PWR Reactor Pressure Vessel (RPV) Upper Head Penetrations Inspection Plan

(MRP-75)

Revision 1

1007337

EPRI Project Manager
C. King

EPRI • 3412 Hillview Avenue, Palo Alto, California 94304 • PO Box 10412, Palo Alto, California 94303 • USA
800.313.3774 • 650.855.2121 • askepri@epri.com • www.epri.com

DISCLAIMER OF WARRANTIES AND LIMITATION OF LIABILITIES

ORGANIZATION(S) THAT PREPARED THIS DOCUMENT

PWR Materials Reliability Program Alloy 600 Issue Task Group

ORDERING INFORMATION

Requests for copies of this report should be directed to EPRI Orders and Conferences, 1355 Willow Way, Suite 278, Concord, CA 94520. Toll-free number: 800.313.3774, press 2, or internally x5379; voice: 925.609.9169; fax: 925.609.1310.

CITATIONS

This report was prepared by Ad-hoc Inspection Plan Subcommittee

Michael Lashley, Chairman	South Texas Project
Scott Boggs	Florida Power & Light
Nat Cofie	Structural Integrity Associates
Greg Gerzen	Exelon Corporation
Craig Harrington	TXU Energy
Steve Hunt	Dominion Engineering, Inc.
Christine King	EPRI
Richard Labott	Public Service Electric & Gas
John Makar	Wolf Creek (currently at INPO)
Larry Mathews	Southern Nuclear Operating Company
Pete Riccardella	Structural Integrity Associates
David Steininger	EPRI
Glenn White	Dominion Engineering, Inc.

This report describes research sponsored by EPRI.

The report is a corporate document that should be cited in the literature in the following manner:

PWR Reactor Pressure Vessel (RPV) Upper Head Penetrations Inspection Plan (MRP-75): Revision 1, EPRI, Palo Alto, CA: 2002. 1007337.

REPORT SUMMARY

Background

Between November 2000 and April 2001 leaks were discovered from reactor vessel top head penetrations at Arkansas Nuclear One-1 and Oconee 1, 2, and 3. The leaks were discovered by visual inspections of the heads, which showed small amounts of boric acid crystal deposits that were determined to have come from the annulus between the nozzles and the vessel head. The CRDM nozzle leaks were traced to predominantly axial PWSCC cracks initiating on the outside surface of the nozzle wall below the J-groove weld. Two of the leaking nozzles at Oconee 3 had circumferential cracks propagating from the OD of the nozzle above the J-groove weld about 165° around the nozzle circumference. Several other nozzles had smaller circumferential cracks on the OD of the nozzle above the top of the J-groove weld. Circumferential cracks above the J-groove weld have the potential to result in nozzle ejection if they reach about 330°.

In August 2001, the NRC issued Bulletin 2001-01 requesting that PWR licensees provide information related to the structural integrity of the reactor pressure vessel (RPV) head penetration nozzles, including the extent of nozzle leakage and cracking that has been found to date, the inspections and repairs that have been undertaken to satisfy applicable regulatory requirements, and the basis for concluding that plans for future inspections will ensure compliance with applicable regulatory requirements. In response to this NRC bulletin, many PWR licensees performed bare metal visual inspections of the RPV head looking for boric acid deposits adjacent to RPV head penetrations. At this time, most of the inspections committed to in response to Bulletin 2001-01 have been completed.

In March 2002, in conjunction with the inspections for most NRC Bulletin 2001-01, Davis-Besse discovered evidence of significant wastage of the low alloy steel head contiguous to CRDM nozzle 3 and less substantial wastage contiguous to CRDM nozzle. The extent of the wastage at nozzle 3 was unanticipated by the utility given the results of previous RPV head inspections at other plants. These previous inspections showed small volumes of leakage from a few nozzles, but little evidence of corrosion of the low alloy steel head. In response to the findings at Davis-Besse, the NRC issued Bulletin 2002-01 focusing on the integrity of the reactor coolant pressure boundary including the reactor pressure vessel head and the extent to which inspections have been undertaken to identify corrosion of the RPV head.

In summary, since November 2000, leaks have been discovered from at least 30 CRDM nozzles at PWRs in the United States. Most of the leaks have been small and have resulted from axially oriented cracks in the nozzle wall or axial/radial oriented cracks in the J-groove welds which produced small volumes of boric acid deposits on the vessel head near the nozzles. In a few cases the PWSCC has included circumferential cracks above the J-groove weld, and in leakage that has resulted in measurable corrosion of the low-alloy steel head material.

Objectives

The objective of the industry inspection plan is to ensure structural integrity by maintaining an acceptably low probability of nozzle ejection or the loss of ASME Code margins due to wastage. The inspection plan applies a graduated approach to inspections to allow early detection of leakage, through-wall cracking, or wastage prior to challenging structural integrity.

Approach

The inspection plan addresses the issue of nozzle ejection due to large circumferential cracks above the J-groove weld by a risk informed analysis for nozzles in B&W designed and manufactured RPV heads with B&W produced nozzle materials. Industry experience to date shows that this head design and nozzle materials has cracked earlier than other designs and materials found in the PWR fleet, therefore the inspection plan is considered to be conservative and applicable to all other domestic PWR plants.

The inspection plan addresses the issue of low-alloy steel wastage, by demonstrating that structural integrity for high and moderate susceptibility plants is ensured by Supplemental Visual (SV) inspections every outage. Less frequent SV inspections are reasonable for lower susceptibility plants given their relatively low head temperatures and resultant low probability of cracking and leakage in these plants.

Results

Bare metal visual (BMV) and non-destructive examination (NDE) frequencies have been conservatively established based on the risk informed analyses to protect against circumferential cracking and potential nozzle ejection (Appendix A). Supplemental visual (SV) examination frequencies have been conservatively established based on deterministic and probabilistic analyses to protect against wastage (Appendices C, D, and E).

EPRI Perspective

Following the identification of OD-initiated circumferential cracks above the J-groove weld at Oconee 3, the Alloy 600 Issue Task Group initiated studies to model PWSCC degradation of the nozzle base material. This probabilistic model conservatively estimates the progression of an axial crack in the nozzle to a leak and to an OD-circumferential crack above the J-groove weld. This model demonstrates that through periodic inspections as defined by this inspection plan that the probability of nozzle ejection is low (i.e. less than 1×10^{-3} per plant year).

Upon discovery of the significant corrosion of the RPV head at Davis-Besse, the Alloy 600 Issue Task Group worked to understand the data available on boric acid corrosion, the progression of the Davis-Besse degradation, and the generic implications for the rest of the PWR fleet regarding detection of leakage before the leakage could lead to wastage of the low-alloy steel material. Deterministic and probabilistic evaluations show that the Supplemental Visual inspections required by this inspection plan will ensure early detection of CRDM nozzle leakage prior to any wastage that would challenge the applicable ASME Code margins. The probabilistic evaluation shows that the probability of exceeding the Code allowables for primary membrane and membrane plus bending stresses is less than 1×10^{-3} given a leaking CRDM nozzle and SV inspections performed during each refueling outage. The statistical inputs to the probabilistic evaluation were designed to capture the process uncertainties. Work is ongoing to further refine

understanding of the wastage process. This work includes MRP and EPRI proposals to DOE's Nuclear Energy Plant Optimization (NEPO) program for specific boric acid corrosion tests.

This document represents a rational method for inspecting RPV head penetrations and safely managing nozzle cracking and RPV head wastage. Revisions can be expected as the industry accumulates RPV head penetration inspection results, experience with the implementation of this inspection plan, and data from relevant laboratory tests.

Keywords
Primary water stress corrosion cracking
PWSCC
Alloy 600
Alloy 82/182
CRDM nozzle
CEDM nozzle
J-groove weld
RPV Head Penetration
Inspection Plan

CONTENTS

LIST OF FIGURES

LIST OF TABLES

1
PURPOSE

The purpose of the industry inspection plan for RPV upper head penetrations is to provide further guidance for PWR licensees subsequent to responding to NRC Bulletins 2001-01 and 2002-01. This inspection plan provides the foundation for a long-term management program for the RPV head penetrations; however, due to the evolving nature of this issue, this plan will be reviewed within three years from issuance. This inspection plan is not intended to supplant previous inspections, evaluations, or site-specific regulatory commitments. The industry inspection plan goal is to preserve structural integrity thereby ensuring safe operation. Structural integrity is defined as maintaining an acceptably low probability of developing primary water stress corrosion cracking (PWSCC) that could lead to nozzle ejection or the loss of ASME Code margins due to consequential wastage. This plan is primarily structured to address PWSCC as the fundamental failure mechanism. However, the inspection plan also applies a graduated approach to inspections to allow early detection of leakage, through-wall cracking, or incipient wastage prior to challenging structural integrity. Industry data is used in conjunction with a risk assessment model to demonstrate that the increase in predicted core damage frequency (CDF) resulting from RPV head penetration cracking is within regulatory guidance (RG 1.174).

2
SCOPE

The guidance provided in this document is applicable to the pressure boundary of the RPV upper head penetrations fabricated from Alloy 600 with Alloy 82/182 weld material. When appropriate technical information is available to define inspection requirements for Alloy 690/52/152 material, this inspection plan will be updated. For the purpose of this plan, through-wall cracks are defined as cracks that provide a leak path from the primary side environment to the nozzle annulus.

3
RISK INFORMED RPV UPPER HEAD PENETRATION INSPECTION METHODOLOGY BASES

3.1 RPV Upper Head Penetration Inspection Bases and Categorization

The RPV head penetration nozzle inspection schedule presented in Section 6.0 is based on a risk informed analysis of nozzle cracking within B&W designed and manufactured RPV nozzle material and head geometry. Pertinent information and bases for this risk informed schedule are provided in Appendix A. The cracking susceptibility of this material is used to bound the materials contained in the PWR fleet based on experience to date and therefore this inspection plan is considered to be conservative and applicable to all other domestic PWR plants.

Probabilistic fracture mechanics (PFM) analyses using the Monte-Carlo simulation algorithm were performed to determine the probability of leakage and failure versus time for a set of input parameters, including head operating temperature, inspection types (visual or non-visual NDE) and inspection intervals. Input into this algorithm included an experience-based time to leakage correlation that uses a Weibull model of plant inspections to date, fracture mechanics analyses of various nozzle configurations containing axial and circumferential cracks and MRP developed statistical crack growth rate data for Alloy 600. The parameters used in the model were benchmarked against the most severe cracking found to date in the industry (B&W Plants) and produced results that are in agreement with experience to date. This analysis assumes there exists an acceptable probability that primary leakage from a through-wall nozzle crack or J-groove weld crack will flow through the nozzle/head penetration interface to the top of the reactor pressure vessel head where it can be visibly identified (see Appendix B).

The moderate susceptibility limit was defined as the number of effective degradation years (EDY) at which a plant reaches either a probability of one leaking nozzle = 20%, or a probability of net section collapse (NSC i.e. nozzle ejection) = 1×10^{-4}. EDY is defined as Effective Full Power Years (EFPY) @ 600°F (RPV head temperature). Explanation of EDY and the method to relate this parameter to Effective Full Power Years at a given head temperature are provided in Appendix A and Reference 2. The high susceptibility limit was defined as the number of EDY at which a plant reaches a probability of nozzle ejection = 1×10^{-3}, which is consistent with NRC RG 1.174 guidance for change in core damage frequency. This NRC guidance specifies an acceptable change in core damage frequency (1×10^{-6} per plant year) for changes in plant design parameters, technical specifications, etc. Therefore, this inspection plan is designed to keep a change in a plant's core damage frequency associated with RPV head penetration cracking to less than 1×10^{-6} per plant year. Since the probability of core damage given a nozzle ejection has been estimated to be 1×10^{-3}, and the probability of nozzle cracking resulting in nozzle ejection is maintained, by implementation of this inspection plan, to be no greater than 1×10^{-3},

the resulting incremental change in core damage frequency under this plan is expected to be less than 1×10^{-6} (i.e., 1×10^{-3} multiplied by 1×10^{-3} equals 1×10^{-6}) per plant year.

A comparison of the PFM results with those from deterministic analyses indicated that the risk-based limits are conservative.

The inspection schedule then employs plant categories defined by these risk-informed susceptibility limits (Appendix A) and specified as follows:

- Low susceptibility: less than 10 EDY, without a leak or identified crack
- Moderate susceptibility: greater than or equal to 10 EDY and less than 18 EDY without a leak or identified through-wall crack, and
- High susceptibility: greater than or equal to 18 EDY or units that have identified leaks or through-wall cracks.

3.2 Penetration J-Groove Weld Inspection Bases

Circumferential cracks in the J-groove weld do not pose a significant risk of nozzle ejection. Cracking that is completely within the weld metal, even if 360^{o} around the nozzle, will not lead to ejection since the portion of the weld that remains attached to the outside surface of the nozzle will not be able to pass through the tight annular fit.

There would be a risk of ejection for the case of lack-of-fusion between the J-groove weld and outside surface of the nozzle over most of the weld circumference. However, the tolerable extent of lack-of-fusion, which still maintains structural integrity, is similar to the acceptable extent of through-wall circumferential cracking (i.e. >75% of the circumference). There is no precedent for such a large area of lack-of-fusion and inspections performed to date do not show significant areas of lack-of-fusion.

Therefore, although the nozzle J-groove weld material is anticipated to have a higher crack growth rate than the nozzle base metal, no inspection requirements and flaw evaluation procedures specific to the weld are required in addition to those otherwise specified or referenced in this document.

4
RPV HEAD FLAW ACCEPTANCE CRITERIA

Boric acid deposits on the RPV head shall be investigated to determine the source and for evidence suggesting general corrosion of the head from primary coolant leakage [1]. When necessary to allow adequate examination, the boric acid crystals and residue shall be removed and a subsequent visual exam (direct or remote) of the previously obscured surfaces shall be performed to evaluate and determine the condition of the underlying base materials. Based on these visual exams, corrective actions shall be taken in accordance with the site's corrective action program.

A penetration whose visual examination detects relevant conditions indicative of boric acid deposits emanating from the nozzle-to-head annulus [1] shall be unacceptable for continued service until supplemental examinations or evaluations are complete and any identified flaws meet applicable acceptance criteria.

Leaks or through wall cracks should be further evaluated per the guidance provided below under Section 6.4, "*Plants with leak(s) or through wall cracks identified"*. Acceptance criteria proposed by the NRC for the flaws were specified in Reference 3. The MRP and ASME Section XI Code are working to develop final criteria, and until those criteria are issued, those of Reference 3 may be used. Additionally, the penetration originally containing relevant conditions shall be acceptable for continued service if the relevant conditions are corrected by a repair/replacement activity or by other corrective measures necessary to meet the acceptance criteria.

5
EXAMINATION REQUIREMENTS (CRITICAL ATTRIBUTES)

5.1 Visual Examinations

The following general prerequisites and performance criteria apply:

- the RPV head penetration area must be accessible consistent with the tools and techniques to be employed and the applicable inspection requirements identified below,
- visual access to the area of interest should not be compromised by the presence of existing deposits on the RPV head, or other factors that could interfere with the examination, and
- written procedure(s) should be developed with appropriate controls over technique and examiner qualification.

5.1.1 Bare Metal Visual (BMV) Examination

A detailed visual examination meeting the following additional requirements:

- Optical aid(s) (for example, camera) used should be able to resolve the 0.158-inch (4-mm) character height under conditions similar to those for the actual inspection (lighting, view angle, etc.) [1],
- The entire intersection between the RPV head and each penetration can be readily viewed as well as approximately one-half (1/2) inch of the adjacent bare surface of the upper head, and
- Additional examinations of uncertain deposits to further discriminate between the possible sources of origin may require additional optical aids with greater resolution, magnification, etc.

5.1.2 Supplemental Visual (SV) Examination

A direct or remote visual examination, which may be addressed through a plant's 88-05 program, with the following additional attributes intended to identify evidence of significant boric acid accumulation that may be associated with incipient wastage:

- RPV heads with accessible upper surface
- Area of interest – the exterior bare surface of the RPV upper head

- Minimum detectable condition – a significant accumulation of boric acid crystals with:
- major dimension greater than 4" (i.e., large enough to not be hidden behind a penetration tube), and
- with thickness such that the condition of the underlying metal cannot be readily determined (i.e., not a film or stain),
- Accessibility – sufficient to observe the minimum detectable condition located anywhere within the area of interest (viewing the entire circumference of each RPV head penetration is not required).
- RPV heads with closely conforming rigid insulation - the following alternative requirements may be met:
- Area of interest - entire periphery and outer surface of the permanently installed insulation (including joints between insulation segments, and annular gaps between the insulation and RPV head penetrations) and exposed portions of RPV head and flange
- Minimum detectable condition - any evidence of RCS leakage such as flow emanating from beneath the insulation, bulging insulation, or boric acid accumulation emerging upward through the joints and gaps between adjoining insulation panels from the RPV head surface,
- Accessibility – sufficient to observe the minimum detectable condition located anywhere within the area of interest.

5.2 Non-Visual Examination (NDE)

- A surface technique intended to identify cracking emanating from the pressure retaining wetted surface of the J-groove weld and the adjacent inside and outside diameter surface of the penetration, or
- a volumetric technique intended to identify cracking propagating through the root of the J-groove weld and/or the penetration base material into the penetration annulus, or
- a combination of the above two examinations such that any cracking that could provide a leak path through the pressure boundary is detected.

6
PLANT-SPECIFIC RPV HEAD PENETRATION INSPECTION SCHEDULE

This inspection plan will be implemented at the next refueling outage (RFO) following completion of the plant's head penetration inspections in response to NRC Bulletin 2001-01 or 2002-01. At the plant's option, the inspections in response to NRC Bulletin 2001-01 or 2002-01 may be substituted for the first inspection required by this plan if they meet the critical inspection attributes required of this plan. The subsequent re-inspection frequency will be based on the completion date of that previous inspection. Inspection methods may be chosen on a per-penetration basis (e.g., non-visual examination may used for some penetrations, while visual is used for others). Figures 6-1 and 6-2 are flowcharts of the inspection plan provided in the text below. The plant categories have been initially defined as noted above (and in Appendix A) based on preliminary bounding risk assessment activities. When a plant moves from one category to another (e.g. by gaining more EDY), the re-inspection frequency is dictated by the new category and the method of the previous exam. If the previous inspection is within the frequency of the new category, no new inspection is required upon entering the new category.

The BMV and NDE examination frequencies have been conservatively established based on the risk informed analyses of nozzle cracking (Appendix A), primarily to protect against circumferential cracking and potential nozzle ejection. The SV examination frequency is conservatively established to enhance detection of incipient wastage from all sources on and around the RPV head and to ensure the subsequent BMV is not obscured by boric acid accumulation (Appendices C, D, and E).

6.1 For low susceptibility plants (< 10 Effective Degradation Years, EDY):

6.1.1 Perform either a Bare Metal Visual (BMV) examination of 100% of the RPV head penetrations once per 10 EFPY; or perform NDE (i.e., non-visual examination) of 100 % of the RPV head penetrations and associated J-groove welds, once per 10 EFPY.

6.1.2 In addition, perform Supplemental Visual examinations every 2nd RFO during those outages when the 6.1.1 examinations are not required. The initial inspection following a 100% non-visual examination of all RPV head penetrations and associated J-groove welds may be performed during the 3rd RFO following the 100% non-visual examination. The SV frequency may be revised at a future date with an appropriate technical basis.

6.1.3 If leakage, or through wall cracking is identified, the plant is reclassified as "high susceptibility". If only part through-wall cracks are identified, the plant is reclassified as "moderate susceptibility".

6.1.4 For plants whose inspection periods are controlled either by EDY or EFPY, the inspection periods may be increased by a maximum of 0.5 EFPY for scheduling purposes.

6.2 For moderate susceptibility plants *(10 EDY ≤ X < 18 EDY)*

6.2.1 Perform a BMV examination of 100% of the RPV head penetrations at the 1st RFO upon entering this category (or not more than 2 EDY since the most recent exam) and once every 2 EDY, not to exceed 5 EFPY. Alternatively, perform NDE (i.e., non-visual examination) of 100 % of the RPV head penetrations and associated J-groove welds at the 1st RFO upon entering this category and once every 4 EDY, not to exceed 10 EFPY.

6.2.2 In addition, perform Supplemental Visual examinations every RFO during those outages when the 6.2.1 examinations are not required. The SV frequency may be revised at a future date with an appropriate technical basis.

6.2.3 If leakage, or through wall cracking is identified, the plant is reclassified as "high susceptibility". If part through-wall cracks are identified, the classification of the plant does not change.

6.2.4 For plants whose inspection periods are controlled either by EDY or EFPY, the inspection periods may be increased by a maximum of 0.5 EFPY for scheduling purposes.

6.3 For high susceptibility plants *(≥ 18 EDY)*

6.3.1 Perform a BMV examination of 100% of the RPV head penetrations at every RFO upon entering this category. Alternatively, perform NDE (i.e., non-visual examination) of 100% of the RPV head penetrations and associated J-groove welds at the 1st RFO upon entering this category and once every 4 EDY, not to exceed 6 EFPY.

6.3.2 In addition, perform Supplemental Visual examinations every RFO during those outages when the 6.3.1 examinations are not required. The SV frequency may be revised at a future date with an appropriate technical basis.

6.3.3 For plants performing visual examinations to meet the requirements of 6.3.1, perform NDE (i.e., non-visual examination) of 100% of the RPV head penetrations and associated J-groove welds, or portions thereof that can be examined without undertaking physical modifications for accessibility, within 4 EDY upon entering this category or issuance of this Plan, whichever is later. This additional NDE requirement is based on providing defense-in-depth.

6.3.4 For plants whose inspection periods are controlled either by EDY or EFPY, the inspection periods may be increased by a maximum of 0.5 EFPY for scheduling purposes.

6.4 Plants With Leak(s) Or Through-Wall Cracks Identified

6.4.1 Discovery Inspection

- Perform a non-visual examination of the leaking RPV head penetration(s) and associated J-groove welds to characterize the crack or leak identified.
- Indications are evaluated or repaired in accordance with approved flaw evaluation guidelines.

Note: Nozzles with through-wall indications shall be evaluated for cavities and corrosion of the reactor vessel head adjacent to the penetration. Any identified corrosion shall be evaluated and repaired as necessary.

6.4.2 Expansion of Inspection

Implement the following expansion guidance either during the Discovery Inspection or no later than the next RFO following discovery of a leak or through-wall crack in any RPV head penetration or associated J-groove weld. Either:

- Perform NDE (i.e., non-visual examination) of 100% of the RPV head penetrations and associated J-groove welds.
    - Indications are evaluated or repaired in accordance with approved flaw evaluation guidelines.
- Or, perform a plant-specific technical evaluation to justify continued visual examination until the component is removed from service.

6.5 Plants With Part Through-Wall Cracks Identified

6.5.1 Discovery Inspection

- Indications are evaluated or repaired in accordance with approved flaw evaluation guidelines.

6.5.2 Indications Left in Service

- Re-inspection of the indication is performed in accordance with the flaw evaluation guidelines and projected crack growth.
- Re-inspection of an embedded flaw is performed at
    - The next scheduled RFO and once every ISI period thereafter, or
    - In accordance with a site-specific evaluation.

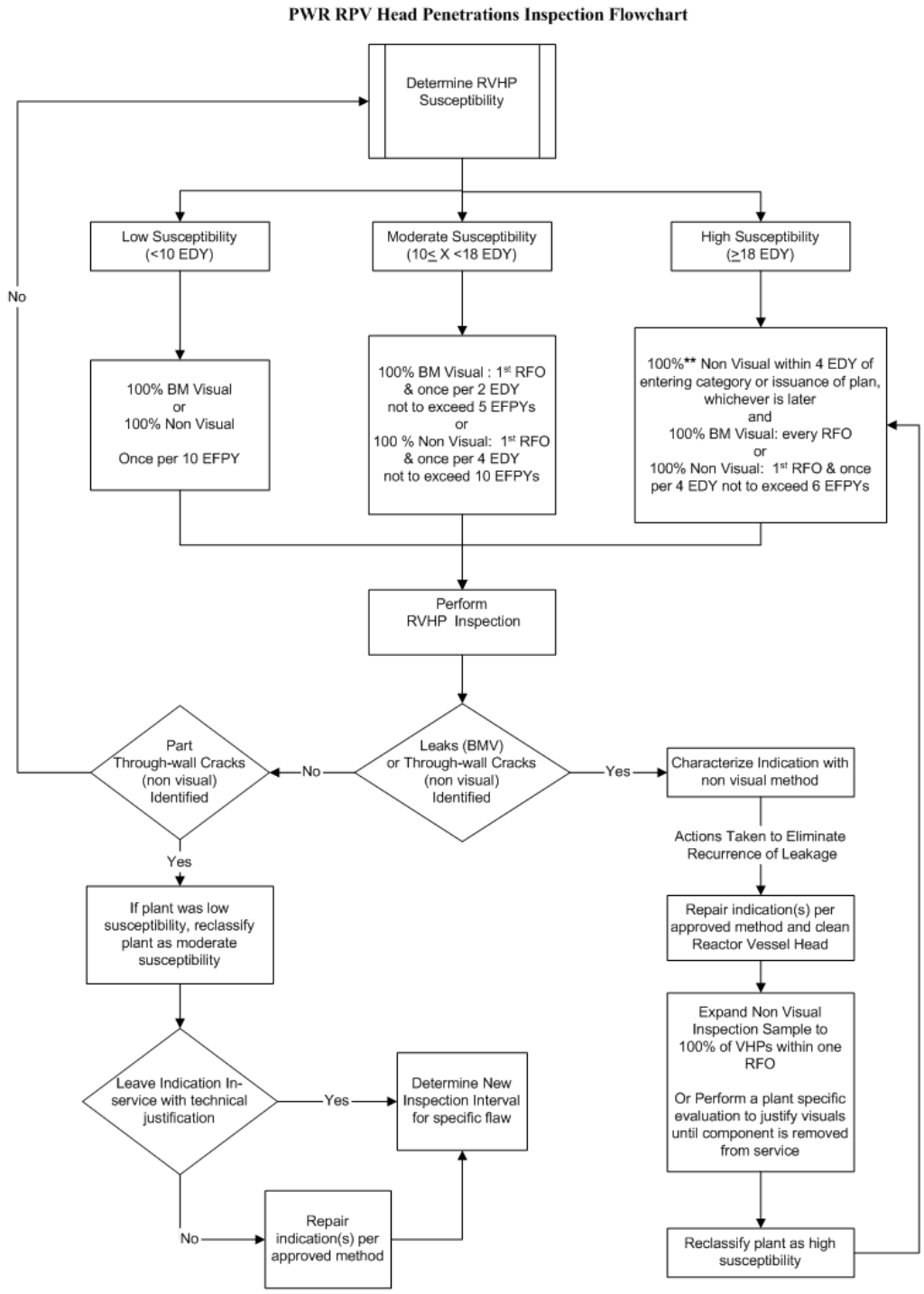

** 100% of the RPV Head penetrations and associated J-groove welds or portions thereof that can be examined without incurring undue hardship.

Note: This flowchart addresses the RPV Head penetration inspection schedule, not the supplemental visual examinations (See Figure 6-2).

Figure 6-1
PWR RPV Head Penetration Inspection Flowchart

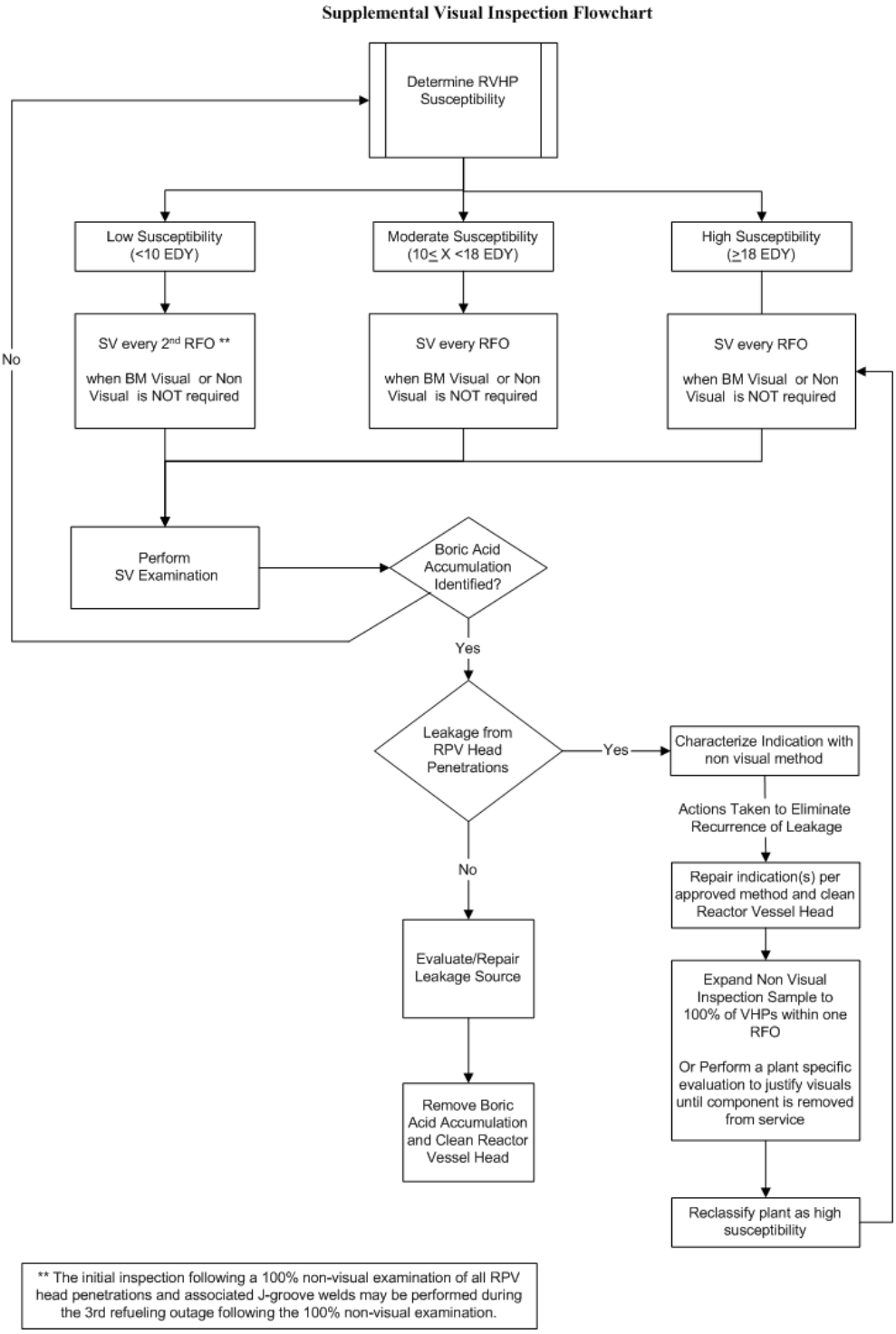

Figure 6-2
Supplemental Visual Inspection Flowchart

7
AS-LEFT RPV HEAD CLEANLINESS CONDITION

Upon completion of each visual examination (BMV or SV), the RPV head upper surface should be clean of debris and deposits consistent with the following guidance to prevent interference with the subsequent detection of leakage:

- Isolated, loosely adherent, boric acid crystal "crumbs" may remain once documented,
- Thin, surface-conforming boric acid films with thickness such that the condition of the underlying metal can be readily determined (i.e., a film or stain) may remain once documented,
- Other cleanliness exceptions may be allowed to remain if fully documented as to composition and extent and provided that a written evaluation concludes that the condition is acceptable and will not interfere with any necessary subsequent visual examination (BMV or SV).

8
REFERENCES

1. EPRI Technical Report, *Visual Examination for Leakage of PWR Reactor Head Penetrations on Top of the RPV Head: Revision 1*, Report 1006899, March 2002.

2. EPRI Interim Report, *PWR Materials Reliability Project Interim Alloy 600 Safety Assessments for US PWR Plants (MPR-44), Part 2: Reactor Vessel Top Head Penetrations*, TP-1001491, Part 2, May 2001.

3. Letter, Jack Strosnider, NRC, to Alex Marion, NEI, *Subject: Flaw Evaluation Criteria*, November 21, 2001.

A
APPENDIX A: TECHNICAL BASIS FOR RPV UPPER HEAD PENETRATION INSPECTION PLAN

Probabilistic Fracture Mechanics (PFM) analyses are described that predict the probability of leakage and failure versus plant operating time for various input parameters that bound the operating characteristics of the US PWR fleet. These include various head operating temperatures, inspection types (visual or non-visual NDE) and inspection intervals. The PFM algorithm includes an experience-based time to leakage correlation based on a Weibull model of plant inspections to date, fracture mechanics analyses of various nozzle configurations containing axial and circumferential cracks, and a statistical representation of crack growth rate data for Alloy 600. The model is benchmarked against the group of plants exhibiting the most severe cracking found to date in the industry (Babcock and Wilcox designed plants) and it produces results that are in agreement with experience to date at these plants. Its application to other plant designs, which have exhibited less severe cracking, is therefore conservative.

The benchmarked PFM model is then used to define susceptibility categories that are designed to keep the worst-case probability of nozzle failure within NRC Regulatory Guide 1.174 guidance for change in core damage frequency. This NRC guidance specifies an acceptable change in core damage frequency (1×10^{-6} per plant year) for changes in plant design parameters, technical specifications, etc. Therefore, the inspection plan is designed to limit the change in any plant's core damage frequency associated with RPV head penetration cracking to less than 1×10^{-6} per plant year. Since the probability of core damage given a nozzle failure (assuming that failure leads to ejection of the nozzle from the head) has been estimated to be 1×10^{-3}, and the probability of nozzle cracking resulting in nozzle ejection is maintained, by implementation of the inspection plan, to be no greater than 1×10^{-3}, the resulting incremental change in core damage frequency under the plan is 1×10^{-6} (i.e., 1×10^{-3} times 1×10^{-3} equals 1×10^{-6}) per plant year. A comparison of the PFM results with those from deterministic analyses indicates that the risk-based inspection criteria are conservative.

A.1 Probabilistic Fracture Mechanics

Development is underway of a generic Probabilistic Fracture Mechanics (PFM) methodology for Control Rod Drive Mechanism (CRDM) top head penetrations. The methodology has been fully developed for the most critical reactor type (Babcock & Wilcox designed plants) with respect to top head nozzle cracking based on field inspection results to date. Elements of the methodology include:

- Experience-based time to leakage computations that use a Weibull model of plant inspections to date.

- Fracture mechanics analyses of various nozzle configurations containing axial and circumferential cracks.
- Statistical crack growth rate (CGR) data for Alloy 600 material developed by the Materials Reliability Program (MRP) Expert Panel [A-1].
- A Monte-Carlo simulation algorithm to determine the probability of leakage versus time and the probability of nozzle ejection (Net Section Collapse or NSC) versus time for various sets of input parameters, including head operating temperature, inspection type (visual or NDE) and inspection intervals.

Details of this methodology are contained in Reference A-2.

The PFM methodology provides a means of evaluating various top head inspection options to determine their relative contributions to safe plant operation.

A.1.1 Assumptions

Several key assumptions are necessary to perform a CRDM PFM analysis with the MRP PFM methodology. These include Weibull parameters for time to leakage, CGR distribution type, correlation factors between time to leakage and crack growth rate, and probabilities of detection (PODs) for the various inspection types. Other required input includes number of CRDM nozzles and heats of nozzle material per head, nozzle angles, yield strengths, and nozzle-to-head shrink-fit conditions. Although this latter group is generally known for each specific plant, assumptions must be made on these parameters as well in order to conduct analyses that simulate the U.S. PWR fleet as a whole. For purposes of this analysis, reasonable values of these parameters were selected that are representative of B&W-designed plants, as summarized in Table A-1. These are considered to be a conservative representation of U.S. PWRs as a whole, since the B&W plants have been seen to lead the U.S. fleet in terms of severity of cracking and leakage (7 out of 7 plants found to have leaking nozzles, several of which contained circumferential cracks). However, before proceeding with production analyses, these assumptions were benchmarked against actual performance of the B&W plants.

Table A-1
Parameters Assumed for PFM Analysis

Weibull Parameters	Alpha	3
	Beta	15 ± 6 (Triang.)
CGR Distribution	Exponent	1.16
	Alpha (heat-to-heat)	-15.25 ± 2.212 (Log-Triang.)
	Alpha (within heat)	0 ± 1.6 (Log-Triang.)
Correlation Factors	Heat-to-Heat	0.8
	Within Heat	0.8
# Nozzles	69	
# Heats	3	
Nozzle Yield Strength	Normal	44.5 ksi; STD=1.5 ksi
Interference Fit	Normal	0.0003"; STD=0.0014"

A.1.2 Benchmarking of PFM Assumptions

The benchmark analysis results obtained with this particular set of assumptions for a B&W plant design are shown in Figure A-1. This figure shows the cumulative probability of leakage, large circumferential cracking, and nozzle net section collapse (NSC) versus time for a plant analyzed with the assumptions listed in Table A-1, operated at a 602°F head temperature (the approximate average head temperature for all B&W plants, which ranged from 601°F to 605°F). The results indicate a high probability of leakage (> 90%), and a moderate probability (~ 12%) of a large circumferential crack at 20.1 EFPY. These results are in agreement with experience, since all of the B&W plants experienced at least one leaking nozzle at about 20 EFPY, and one out of seven experienced a large circumferential crack. Thus, the above parameters are considered reasonable and conservative for evaluation of an inspection plan for the entire U.S. PWR fleet, since they are benchmarked against the worst performing group of plants in the fleet.

One final requirement for the evaluation is to specify limits on probability of leakage and net section collapse. Using the NRC guidance for risk-informed decisions [A-3], a value of 1×10^{-6} has been selected as an acceptable change in core damage frequency per year associated with the nozzle cracking issue. That is, an inspection program will be considered acceptable if it keeps the incremental core damage frequency associated with the CRDM nozzle cracking issue less than this limit for any plant in the fleet. Since the conditional core damage frequency given nozzle ejection (i.e. NSC) has been estimated at approximately 1×10^{-3}, it is assumed for purposes of this analysis that a plant enters the high-risk category when the probability of a nozzle NSC equals 1×10^{-3} per year. It will be seen that this limit also corresponds to a cumulative probability of leakage of ~75% if no inspections are performed up to that point.

To further reduce risk, a second, moderate-risk category is defined as the point when a plant enters a region where either the probability of nozzle NSC equals 1×10^{-4} per year or the cumulative probability of leakage reaches 20%.

A.2 PFM Results

A.2.1 Definition of Risk Categories

The results of the aforementioned PFM analyses are summarized in Figures A-2 and A-3. Referring to Figure A-3, it is seen that the NSC curves intersect the 1×10^{-3} per year limit (upper dashed line) at decreasing times as the temperature increases from 560°F to the maximum of 605°F. These intersection points have been translated to a locus of EFPY versus temperature (upper red, chain-link curve) in Figure A-4. Similar loci have been constructed from intersections with the lower dashed line in Figure A-3 (probability of NSC = 1×10^{-4} per year) and from the intersections of the probability of leakage curves with the two dashed lines in Figure A-2 (20% and 75% cumulative leakage probability). The lower NSC limit (1×10^{-4}) is shown as the brown chain-link curve in Figure A-4. The leakage limits are shown by the two solid curves in Figure A-4 (blue for 75% and orange for 20%). It is seen that there is reasonable correspondence between the two sets of curves. That is, both the upper and lower leakage and NSC curves lie close to one another, such that a single set of limits will address both risks. Plants that plot above and to the right of the upper two curves are considered to be in a high-risk category, since their probability of NSC would exceed 1×10^{-3} per year, and they would also have a 75% cumulative probability of leakage. Plants that plot between the upper and lower sets of curves are considered to be in a moderate risk category, since their probability of NSC would exceed 1×10^{-4} per year, and they would have a 20% cumulative probability of leakage. Plants that plot below and to the left of the bottom set of curves are considered to be at low-risk with respect to the CRDM nozzle cracking issue.

Also shown in Figure A-4 are data points corresponding to plant inspections, along with the current head operating temperatures at each plant and an estimate of EFPY at the times of inspection. The red triangles represent the nine plants in which leakage has been detected (seven B&W plants and two Westinghouse plants). The yellow-filled squares represent the plants in which cracking (but no leakage) has been detected. The solid blue, diamond-shaped data-points represent plants that have performed visual examinations with no leakage detected, and the solid blue squares represent plants that have performed non-destructive examinations with no indications of cracking. Note that in some cases, multiple inspections have been performed at a given plant. These are identified in Figure A-4 by vertical lines connecting the data-points for that plant.

It can be seen from these data that the proposed risk-based categorization curves line up well with plant inspection results to date. All of the inspections that resulted in either leakage or cracking lie in the moderate or high-risk regions, and all except one of the plants with leaks lie on or above the high-risk curve. The plant with large circumferential cracks (Oconee-3) was well into the high-risk region at the time the cracks were observed. Also shown are data-points corresponding to planned future inspections (Fall 2002 or Spring 2003). It is seen from these data that all plants in the high-risk region and the large majority of the plants in the moderate-risk region have been inspected at least once.

Finally, the curves and data-points from Figure A-4 are re-plotted in Figure A-5, along with several light-blue curves that represent various numbers of Effective Degradation Years (EDYs,

or equivalent EFPYs at 600°F). EDYs are computed in accordance with the following activation energy equation [A-4]:

$$EDY_{600°F} = \sum_{j=1}^{n} \left\{ \Delta EFPY_j \exp\left[-\frac{Q_i}{R}\left(\frac{1}{T_{head,j}} - \frac{1}{T_{ref}} \right) \right] \right\} \qquad \text{[Equation A-1]}$$

where:

$EDY_{600°F}$ = total effective degradation years through February 2001, normalized to a reference temperature of 600°F
Q_i = activation energy for crack initiation (50 kcal/mole)
R = universal gas constant (1.103×10^{-3} kcal/mol-°R)
$T_{head,j}$ = 100% power head temp. during time period j (°R = °F + 459.67)
T_{ref} = arbitrary reference temperature (600°F = 1059.67°R)
n = number of different head temperatures during plant history

It is seen from Figure A-5 that the risk categories defined above correspond to the following limits in terms of EDYs:

Low-Risk: $0 < \text{EDYs} < 10$

Moderate-Risk: $10 \leq \text{EDYs} < 18$

High-Risk: $18 \leq \text{EDYs}$

A.2.2 Inspection Interval Sensitivity Studies

PFM analysis was also used to perform sensitivity studies of the effects of various inspection intervals for plants in the moderate and high-risk categories. These studies were all performed at an assumed head operating temperature of 600°F, so they yield results directly in EDYs, which can be translated to other operating temperatures via the above activation energy equation.

One additional assumption needed for the inspection interval studies is probability of detection (POD) for the two inspection types, bare metal visual (BMV) and non-destructive examination (NDE). For BMV, it was assumed that, if a penetration is leaking when the initial visual inspection is performed, there is a 60% probability that the leakage will be detected. For subsequent visual examinations of a penetration that was previously inspected but leakage was missed, the 60% POD is multiplied by a factor of 0.2, yielding a POD of 12% for repeat inspections. These conservatively low PODs, account for a combination of effects including tight shrink fit conditions, difficult accessibility for inspections and human error. For NDE, a previously developed curve for "Full-V" ultrasonic inspection of reactor vessels was obtained from Reference A-5, and then multiplied by a factor of 0.8. The resulting curve of POD versus crack depth, shown in Figure A-6, is also considered to be conservative for the types of NDE currently being performed on CRDM nozzles.

Figure A-7 illustrates the effect of BMV at various intervals, beginning when a plant first enters the High Risk category (18 EFPYs at 600°F = 18 EDYs). BMVs every 4 EDY, 2 EDY and at each refueling outage (RFO) were evaluated. It is seen that in all cases, the yearly probability of

NSC, which is just approaching 1 x 10^{-3} at the time of initial inspection, is approximately halved immediately following the inspection. The curves for 2 and 4 EDY intervals increase after that, however, and after some period of time are predicted to again exceed the 1 x 10^{-3} limit. Inspection each RFO, on the other hand, reduces the probability of net section collapse below the 1 x 10^{-3} limit throughout the time period analyzed.

Figure A-8 presents similar results for NDE beginning when a plant first enters the high-risk category, considering inspection intervals of 4 and 8 EDY. It is seen that, for the POD assumed, NDE at 4 EDY intervals is even more effective than BMV each RFO at reducing the probability of NSC to an acceptable level, and keeping it there indefinitely. NDE at 8 EDY intervals is less effective, and does allow the probability to re-approach 1 x 10^{-3} between inspections.

Finally, Figure A-9 illustrates that the recommended inspections for plants in the Moderate category (BMV at 2 EDY or NDE at 4 EDY intervals) are more than adequate to maintain the probabilities of NSC at acceptable levels for the time period until the plants reach the high risk category. These inspections provide an extra measure of assurance, which would not be required just based on the PFM analysis by itself, to keep the probability of NSC of the entire PWR fleet at an extremely low level.

A.3 Deterministic Crack Growth Analysis

A deterministic crack growth evaluation has also been performed to determine the time it will take for an assumed initial circumferential flaw to reach the ASME Code Section XI allowable through-wall length. Inputs into this deterministic analysis include crack growth law, stress intensity factor versus flaw length distribution and assumed initial flaw size. Each of these inputs is described in the following paragraphs.

A.3.1 Crack Growth Law for Alloy 600

Reference A-1 provides the MRP recommended curve to be used to evaluate growth of SCC flaws in Alloy 600 materials, such as RHV nozzle and is given by:

$$\dot{a} = \exp\left[-\frac{Q_g}{R}\left(\frac{1}{T}-\frac{1}{T_{ref}}\right)\right]\alpha\left(K-K_{th}\right)^{\beta} \qquad \text{[Equation A-2]}$$

where:

$\dot{a}$ = crack growth rate at temperature T in m/s (or in/yr)

Q_g = thermal activation energy for crack growth
= 130 kJ/mole (31.0 kcal/mole)

R = universal gas constant
= 8.314 x 10^{-3} kJ/mole·K (1.103□10^{-3} kcal/mole·°R)

T = absolute operating temperature at location of crack, K (or °R)

T_{ref} = absolute reference temperature used to normalize data
= 598.15 K (1076.67°R)

α = crack growth amplitude

= 2.89×10^{-12} at 325°C for $\dot{a}$ in units of m/s and K in units of MPa $\sqrt{\text{m}}$
(4.00×10^{-3} at 617°F for $\dot{a}$ in units of in/yr and K in units of ksi $\sqrt{\text{in}}$)

K = crack tip stress intensity factor, MPa $\sqrt{\text{m}}$ (or ksi $\sqrt{\text{in}}$)

K_{th} = crack tip stress intensity factor threshold

= 9 MPa $\sqrt{\text{m}}$ (8.19 ksi $\sqrt{\text{in}}$)

β = exponent

= 1.16

This curve represents the 75th percentile level of the CGR data contained in Reference A-1. Furthermore, for deterministic analysis, the MRP recommends a factor of two be applied to the above crack growth law. The MRP equation, including the factor of two can be written in a simpler form, as:

$$\frac{da}{dt} = C\left(K - 8.19\right)^{1.16} \quad in/hr \qquad \text{[Equation A-3]}$$

where:

K = stress intensity factor ($ksi\sqrt{in}$)

C = function of temperature and whose values are indicated in Table A-2.

Table A-2
Value of Parameter C for Deterministic Analysis as a Function of Temperature

Temperature (ºF)	C
580	3.604×10^{-7}
590	4.665×10^{-7}
600	6.008×10^{-7}
602	6.316×10^{-7}
605	6.806×10^{-7}

A.3.2 Stress Intensity Factor Distribution

In previous work done to support the MRP risk assessment, the stress intensity factor (K) for circumferential flaws of two plant types was determined. This information is shown in Tables A-3 and A-4. As can be seen from these tables, K is a strong function of the nozzle angle. For this deterministic evaluation, the most conservative nozzle angle location (38º for the B&W-type plants and 43.5º for the Westinghouse-type plant) is used. It can be seen further from these

tables that K is also dependent on whether the crack is in the uphill or downhill direction. The uphill direction, being the most conservative distribution of the two, is used in this deterministic evaluation for B&W plants. For Westinghouse plants, the conservative downhill distribution is used. Although generic analyses have not yet been performed for Combustion Engineering designed plants, the stress intensity factors in Tables A-3 and A-4 are considered to be representative of the bounding CEDM nozzles in this plant design.

Table A-3
Typical Stress Intensity Factor Distribution for B&W Type Plant

Nozzle Angle	Circumferential Crack Length		Stress Intensity Factor (ksi*(in)$^{1/2}$)	
	Degrees	Inches	Uphill	Downhill
0°	30	0.9664	20.8	N/A
	70	2.2550	18.8	N/A
	160	5.1540	20.3	N/A
	180	5.3140	0.64	N/A
	220	6.4950	0.63	N/A
	260	7.6760	0.63	N/A
	300	8.8570	0.62	N/A
18°	30	1.0170	27.2	27.2
	70	2.3730	24.0	24.0
	160	5.4240	24.5	24.5
	180	5.5920	23.4	1.0
	220	6.8350	23.8	2.4
	260	8.0770	26.9	6.0
	300	9.3200	26.5	11.5
26°	30	1.0830	29.7	29.7
	70	2.5260	26.1	26.1
	160	5.7750	26.5	26.5
	180	5.9530	28.4	0.4
	220	7.2760	23.2	1.7
	260	8.5990	23.6	7.5
	300	9.9220	24.9	16.6
38°	30	1.2380	34.4	34.4
	70	2.8830	27.1	27.1
	160	6.6020	29.2	29.2
	180	6.8060	37.7	4.5
	220	8.3190	31.2	6.7
	260	9.8310	26.6	12.7
	300	11.3440	29.9	25.9

Table A-4
Typical Stress Intensity Factor Distribution for Westinghouse-Type Plant

Nozzle Angle	Circumferential Crack Length		Stress Intensity Factor (ksi*(in)$^{1/2}$)	
	Degrees	Inches	Uphill	Downhill
0°	30	0.9653	20.8	N/A
	70	2.2525	18.8	N/A
	160	5.1487	20.3	N/A
	180	5.3014	0.64	N/A
	220	6.4790	0.63	N/A
	260	7.6576	0.63	N/A
	300	8.8357	0.62	N/A
13.6°	30	0.9793	27.2	27.2
	70	2.2851	24.0	24.0
	160	5.2232	24.5	24.5
	180	5.3782	6.9	28.3
	220	6.5733	10.1	29.7
	260	7.7684	12.4	29.8
	300	8.9636	16.7	28.7
30°	30	1.0413	29.7	29.7
	70	2.4299	26.1	26.1
	160	5.5541	26.5	26.5
	180	5.7188	6.9	37.2
	220	6.9897	8.0	39.8
	260	8.2605	11.7	41.3
	300	9.5314	18.5	41.0
43.5°	30	1.1554	34.4	34.4
	70	2.6959	27.1	27.1
	160	6.1622	29.2	29.2
	180	6.3449	14.8	47.2
	220	7.7549	13.5	51.9
	260	9.1649	16.7	58.1
	300	10.5749	23.8	63.7

A.3.3 Initial Flaw Size and Allowable Flaw Size

The initial flaw size for this evaluation is assumed to be a through-wall circumferential flaw that is 30 degrees of the circumference, corresponding to the first crack length for which a K value is provided in Tables A-3 and A-4. This assumed initial crack length is very conservative and should provide a conservative estimate of time to reach allowable flaw size.

From Reference A-4, the allowable flaw size based on a safety factor of 3, consistent with ASME Code Section XI, is about 300º of the circumference. This allowable flaw size is used in the evaluation.

A.3.4 Crack Growth Evaluation and Results

The evaluation is performed separately for the two plant types. The temperatures, as shown in Table A-2, were considered in the crack growth evaluation using the input parameters discussed above. The results of the evaluation are shown in Figures A-10 and A-11, and are summarized in Table A-5.

It can be seen that in the worst case corresponding to a temperature of 605ºF, the time for an initial 30º flaw to reach the allowable flaw size is 24.3 EFPY for B&W plant-type, and 16.8 EFPY for the Westinghouse plant-type. For reference, the time to reach Oconee Unit 3 type flaw (165º) is also noted. For a B&W plant at 605ºF, it takes 13.4 EFPY to reach this flaw size, while for a Westinghouse-type plant, it takes 12.5 years.

Table A-1
Summary of Deterministic Crack Growth Results

Temperature (ºF)	Time for Initial Flaw Size of 30º Circumference to Grow to 165º and Allowable Flaw Size of 300º (EFPY)			
	B&W-Type Plants		Westinghouse-Type Plant	
	165º	300º	165º	300º
580	25.3	>40	23.7	31.7
590	19.6	35.3	18.3	24.6
600	15.2	27.3	14.2	19.1
602	14.4	26.0	13.5	18.2
605	13.4	24.3	12.5	16.8

Referring to Figure A-12, the deterministic crack growth times reported in Table A-5 for the Westinghouse-type plant were added to the lower, 20% probability of leakage curve in Figure A-4. This equates to the amount of time, conservatively, that a crack would require to grow from the initial assumed size at leakage (30°) to the allowable flaw size of 300°. It is seen that these times exceed the high-risk curve from the risk-based analysis, indicating that the risk-based limits are conservative with respect to deterministic crack growth analysis.

A.3.5 REFERENCES

A-1. *Crack Growth Rates for Evaluating Primary Water Stress Corrosion Cracking (PWSCC) of Thick-Wall Alloy 600 Material*, EPRI Document MRP-55, July 2002.

A-2. S.S. Tang and P. C. Riccardella, *M R P E R C R D Evaluation of Reliability for Control Rod Drive Nozzles in Vessel Top Head,* Materials Reliability Program, Structural Integrity Report (Draft), January 2002.

A-3. NRC Reg. Guide 1.174. *An Approach for Using Probabilistic Risk Assessment in Risk-Informed Decisions on Plant Specific Changes to the Current Licensing Basis,* U.S. Nuclear Regulatory Commission, January 1998.

A-4. PWR Materials Reliability Report, *Interim Alloy 600 Safety Assessments for US PWR Plants (MRP-44), Part 2: Reactor Vessel Top Head Penetrations,* EPRI Report No. TP-1001491, Part 2, May 2001.

A-5 Dimitrijevic, V. and Ammirato, F., *Use of Nondestructive Evaluation Data to Improve Analysis of Reactor Pressure Vessel Integrity,* EPRI Report TR-102074, Yankee Atomic Electric Co. March 1993

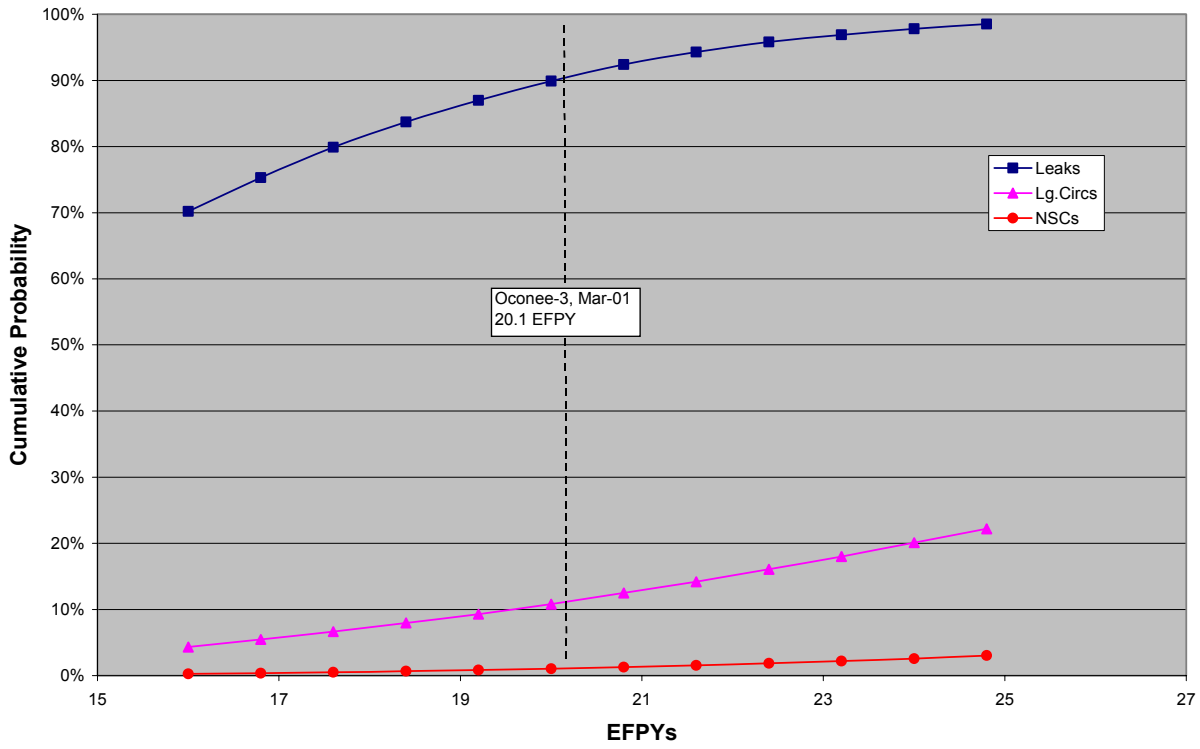

Figure A-1
Results of PFM Calibration Analysis at 602°F Showing Comparison to Oconee 3 Inspection Results

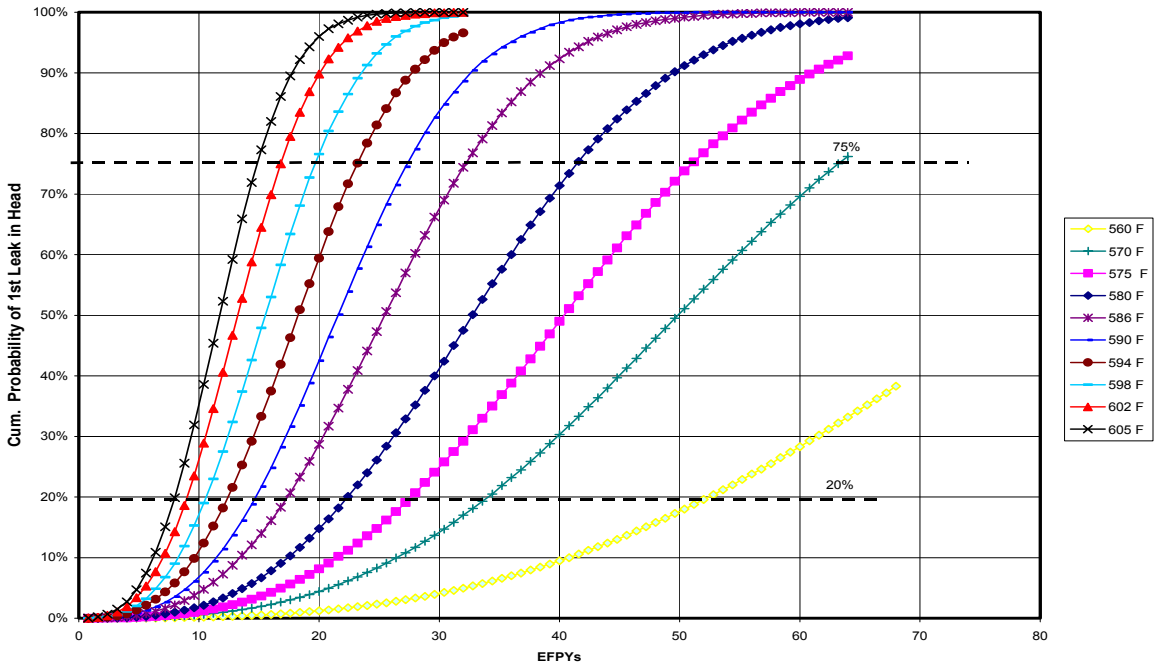

Figure A-2
Cumulative Probability of Leakage versus Time for Various Head Temperatures

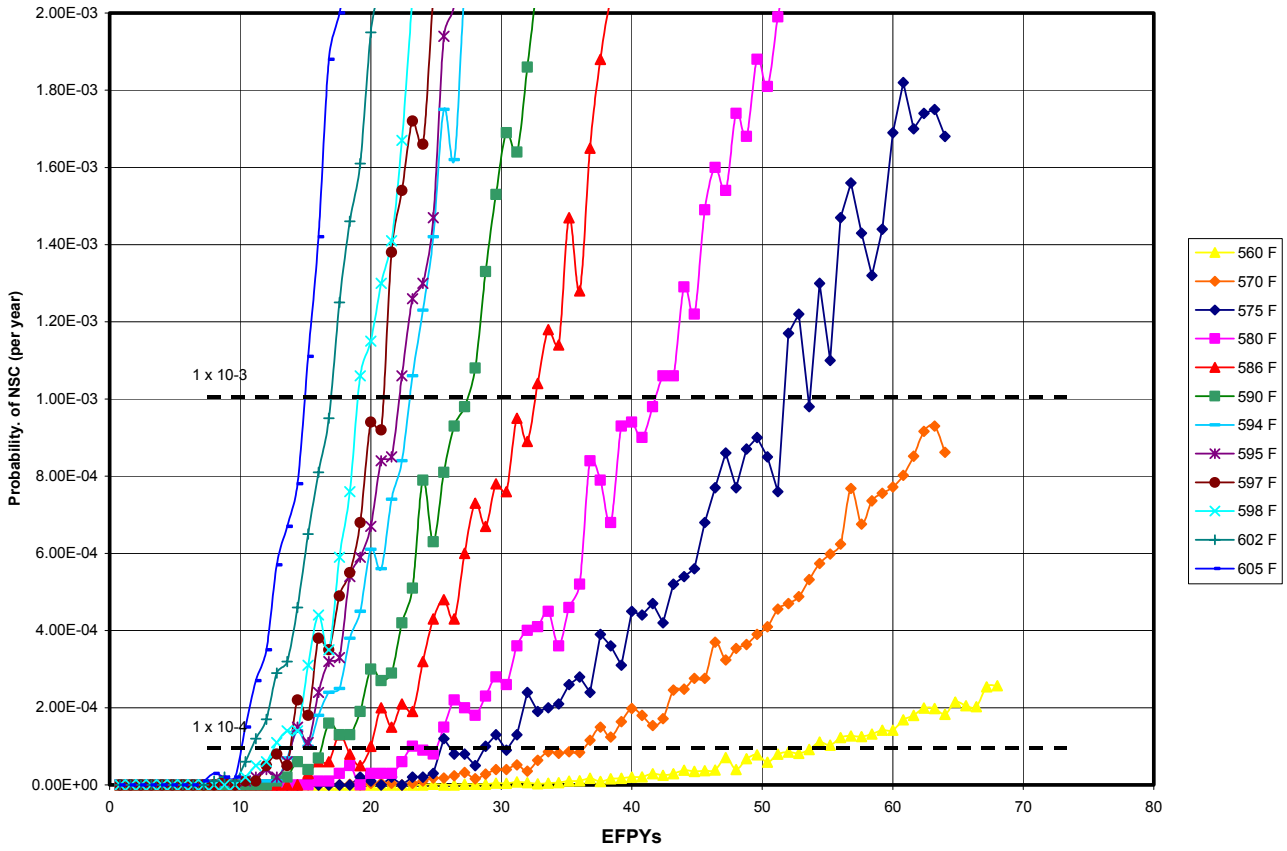

Figure A-3
Probability Density (per year) of Net Section Collapse versus Time for Various Head Temperatures

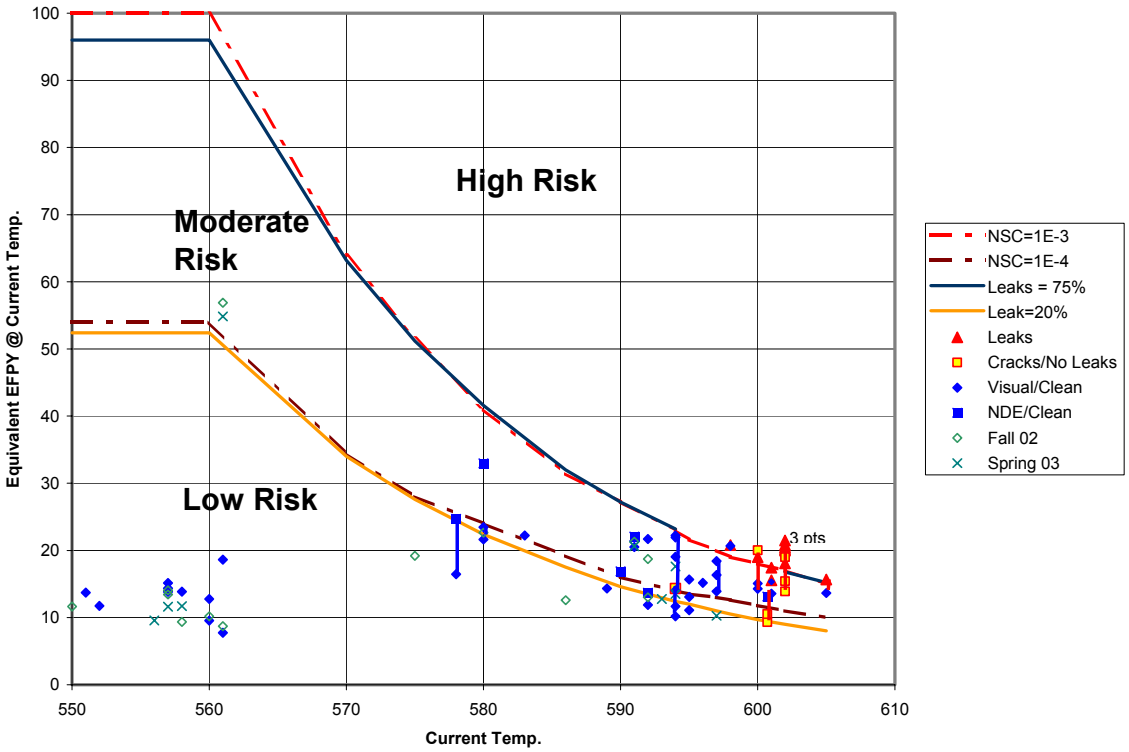

Figure A-4
Definition of Low, Moderate, and High Risk Time-Temperature Regimes Based on PFM Results. Plant Inspection Results Also Indicated

Notes Regarding Plant Data in Figure:

- Vertical lines connecting the data points for a given plant indicate multiple inspections at that plant.

- For plants that have operated at more than one head temperature, the EFPYs have been normalized to the current temperature (per Equation A-1), and the data points have been plotted at that temperature.

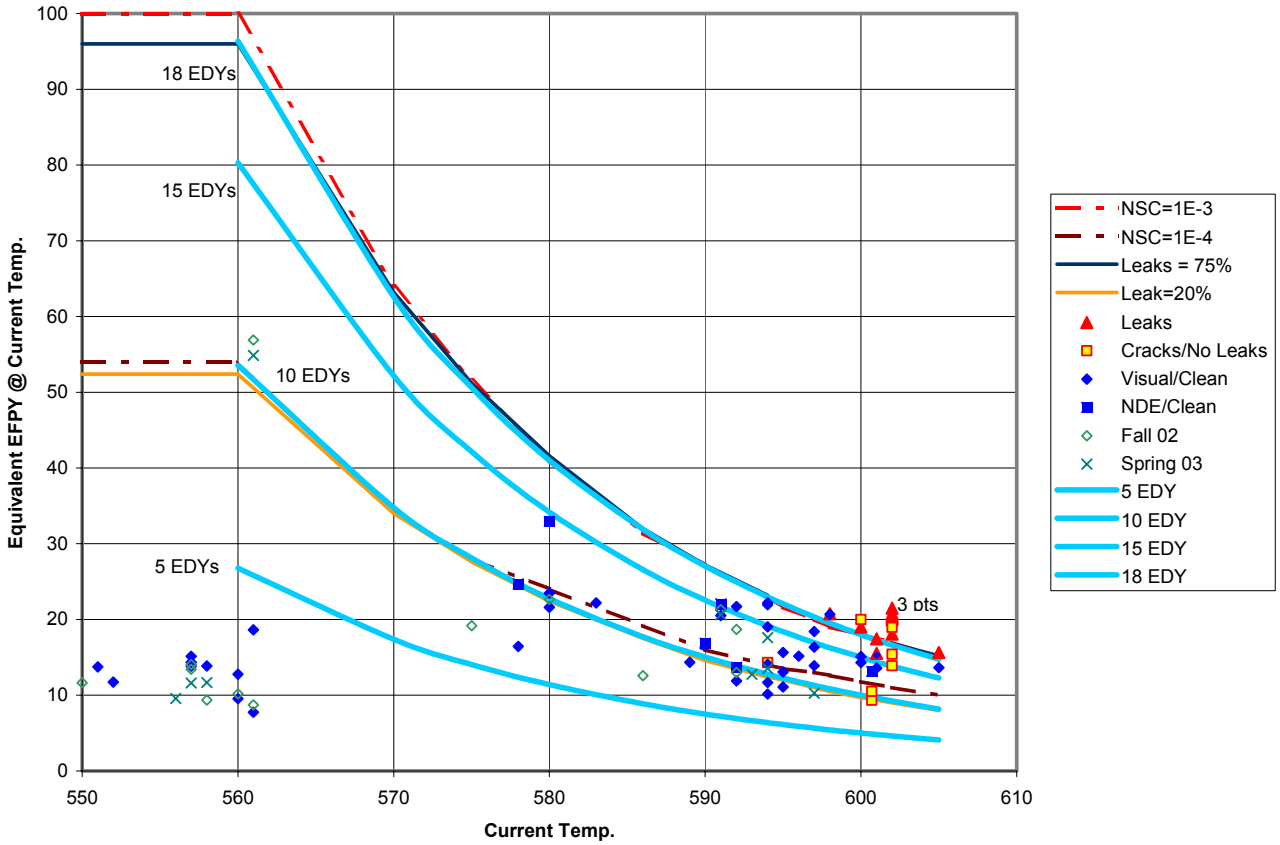

Figure A-5
Correspondence of Time-Temperature Regimes Based on PFM Results to Effective Degradation Years

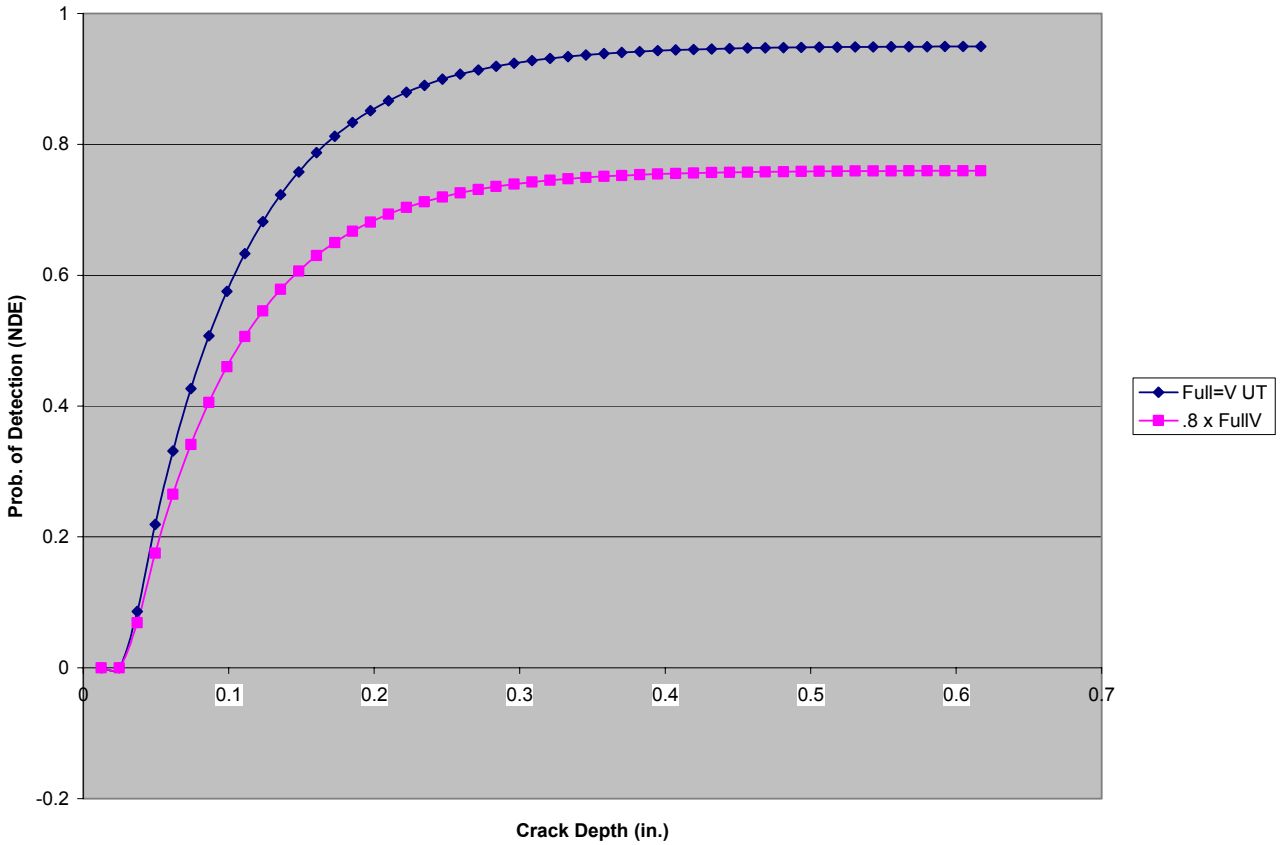

Figure A-6
Probability of Detection Curves for Non-Destructive Examination

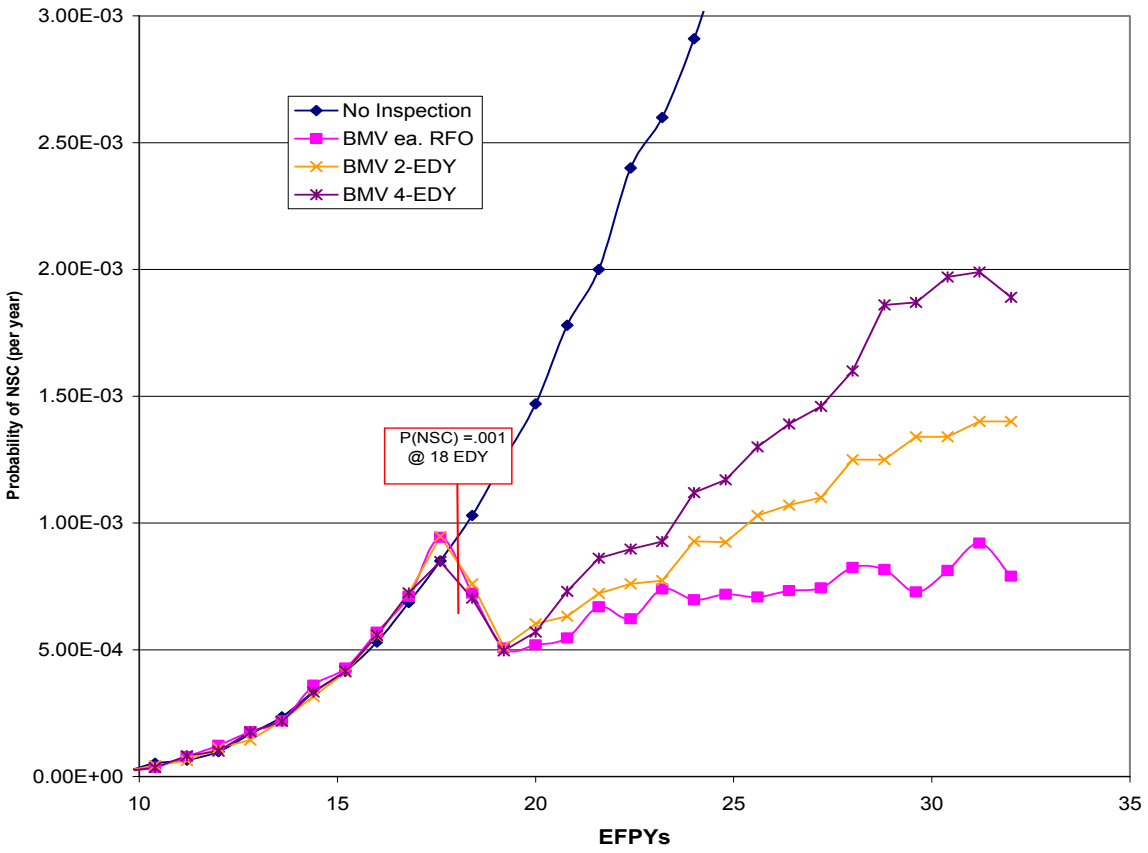

Figure A-7
Effect of Bare Metal Visual Inspection on Net Section Collapse Probability for Plants in the High Risk Inspection Category (Analysis run at 600°F)

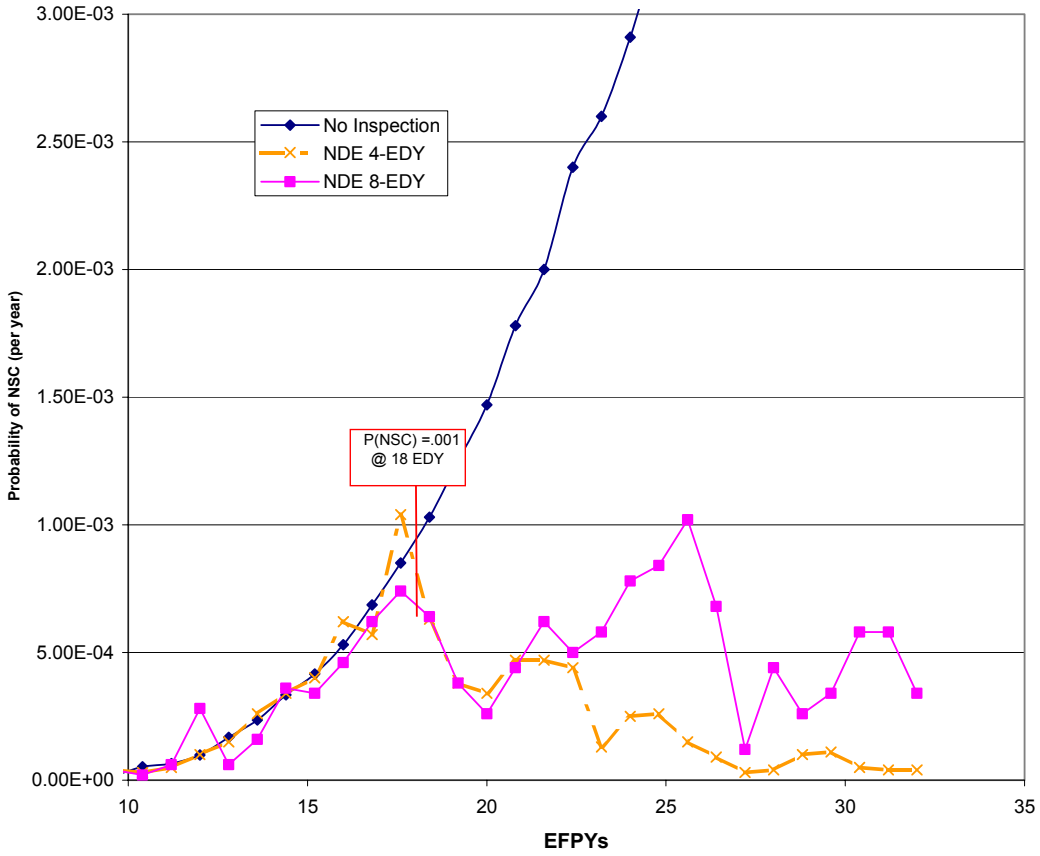

Figure A-8
Effect of Non-Destructive Examination on Net Section Collapse Probability for Plants in the High Risk Inspection Category (Analysis run at 600°F)

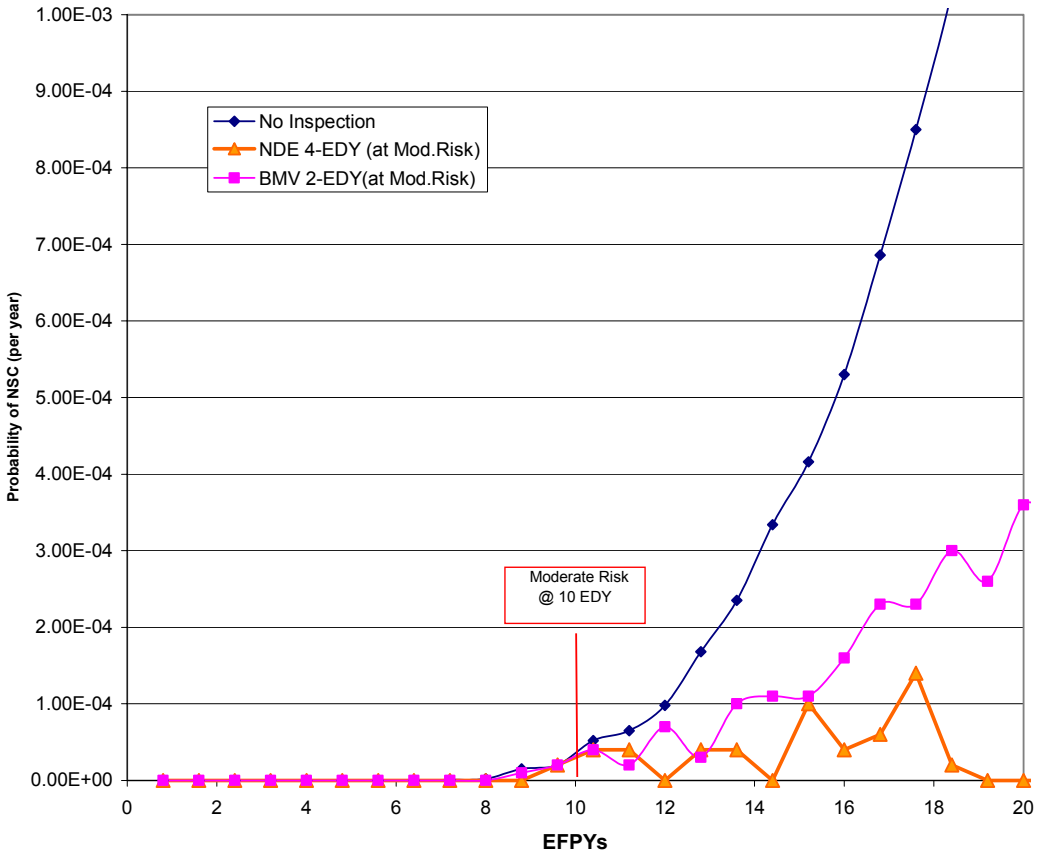

Figure A-9
Effect of Recommended Inspections on Net Section Collapse Probability for Plants in the Moderate Risk Inspection Category (Analysis run at 600°F)

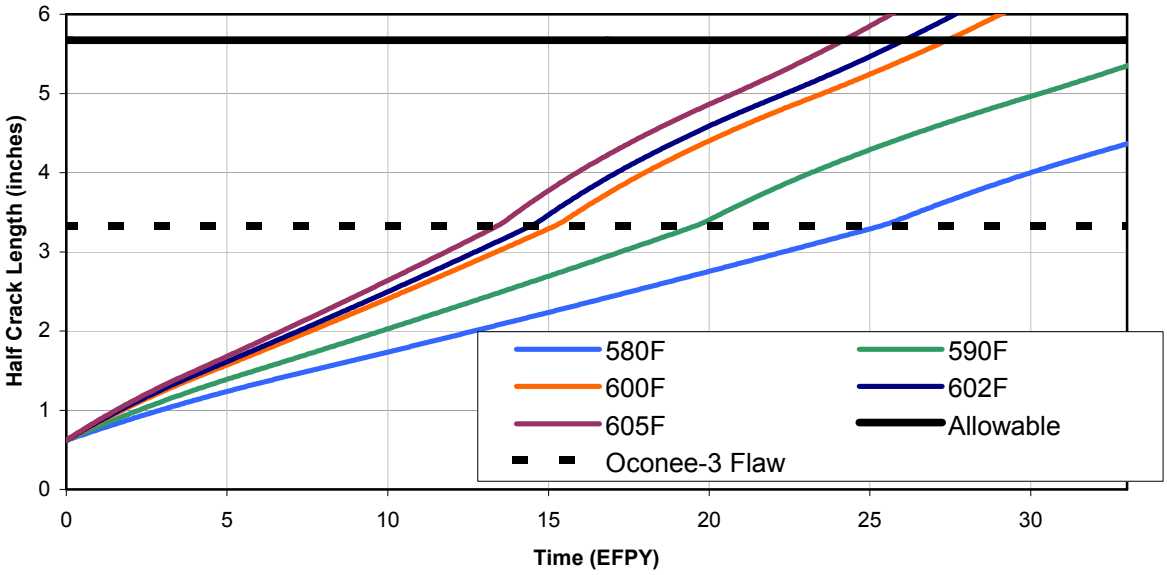

Figure A-10
Results of Deterministic Crack Growth Evaluation for B&W-Type Plant

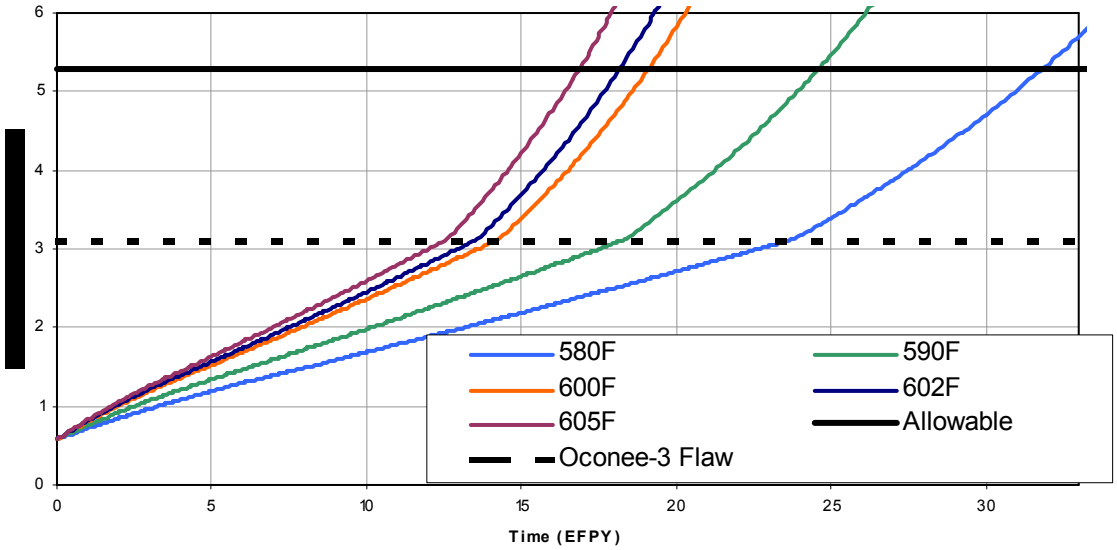

Figure A-11
Results of Deterministic Crack Growth Evaluation for Westinghouse-Type Plant

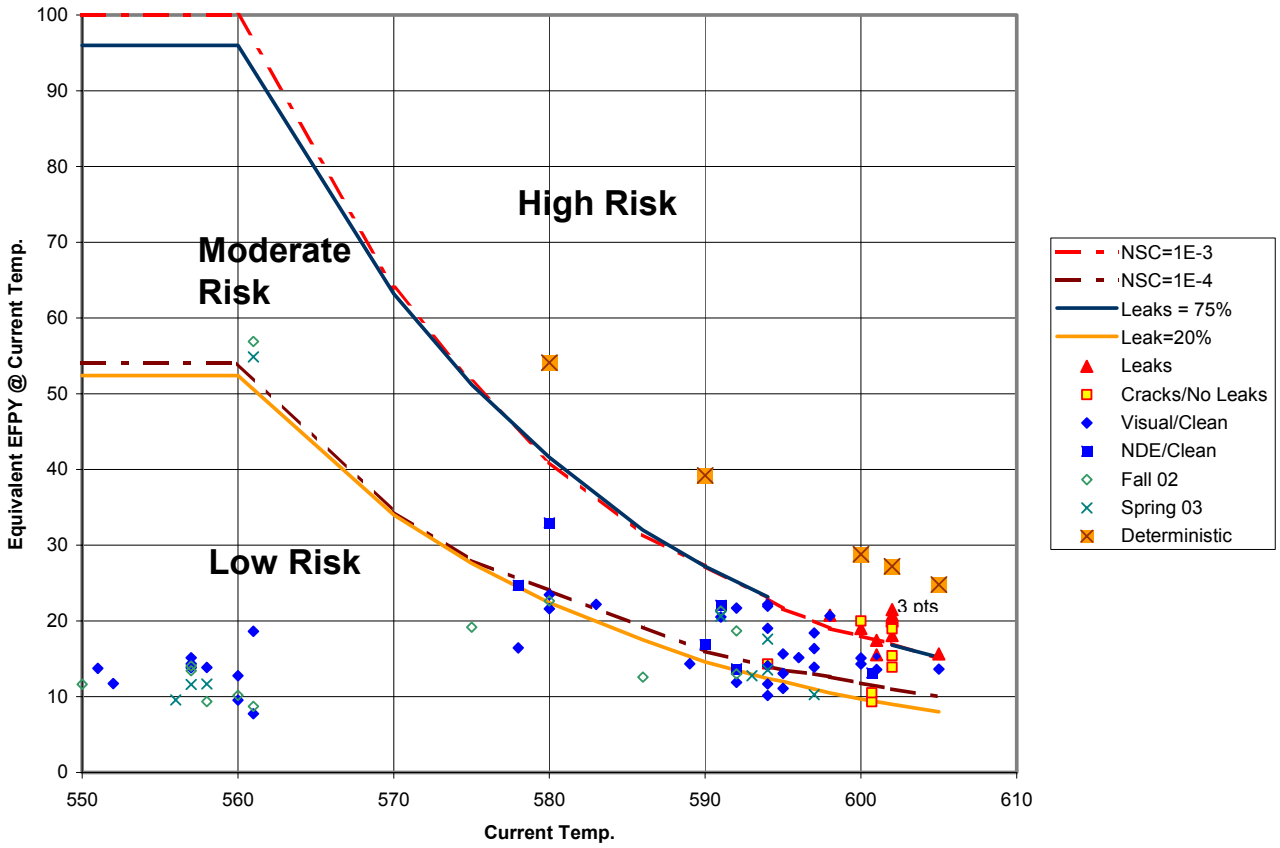

Figure A-12
Deterministic Crack Growth Results for Westinghouse-Type Plant Added to Figure A-4, Illustrating Conservatism of Risk-Based Limits

B
PROBABILITY OF DETECTING LEAKS IN RPV UPPER HEAD NOZZLES BY BARE METAL VISUAL INSPECTION

B.1 Background

Visual inspections of the reactor coolant system pressure boundary have proven an effective method for identifying leakage from PWSCC cracks in Alloy 600 base metal and Alloy 82/182 weld metal. Specifically, visual inspections have detected leaks in reactor pressure vessel (RPV) head CRDM nozzles, RPV head thermocouple nozzles, pressurizer heater sleeves, pressurizer instrument nozzles, hot leg instrument nozzles, steam generator drain lines, an RPV hot leg nozzle weld, a pressurizer PORV safe end, and a pressurizer manway diaphragm plate.

Visual inspections are an important element of Alloy 600 inspection programs since they have been proven effective, are cost effective, and, depending upon conditions as outlined below, are capable of detecting very small leaks.

The purpose of this document is to demonstrate that a bare-metal visual inspections of reactor vessel top head surfaces will result in a high probability of leak detection (POD) provided that there is visual access to the locations where the nozzles penetrate the vessel top head surface, and the access is not hindered by pre-existing boric acid deposits.

B.2 Probability of Detecting Leaks by Bare Metal Visual Inspection

An estimate of the probability of leak detection (POD) by visual means can be developed based on recent field experience, the calculated annulus gap under operating conditions, tribology considerations, and experience with leaks for nozzles that are roll-expanded into the pressure vessel shell. The estimated POD will continue to be refined as the results of visual inspections are correlated with increasing numbers of non-visual (non-destructive) examinations.

1. Field Experience

   - Through May 2002, thirty-two CRDM nozzles at eight plants (ANO-1, Crystal River 3, North Anna 2, Oconee 1-3, Surry 1 and TMI-1) have been found to have leaks based on visual inspections.

   - Non-visual NDE inspections have been performed on 578 CRDM and CEDM nozzles at sixteen plants. The sixteen plants consist of the eight plants with visually detected leaks plus eight other plants (ANO-2, Cook 2, Davis-Besse, Ginna, Millstone 2, North

Anna 1, Palo Verde 2, and SONGS 2). The non-visual NDE inspections were performed for the following reasons:

- 62 nozzles (11%) were inspected to confirm the visually identified leak path or to assess locations where visual inspections were masked.
- 80 nozzles (14%) were inspected to assess the extent of condition in plants where leaking nozzles were discovered.
- 367 nozzles (63%) were inspected at plants where bare metal visual inspections were not possible.
- 69 nozzles (12%) were inspected based on a regulatory commitment even though a visual inspection would have been possible.

- The 578 non-visual inspections identified three leaking nozzles in addition to the 32 discovered by visual means. However, these three additional leaking nozzles were at Davis-Besse where it is considered that they would have been discovered by the type of bare metal visual inspections performed subsequent to discovery of a leak at Oconee 1 in 1999.

- In summary, all 35 leaking nozzles to date in domestic PWR plants have been, or would have been, discovered by top head bare metal visual inspections using industry guidance developed subsequent to discovering the first leak at Oconee 1. No leaking nozzles have been discovered by non-visual examinations, except for the three nozzles at Davis-Besse that would have been detected visually.

- A case can be made that visual inspections may have missed some leaking nozzles. Two situations warrant discussion:

- It is likely that some of the leaking nozzles had been leaking for several years and that the leakage was missed during prior visual inspections. However, industry guidance developed over the past year with regard to the size of leaks to be anticipated, evidence of leakage, the need for clean heads, etc. is considered to have improved the bare metal visual inspections to the level that these leaks would be detected at the first evidence of leakage.
- It is reported that the Bugey 3 nozzle leaked during hydrostatic testing with no evidence of boric acid deposits on the vessel top head surface. However, inquiries by the MRP have failed to establish the level of visual inspections that had been performed, or the condition of the vessel top head surface, prior to the leak being identified during the hydrostatic testing. The case of Bugey 3 also illustrates that there must be some crack extension above the J-groove weld for there to be visually detectable leakage. At Bugey 3 the through-wall portion of the crack only extended 2 mm (0.08 inch) above the top of the J-groove weld.

2. Annulus Gap Opening

- The eight plants with visually identified leaks (not including Davis-Besse) had maximum specified interference fits ranging from 0.0012" to 0.0015". The actual interference fit was measured during fabrication for several of the plants with identified leaks. Leaks have been visually identified in three nozzles with 0.0014" interference at Oconee 2.

- Leaks at Davis-Besse nozzles 2 and 3 were originally identified by non-destructive examinations from under the vessel head but it is considered that both of these leaks would clearly have been identified by a bare metal visual inspection of a previously cleaned head. Davis-Besse nozzles 3 and 2 are reported to have had 0.0015" and 0.002" interference respectively.

- Many plants have specified interference fits greater than the 0.002" for which leakage has been visually confirmed. Forty plants have specified maximum interference fits of 0.003", two plants have specified maximum fits of 0.0035", and three plants have specified maximum fits of 0.004".

- Finite element gap displacement calculations have been performed for several plants with specified interference fits ranging from 0.0015 – 0.003". These analyses have demonstrated a leak path through the annulus region. In some cases the analyses have included the fact that a leak into the annulus region results in application of pressure on the outside of the nozzle and the inside of the hole in the vessel head. This change in boundary conditions from the as-designed configuration increases the pressure dilation of the vessel head (pressure applied to a larger diameter than the inside of the nozzle) and eliminates the pressure deflection of the nozzle. The net effect of the leak is therefore to increase the gap opening.

- Figure B-1 shows the specified interference fits relative to the vessel head radius to thickness ratio (R/T), and the status of cases analyzed and confirmed leakage. These results show that calculations have demonstrated a leak path for nozzles with up to 0.003" specified maximum interference fit with the smallest R/T ratios. Heads with small R/T ratios will have smaller gap opening displacement than heads with large R/T ratios since they will have lower membrane stresses in the head and less pressure dilation of the vessel shell.

- With the exception of Cook 2 which has already performed non-visual NDE of all nozzles, the plants with 0.0035" and 0.004" specified maximum interference fit all have relatively low predicted PWSCC susceptibility based on time and temperature.

- Finally, it should be noted that the actual interference fits for most nozzles will be less than the maximum specified for two reasons. First, there is likely to be a statistical distribution of fits within the specified range. Second, from a manufacturing assembly standpoint, it is desirable to avoid large interference fits since large interference fits increase the potential that a nozzle will become stuck in the head at the wrong elevation during installation. It has been confirmed for plants where the nozzle and hole dimensions have been recorded that the actual interference for most nozzles is significantly less than the maximum specified.

3. Flow Passages for Cases With Predicted Interference Fit

   - Even for cases where there is a nominal interference fit between the CRDM nozzle and hole in the vessel head under operating conditions, the actual area of metal-to-metal contact is quite small. *Friction and Wear of Materials* (Rabinowicz, John Wiley & Sons, 1995), gives the actual contact area between two adjacent metal surfaces as the applied load divided by three times the material yield strength. For a typical CRDM nozzle with 0.003" of interference and a yield strength of 50 ksi, the actual metal-to-metal contact area is about 5% of the interface surface area. The remaining approximately 95% of the surface area has small flow passages with an RMS height equal to the sum of the RMS surface roughness of the mating parts, or about 60-90 $x10^{-6}$ inches (0.00006-0.00009").

   - Other manufacturing considerations such as straightness and out-of-roundness tolerances, etc. will result in actual flow passage sizes being greater than the minimum sizes based on surface roughness considerations.

4. Roll Expansion Experience

   - Finally, there have been several cases where leaks have occurred from Alloy 600 penetrations despite the penetrations having been roll expanded into the hole in the pressure vessel. Two cases documented in EPRI TR-103696, *PWSCC of Alloy 600 Materials in PWR Primary System Penetrations*, are steam generator drain pipes at Shearon Harris in 1988 and pressurizer instrument nozzles at Nogent 1 and Cattenom 2 in 1989.

Based on the above, the probability of visual detection for bare-metal visual inspections which are not compromised by pre-existing boric acid on the vessel head is expected to be high.

For probabilistic analyses, it has been conservatively assumed that leaks will not be detected from any nozzle with greater than a 0.002" interference for which leakage has been confirmed at an operating plant. Based on a normal distribution of fits with the maximum and minimum specified values representing 2σ upper and lower bounds, 75% of the nozzles with a specified interference range of 0.000" to 0.003" will have an interference less than 0.002". The probability of detection assumed for probabilistic fracture mechanics analyses was conservatively taken as 0.6.

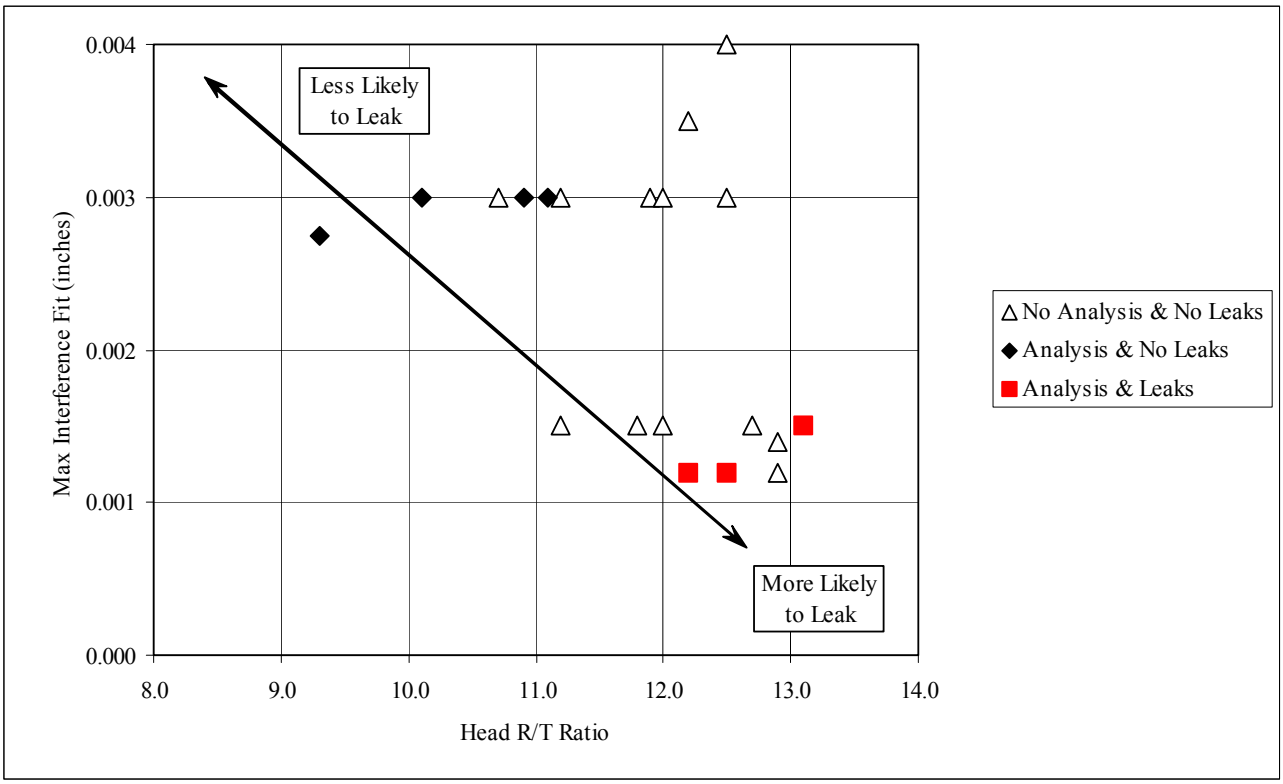

Figure B-1
Reactor Vessel Head Designs for Which Leak Path Has Been Confirmed

C
SUPPLEMENTAL VISUAL INSPECTIONS TO ENSURE RPV CLOSURE HEAD STRUCTURAL INTEGRITY

C.1 Background

The MRP Inspection Plan for RPV head nozzles and closure heads provides inspection criteria for three categories of plants based on the effective degradation years (EDY) at 600°F, which is a function of plant operating time and operating vessel head temperature. The main inspection requirements are as follows:

- For High Susceptibility Plants (≥18 EDY), which have long operating times and high head temperatures, the inspection plan requires a baseline non-visual examination (NDE) and repeat non-visual examinations at periodic intervals or bare metal visual inspections every outage. If a program of non-visual examination is chosen instead of bare metal visual inspections, then Supplemental Visual inspections are required to be performed at each refueling outage that a non-visual examination is not performed.

- For Moderate Susceptibility Plants (10 EDY ≤ x < 18 EDY), which have intermediate operating times and/or lower head temperatures, the inspection plan requires bare metal visual inspections or non-visual examinations at specified intervals. The reinspection intervals are a function of the vessel head temperature. For plants operating at 600°F the bare metal visual reinspection interval is every 2 EFPY and the non-visual examination is every 4 EFPY. Reinspection intervals are longer for lower temperature plants. In addition, for all refueling outages when no bare metal or non-visual examination is performed, then a Supplemental Visual inspection is to be performed.

- For Low Susceptibility Plants (<10 EDY), which have short operating times and/or low head temperatures, the bare metal or non-visual examinations are specified at intervals of 10 EFPY. For periods where no bare metal visual or non-destructive examinations are performed, a Supplemental Visual inspection shall be performed every other outage.

C.2 Purpose

The purpose of this document is to confirm that the specified Supplemental Visual (SV) inspections in the MRP Inspection Plan will ensure that ASME Boiler & Pressure Vessel Code margins for structural integrity of the RPV closure head are maintained. Specifically, this technical assessment confirms that the SV inspections will detect CRDM nozzle leakage before that leakage could lead to low-alloy steel wastage having a volume such that the primary membrane and primary membrane plus bending stresses exceed the code allowable values.

Both deterministic and probabilistic approaches are taken to evaluate the single-cycle SV inspection interval for high and moderate susceptibility plants. A description of the probabilistic wastage model is included as Appendix D, and the stress calculation used to determine the allowable wastage volume to maintain stresses below the code allowables is presented in Appendix E. The specified interval for low susceptibility plants is appropriate given the lack of cracking and leakage identified in low susceptibility plants and their relatively low predicted probability of leakage [C-1].

C.3 Volume of Boric Acid Deposits Detectable by SV Inspection

The Inspection Plan describes two levels of visual inspection.

A *Bare Metal Visual* (BMV) inspection requires that the entire circumference of each RPV head penetration can be viewed such that very small amounts of leakage (e.g., 0.5 in^3 of deposits) can be located, even if at isolated spots around the nozzle.

A *Supplemental Visual* (SV) inspection is intended to locate greater, but still relatively small, amounts of leakage. *Supplemental Visual* inspections can be performed for plants with and without closely conforming rigid insulation. The inspection plan specifies that:

- For cases where the top surface of the vessel head is visible, the Supplemental Visual inspection should be able to locate deposits from leakage that cover an area greater than 4" diameter with a thickness great enough that the condition of the underlying metal surface cannot be determined.

- For cases where the top surface of the vessel head is covered by closely conforming rigid insulation, 1) the entire periphery and outer surface of the permanently installed insulation (including joints between insulation segments, and annular gaps between the insulation and RPV head penetrations) and exposed portions of RPV head and flange must be visible, and 2) the visual inspection must be capable of finding any evidence of RCS leakage such as flow emanating from beneath the insulation, bulging insulation, or boric acid accumulation emerging upward through the joints and gaps between adjoining insulation panels from the RV head surface.

The limiting condition will be for the case of the head with closely conforming rigid insulation. For this technical evaluation, it is assumed that the SV inspections performed at a particular plant are capable of detecting a volume of 500 in^3 of boric acid deposits produced by a leaking CRDM nozzle, either by direct observation or through bulging or displacement of closely conforming insulation. Given the density of solid boric acid crystals of 1.44 g/cm^3, the mass of boric acid deposits corresponding to this volume is 26 pounds, in comparison to the 900 pounds of deposits reported to be located on top of the head at Davis-Besse in 2002 [C-2]. For illustrative purposes the 500 in^3 volume roughly corresponds to a ½-inch thick layer covering 10% of the vessel head surface in the area of the CRDM nozzles. If concentrated at one point, the 500 in^3 volume would result in a sphere of boric acid about 10 inches in diameter. For the probabilistic calculations, the detection limit is assumed to follow a triangular distribution with a lower bound of 250 in^3 and an upper bound of 1000 in^3. Note that for heads that have closely conforming insulation that

is directly in contact with the top head surface, the insulation will prevent any of the released boric acid crystals from escaping to a remote area of the containment building.

C.4 Volume of Boric Acid Deposits versus Leak Rate

Based on a simple mass balance, Figure C-1 shows the volume of boric acid deposits produced as a function of leak rate over the typical 1.5 years for one operating cycle. In this figure an effective average boron concentration in the primary coolant of 750 ppm is assumed. This concentration is a conservatively low value for the actual average over an operating cycle. Note also that Figure C-1 conservatively assumes no porosity for the accumulated boric acid deposits.

Also shown on this figure is the volume of boric acid deposits produced through leakage that is assumed to be detectable by an SV inspection of the vessel head during a refueling outage. The boron mass balance calculation shows that an SV inspection capable of detecting 500 in^3 of released deposits will detect a leak rate of about 0.001 gpm over a period of 1.5 years. Note that the probabilistic evaluation presented below specifically considers the change in boron concentration over the fuel cycle.

C.5 Leak Rate to Produce Rapid Corrosion

The main conclusion of an analytical assessment of the Davis-Besse degradation performed by the MRP [C-3] is that local cooling to temperatures approaching the boiling point of water at atmospheric pressure (212°F) is a necessary condition for the rapid corrosion rates and large wastage volume observed at Davis-Besse to occur. Large local cooling creates the conditions for rapid corrosion by allowing aerated, concentrated boric acid solution to pool on the top head surface. Calculations have also shown that an aggressive chemical environment (e.g., low pH) is more likely to occur for solution temperatures approaching 212°F [C-3]. As discussed in Appendix D, the extent of local cooling is primarily a function of the leak rate. The leak rate is also the main driver for any erosion or flow accelerated corrosion mechanisms—to the extent that they may supplement the boric acid wastage—because the leak rate is the main factor that determines the magnitude of the flow velocities along the leak path.

There are three potential sources of information that are available for determining the minimum, or critical, leak rate that may lead to rapid corrosion. These are (1) the results of two sets of boric acid corrosion tests for leakage into an annulus, (2) the plant experience including Davis-Besse and leaking CRDM nozzles at other plants that produced little or no wastage, and (3) the results of a thermal analysis performed by the MRP and described in Appendix D. Unfortunately, several limitations in the two experiments (Test Series M and EPRI-6 in the EPRI *Boric Acid Corrosion Guidebook* [C-4]) make application of the experimental data very difficult. Such limitations for one or both of the tests include a limited range of tested leak rates, lack of control and measurement of the thermal-hydraulic and chemical environments along the leak path, limited test length, lack of data on time dependence of corrosion rate, size of initial annulus gap, and nozzle orientation (down versus up for CRDM nozzles). After evaluation of all the available information for these two tests, it was decided to base the determination of the critical

leak rate that leads to rapid corrosion on the MRP thermal analysis, with the plant experience as a consistency check.

As described in Appendix D, the thermal analysis is based on an enthalpy balance for the leakage flow in combination with a three-dimensional finite element model of an RPV head. This calculation shows that a leak rate of roughly 0.1 gpm is required to permit pooling of concentrated boric acid solution on the head top surface. This value is consistent with the Davis-Besse root cause report [C-2], which indicates that the leak rate through nozzle #3 at the time of the adjacent rapid corrosion was likely in the range of 0.04 to 0.2 gpm. On the other hand, little (i.e., less than 1 in^3) or no wastage has been reported for the over 30 leaking CRDM nozzles at US plants other than Davis-Besse, despite the direct inspection of the lower section of the annulus made possible by the repair process used for many of these nozzles. This experience is also consistent with the 0.1 gpm value for the critical leak rate since the volume of boric acid deposits associated with all the leaking CRDM nozzles other than those at Davis-Besse indicates leak rates much lower than 0.1 gpm, typically on the order of 1 gallon per year or 2×10^{-6} gpm.

Therefore, a leak rate of 0.1 gpm is used in the deterministic calculation as the critical leak rate that produces rapid corrosion. The deterministic evaluation presented below is based on the time for the leak rate to increase from that which is detectable by an SV inspection to the critical value of 0.1 gpm. The probabilistic calculation uses 0.1 gpm for the nominal critical leak rate, but also uses a corresponding lower bound of 0.02 gpm to account for uncertainties in the thermal analysis as well as those related to the role of molten boric acid, which may retain some moisture even at atmospheric pressure and temperatures significantly higher than 212°F (e.g., 450°F).

C.6 Supplemental Visual Inspection Interval Based on Davis-Besse Operating Experience

Despite uncertainties in the exact progression of the Davis-Besse leak rate and wastage volume over recent operating cycles, it is instructive to examine the Davis-Besse nozzle #3 experience in greater detail. First, it should be noted that Davis-Besse has the highest reported head temperature of any PWR plant in the United States (605°F). In addition, the original Davis-Besse head has several nozzles that have demonstrated the greatest potential for cracking of any heat of CRDM nozzle material in the United States based on inspections performed to date.

The evidence indicating the likely progression for the leak through Davis-Besse CRDM nozzle #3 and the associated large corrosion cavity is summarized in Figure 26 of the Davis-Besse root cause report [C-2], *Timeline of Key Events Related to Reactor Vessel Head Boric Acid Corrosion*. This figure shows that after cleaning the vessel head in 1994, the first evidence of leakage on the head was reported at 10RFO in 1996. This leakage was such that it blocked visual inspection of four of the 69 nozzles, including nozzle #3. A calculation of the volume of the space between the horizontal insulation (minimum 2-inch gap at the center of the head) and the head in the region of the four center nozzles indicates that the deposits accumulated in 1996 would likely have exceeded 500 in^3, the volume assumed to be detectable by an SV inspection at all plants including those having closely conforming insulation.

The timeline figure from the root cause report [C-2] documents several indications that it took more than 2 years of operation after the 1996 refueling outage for the leak rate to increase to the 0.1 gpm considered necessary for rapid corrosion of relatively large areas of the head. These indications include the progression of the unidentified primary system leakage rate, video evidence of the increase in the size of the pile of boric acid deposits on the head surface, clogging of the containment air coolers, and plugging of the containment radiation monitor filters.

On this basis, a Supplemental Visual inspection at 1.5–2.0 year intervals would have detected the leakage at least 4 years prior to the relatively large volume of wastage being discovered at 13RFO in 2002, assuming a hypothetical timing of refueling outages such that the boric acid accumulation was just missed in 1996. The presence of red-colored boric acid deposits on the vessel flange at 11RFO in 1998 was another indicator that the situation warranted evaluation because a red or orange color for boric acid deposits indicates the presence of iron corrosion products, whereas boric acid deposits that do not incorporate corrosion products are white in appearance. While the significance of these indications was missed at Davis-Besse, it is highly unlikely that their significance will be improperly interpreted in the future by any plant. Plants with lower head temperatures than Davis-Besse would tend to require more time to reach equivalent conditions due to lower crack growth rates.

C.7 Deterministic Evaluation: Supplemental Visual Inspection Interval Based on Crack Growth Rate

The deterministic evaluation is based on the time for the leak rate to increase from the level that is detectable over a single cycle (0.001 gpm) to the estimated leak rate that is necessary for rapid corrosion (0.1 gpm). Based on plant experience and leakage modeling work, the primary driver for the increase in leak rate is the length of the nozzle crack above the top of the J-groove weld.

The left side of Figure C-2 illustrates the fundamental industry experience with leakage through CRDM nozzles. Inspections of nozzles with reported small amounts of leakage (order of 1 gallon per year or 2×10^{-6} gpm) have shown that the lengths of deep axial cracks in these nozzles tend to be in the range of 0.25 to 0.6 inches above the top of the J-groove weld. There is no report of any of these leaks resulting in significant corrosion (i.e, greater than 1 in^3)[1]. On the other hand, the crack at Davis-Besse opposite the large wastage cavity extended 1.3 inches above the top of the weld. This crack produced a best-estimate leak rate of 0.15 gpm based on the Davis-Besse root cause report [C-2].

The results of the leakage modeling work are presented in Figure C-3, which shows the predicted leak rate as a function of the crack length above the top of the weld. This figure was originally published in the Davis-Besse root cause report [C-2], and this work was extended to show that

[1] There have been reports of relatively small amounts of wastage (likely much less than 1 in^3) adjacent to two leaking CRDM nozzles at plants other than Davis-Besse. The repair process for one leaking nozzle indicated a small cavity in the low-alloy steel material at the bottom of the annulus that was approximately 3/16" deep [C-6]. Visual inspection of the head top surface adjacent to another leaking nozzle indicated small areas of corrosion on the head top surface. These two cases of wastage were clearly insignificant in terms of the structural integrity of the head.

the effect of the flow resistance of the annulus is small after the initially tight annulus opens slightly (e.g., by a few thousandths of an inch) in work presented to the NRC staff on May 22, 2002 [C-3]. Pages 17 and 18 of the root cause report [C-2] describe the methodologies used, including (1) either an analytical model for a through-wall axial crack in a pipe (Zahoor) or a custom finite element analysis for calculation of the crack opening displacement (COD) in a CRDM nozzle with welding residual stresses and (2) the methodology for predicting leak rate as a function of COD and crack opening area (COA), which was developed by Laborelec for leaks through PWSCC cracks in steam generator tubes[2]. However, these models do not predict the low leak rates observed for cracks extending on the order of 0.5 inches above the top of the weld. This may at least partially be due to the actual through-wall crack profile, for which data are not readily available except for Davis-Besse. A highly uneven through-wall profile would tend to decrease the flow area through the crack compared to the case of an even through-wall profile having the same extent above the weld by reducing both the COD and the crack length on the nozzle ID. Another factor not well captured by the leakage models is the initially tight, three-dimensional intergranular crack structure and its potential clogging by particulates in the primary coolant or boric acid deposits.

Given the above difficulties in directly applying the leakage models, the empirical leak rate curve shown in Figure C-4 was developed to predict the leak rate as a function of axial crack extent above the top of the weld. The power-law shape of the curve was chosen based on the shape of the curves in Figure C-3. Figure C-4 predicts that about 0.41 inches of crack growth would be required for the leak rate to increase from the rate that produces detectable leakage over one 18-month operating cycle (0.001 gpm) to the rate that may produce rapid top-down corrosion, the critical leak rate (0.1 gpm). Note that the unavailable profiles for the cracks that extended about 0.5 inches above the top of the weld, but produced low leakage, are a potential source of conservatism for the evaluation because the distance traveled by the crack front averaged across the nozzle wall is greater for the case of the initially uneven crack front.

The final step in the deterministic evaluation is to calculate the time for the crack to grow the 0.41 inches in the axial direction cited above. For this purpose, the standard methodology that assumes that the crack growth rate follows a power-law dependence to the stress intensity factor is assumed [C-5]. In addition, a uniform through-wall crack profile is assumed as shown on the right side of Figure C-2. Calculations have shown that the stress intensity factor for such cracks growing axially above the top of the J-groove weld is in the range of 40–70 ksi√in for crack lengths of 0.5 to 1.3 inches above the top of the weld. Figure C-5 shows that, for a conservative average stress intensity factor of 65 MPa√m (59.2 ksi√in) and the deterministic MRP crack growth rate curve developed in report MRP-55 [C-5] for cracks in contact with the nozzle annulus environment, it would take about 1.7 EFPYs at a head temperature of 602°F[3] for a crack to grow the 0.41 inches cited above. Therefore, the deterministic evaluation shows that the SV inspection interval is sufficient to prevent the rapid top-down corrosion mode from occurring in high and moderate susceptibility plants having fuel cycles lasting less than 1.7 EFPYs. For

[2] For reference, the Laborelec methodology [C-10] predicts a leak rate of about 0.054 gpm for an axial crack having a length of 1.0 inch and an average crack opening displacement (crack width) of 0.001 inches

[3] The highest head temperature for all plants is 602°F except for Davis-Besse (605°F), where the head is being replaced.

plants that operate with two-year fuel cycles (approaching 2.0 EFPYs), the potential 0.3 EFPY of operation with rapid corrosion will not exhaust the ASME Code stress margins as is apparent considering an upper bound corrosion rate of 5 in/yr based on the available test data for aerated, concentrated boric acid solutions [C-4] and the approximate 150 in^3 volume of allowable wastage calculated in Appendix E. The time to reach the critical leak rate for a head temperature of 595°F is about 2.0 EFPYs. At lower head temperatures typical of low susceptibility plants, the time would be longer.

It should be noted that the preceding evaluation considers the leak rate that results from leak-path cracks in the Alloy 600 base metal material. Leaks can also result from cracks in the Alloy 182 weld metal material. Such cracks can potentially have either a radial-axial or a circumferential orientation. Radial-axial weld cracks are expected to result in relatively small leak rates based on the small flow area at the intersection between the weld material and the bottom of the annulus. Such small leak rates are expected to be insufficient to cause the local cooling that is required to produce rapid corrosion. Circumferential weld cracks cannot be ruled out since highly branched flaws confined to the weld metal have been identified as the source of leakage for two CRDM penetrations at one plant. However, these cracks and resultant leaks resulted in no reported low-alloy steel wastage. The probabilistic evaluation presented below—through its large tolerance bands for many of the input parameters such as the crack growth rate power-law constant *A*—is considered to addresses the possibility of leaks from circumferential weld cracks.

C.8 Probabilistic Evaluation: Supplemental Visual Inspection Interval Based on Monte Carlo Wastage Model

The probabilistic wastage model takes the same basic form as the deterministic model—leak rate increase driven by axial crack growth in the nozzle until cooling is sufficient to cause rapid corrosion—but allows the key inputs to take on distributions of values. The flowchart in Figure C-6 shows the basic approach of the probabilistic model, and Appendix D provides a further description of the model. The probabilistic wastage model explicitly calculates the volume of wastage as the leak rate increases from zero to values greater than the critical leak rate and also the volume of boric acid deposits produced over time.

The wastage cavity progression assumed in the model is based on the Davis-Besse experience [C-2] in combination with the analytical results that show the potential for aerated, concentrated boric acid solutions to pool on the head top surface at relatively high leak rates (Appendix D). Figure C-7 shows the assumed progression through three stages of growth:

- Stage 1: Radial growth of the annulus
- Stage 2: Top-down growth on head top surface
- Stage 3: Outward growth after the cladding is exposed

The tapered shape of the cavity at the head top surface is strong evidence that the top-down mode dominated most of the material loss at Davis-Besse. As the top-down corrosion mode initiated, the wastage cavity became large enough to hold the boiling effluent, and subsequently the edges of the liquid pool receded back toward the leaking nozzle as the cavity grew down, the

result being the tapered appearance at the edges of the top of the cavity. The horizontal striations for the large Davis-Besse wastage cavity shown in Figure C-8 are further evidence of a top-down corrosion progression. Moreover, the closure head wastage experience at Turkey Point in 1986 [C-4, C-6] and Beznau in 1970 [C-6] demonstrate the top-down corrosion mode that can occur when concentrated boric acid solution pools on the top head surface. Unlike at these two plants, the Davis-Besse corrosion, which resulted from nozzle leakage rather than leakage from mechanical joints located above the head, was allowed to continue until the cladding was uncovered.[4]

The corrosion rate at which the cavity grows, on the active portion of the annulus area for Stage 1 growth or on an assumed area of the head top surface for Stage 2 growth, was developed using the model shown in Figure C-9. This figure shows the nominal dependence of the wastage rate in inches per year as a function of leak rate. Note the assumed upper shelf behavior for leak rates greater than the critical value. The exponential behavior in wastage rate shown in the figure was assumed based on the premise that the corrosion rate accelerates nonlinearly as the degree of local cooling increases. However, the results of the model are not very sensitive to the form of the assumed curve linking the values for WR_{low} and WR_{crit}. At each time step, the probabilistic model calculates the incremental volume of material corroded using the current wastage rate and the assumed geometry of the growing cavity. Figure C-10 illustrates the assumed cavity geometry and also compares the model geometry progression with that believed to have characterized the large Davis-Besse cavity.

The results of the probabilistic wastage calculation are shown in Figure C-11. This figure shows the cumulative distribution function (CDF) of the cavity size at the time of detection, either through observation of boric acid accumulation during an SV or by the leak rate exceeding the typical technical specification limit of 1.0 gpm for on-line unidentified leakage. For example, there is a 95% probability that the wastage cavity adjacent to a leaking CRDM nozzle will have a volume less than 36 in^3 for a plant operating at 602°F given a program of SV inspections performed every refueling outage at 1.5 EFPY intervals. This compares to the allowable wastage volume to maintain ASME Code margins of about 150 in^3 as shown in Appendix E. The model shows that the probability of the wastage cavity size exceeding the allowable wastage volume of about 150 in^3 is less than 1×10^{-3} for both 1.5 and 2.0 EFPY cycles given a head temperature of 602°F. Therefore, the SV inspection schedule for high and moderate susceptibility plants will ensure that Code margins are maintained with high confidence. Note that the probabilistic wastage model predicts that there is about a 90–95% probability that the wastage cavity would be detected during an SV inspection, as opposed to through the unidentified leak rate exceeding the typical technical specification limit for leakage of 1.0 gpm.

Finally, it should be noted that there are several factors that may tend to make the probabilistic evaluation described above conservative, i.e., predict a greater wastage volume than would actually be expected:

[4] The average leak rate for the Turkey Point 4 incident (0.25 inches maximum corrosion depth) was reported to be less than 0.45 gpm [C-4]. For the reported six months of leakage and assuming a boron concentration of 750 ppm, the required leak rate to produce the reported minimum of 500 pounds of boric acid deposits is 0.053 gpm. The 1–2 m^3 (60,000–120,000 in^3) of boric acid deposits reported for Beznau [C-6] (1.6 inches maximum corrosion depth) indicate a leak rate during the corrosion progression likely greater than 0.1 gpm.

- The probabilistic evaluation is based on a simulation of a single CRDM nozzle that immediately begins to leak. To date, the B&W plants have been seen to lead the US fleet in terms of severity of cracking and leakage [C-1, C-7]. Therefore, the probability of a CRDM nozzle leaking in a non-B&W plant is expected to typically be significantly lower than that for a B&W plant. All B&W plants have adopted a program of bare metal inspections every refueling outage.

- The wastage model does not take credit for the volumetric and bare metal visual inspections that are provided for by the MRP Inspection Plan.

- The simulation uses the typical technical specification limit of 1.0 gpm for triggering of plant shutdown based on on-line leak detection. In practice, it is expected in the future that unidentified leak rates significantly less than 1.0 gpm would trigger corrective action and that clogging of the containment air coolers would also trigger corrective action soon after the leak rate reaches 0.1 gpm [C-6].

C.9 Summary

Deterministic and probabilistic evaluations show that the Supplemental Visual inspections required by the MRP Inspection Plan will ensure that any wastage due to CRDM nozzle leakage will be detected before the applicable ASME Code margins are exhausted. The probabilistic evaluation shows that the probability of the Code allowables for primary membrane and membrane plus bending stresses being exceeded in the head material is less than 1×10^{-3} given a leaking CRDM nozzle and SV inspections performed during each refueling outage. Moreover, the Davis-Besse experience indicates that Supplemental Visual inspections performed every outage with proper follow-up action would have caught the head degradation relatively early in the material loss process.

Work is ongoing to further refine understanding of the wastage process. The statistical inputs to the probabilistic evaluation presented here were designed to capture the process uncertainties to the extent possible at the current time. The MRP and EPRI have proposed specific testing to DOE's Nuclear Energy Plant Optimization (NEPO) program that are designed to address the process uncertainties [C-8].

C.10 References

C-1. *Technical Basis for RPV Upper Head Penetration Inspection Plan*, by Peter C. Riccardella and Nathaniel G. Cofie, September 2002 [Appendix A of this report]

C-2. *Root Cause Analysis Report: Significant Degradation of the Reactor Pressure Vessel Head*, Davis-Besse Nuclear Power Station report CR 2002-0891, April 2002.

C-3. White, G., C. Marks, and S. Hunt. *Technical Assessment of Davis-Besse Degradation,* prepared for meeting with NRC technical staff, May 22, 2002, Rockville, MD.

C-4. *Boric Acid Corrosion Guidebook, Revision 1: Managing Boric Acid Corrosion Issues at PWR Power Stations*, EPRI, Palo Alto, CA: 2001. 1000975.

C-5. *Crack Growth Rates for Evaluating Primary Water Stress Corrosion Cracking (PWSCC) of Thick-Wall Alloy 600 Material (MRP-55),* EPRI, Palo Alto, CA: July 2002.

C-6. *Proceedings: EPRI Boric Acid Corrosion Workshop*, (MRP-75), EPRI, Palo Alto, CA: September 2002, 1007336.

C-7. *Probability of Detecting Leaks in RPV Upper Head Nozzles by Visual Inspections*, by Steve Hunt and Mark Fleming, September 2002.

C-8. *Support of Boric Acid Corrosion Management Program,* NEPO Project ID No. FY03-44 (Proposed for FY 2003 Funding), presented at the NEPO DOE Coordinating Committee Meeting, Charlotte, NC, August 21, 2002 [Appendix B of this report]

C-9. US NRC Website, *Reactor Vessel Head Degradation – Images,* http://www.nrc.gov/reactors/operating/ops-experience/vessel-head-degradation/images.html.

C-10. *PWR Steam Generator Tube Repair Limits: Technical Support Document for Expansion Zone PWSCC in Roll Transitions – Rev. 2*, EPRI, Palo Alto, CA: 1993. NP-6864-L, Rev. 2.

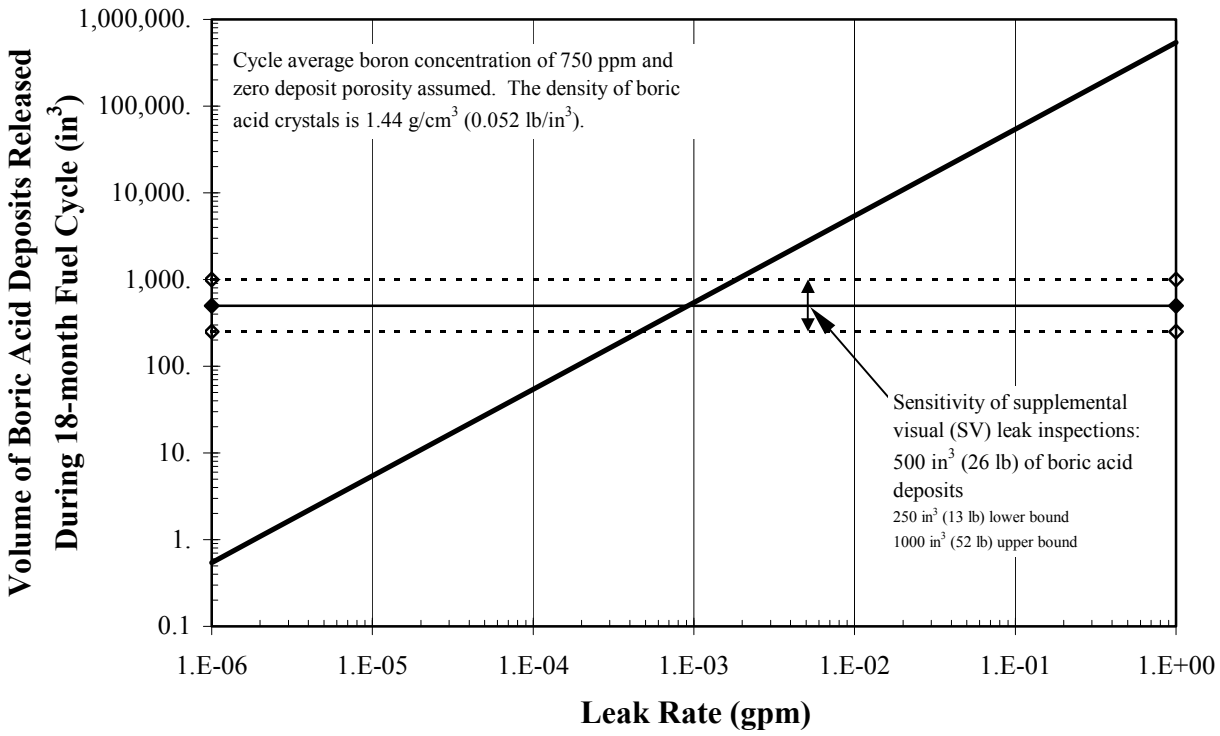

Figure C-1
Leakage Detectability

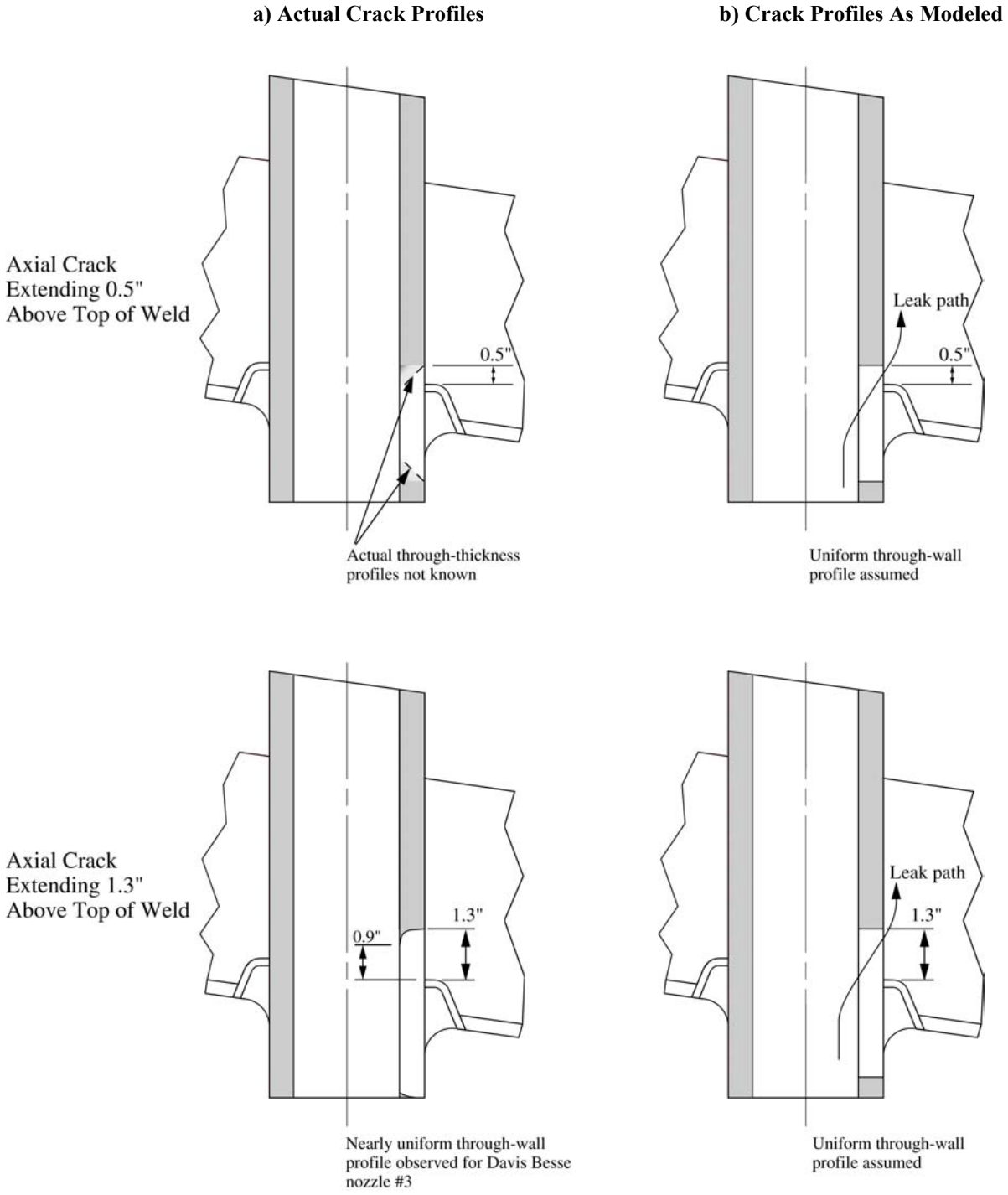

Figure C-2
Through-Wall Axial Crack Profiles: a) Crack geometry based on available plant data; b) Uniform crack profile assumed in leak rate and crack growth modeling

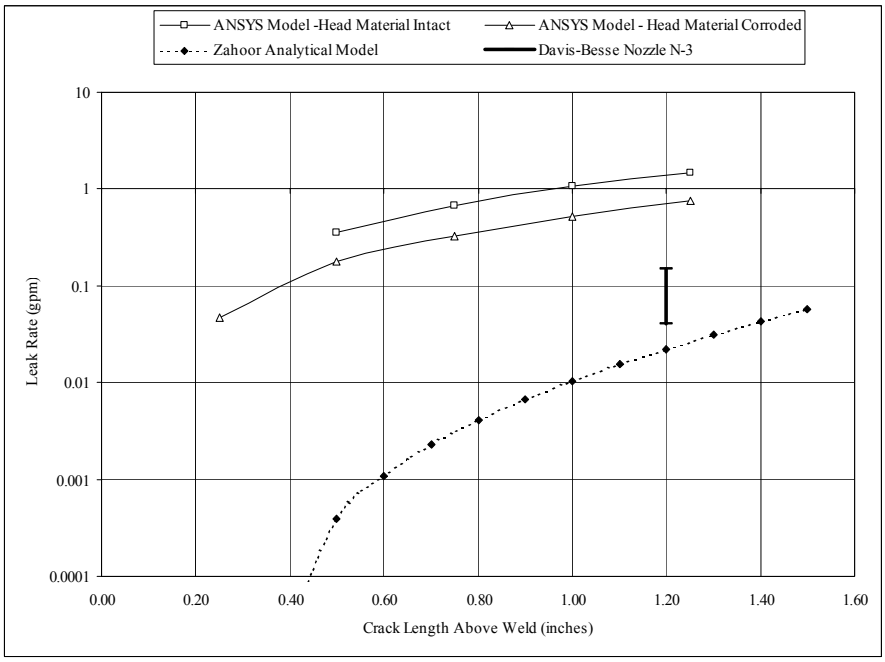

Figure C-3
Leak Rate versus Crack Length According to Analytical Models

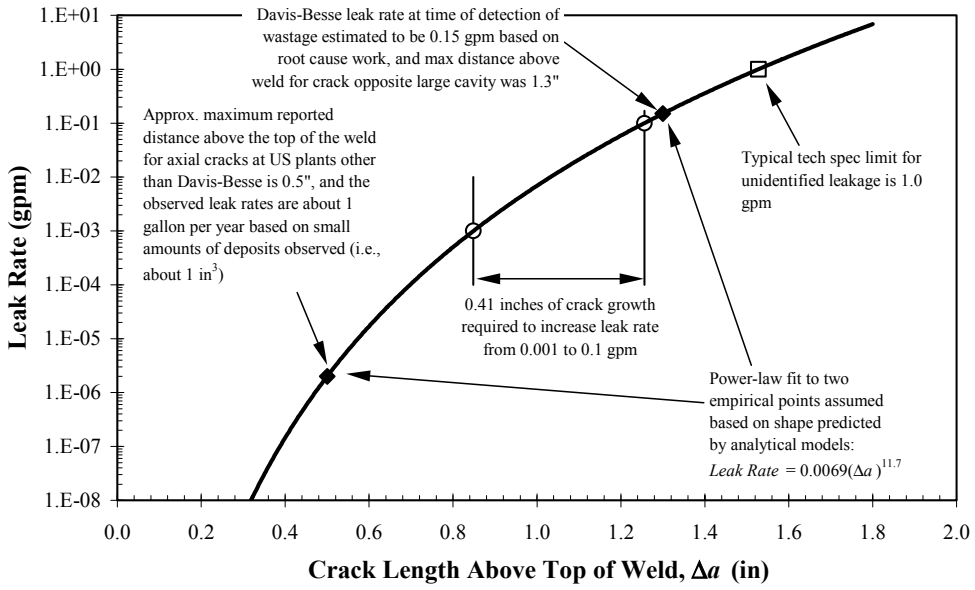

Figure C-4
Assumed Nominal Leak Rate versus Crack Length Relationship Based on Available Plant Data

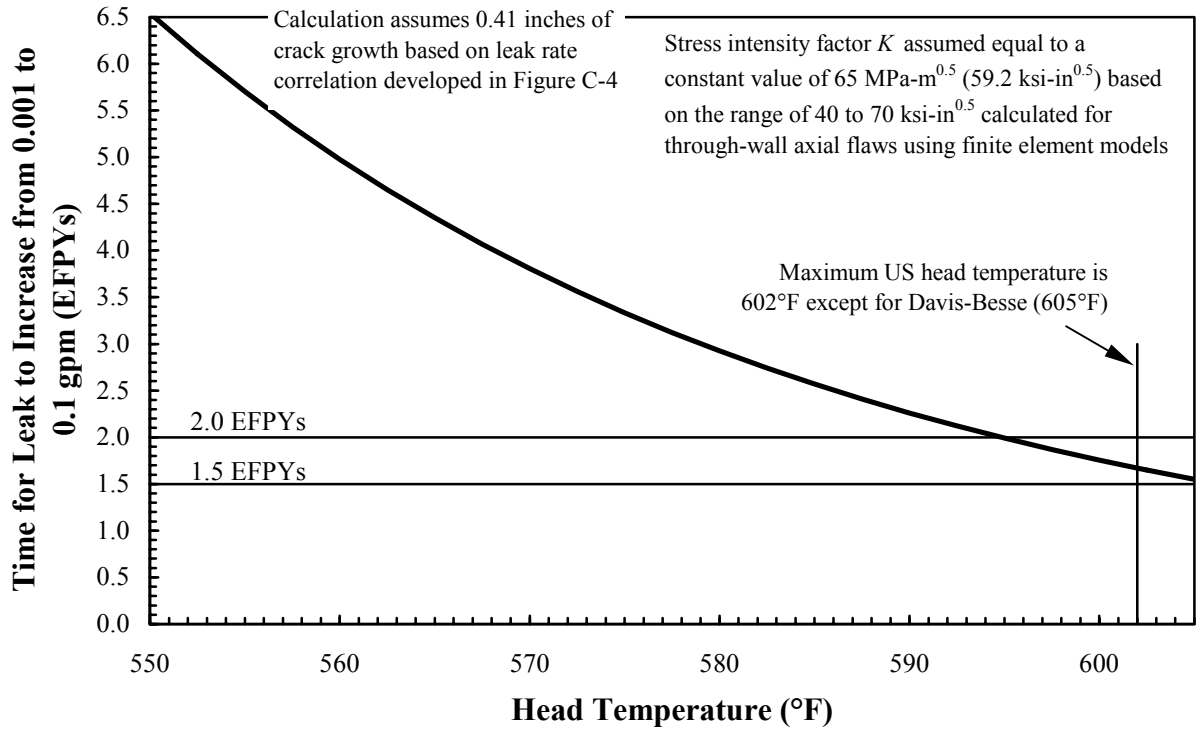

Figure C-5
Time for Leak Rate to Increase from Level Detectable by Supplemental Visual (SV) Inspections (0.001 gpm) to the Critical Leak Rate that May Lead to Rapid Corrosion (0.1 gpm) Using the Deterministic Crack Growth Rate Curve Recommended by the MRP for Cracks in Contact with the OD Annulus Environment [C-5].

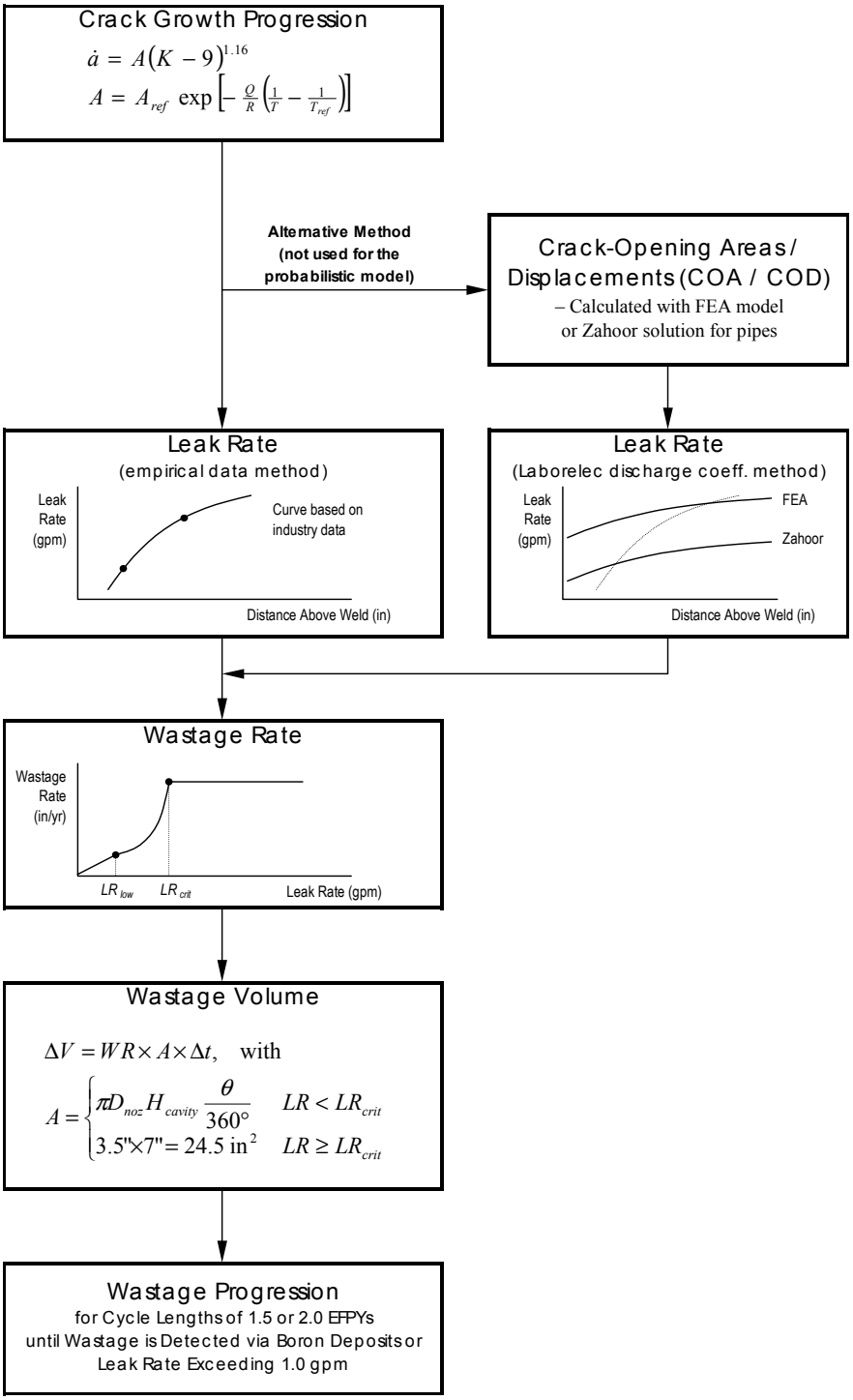

Figure C-6
Simplified Flowchart for the Probabilistic Wastage Model

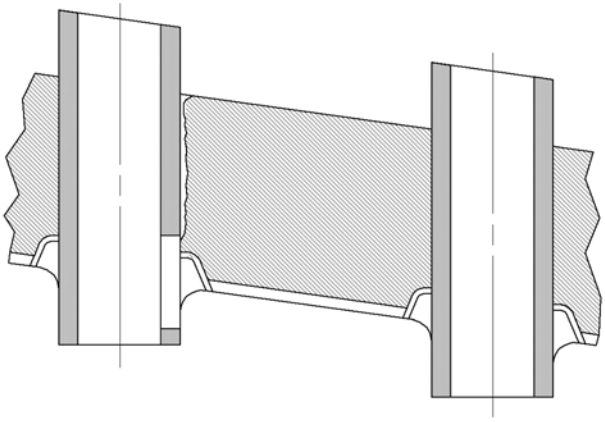

Stage 1: For relatively small initial leak rates, cooling is insufficient to support liquid on the top head surface and the rate of corrosion in the annulus is limited by the lack of oxygen. Steam cutting may act to open up the initially tight annulus.

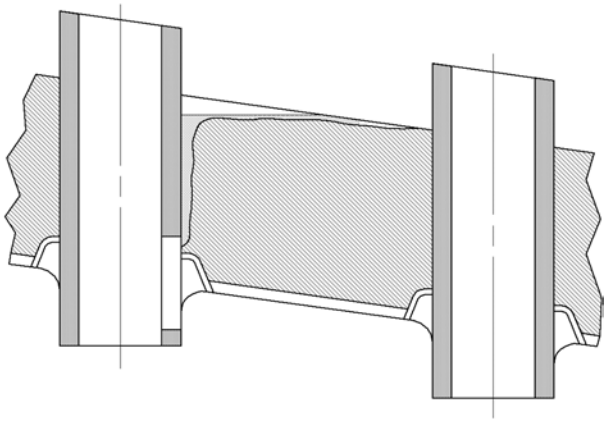

Early Stage 2: The leak rate increases with increasing crack length. Oxygen begins to penetrate into the increasing gap between the nozzle and vessel head and liquid begins to flow out onto the head surface, concentrating boric acid as the water evaporates. The oblong shape of the cavity viewed from above is the result of gravity displacing the liquid in the downhill direction. Corrosion behavior on the top head surface is somewhat analogous to borated water dripping onto a hot metal surface.

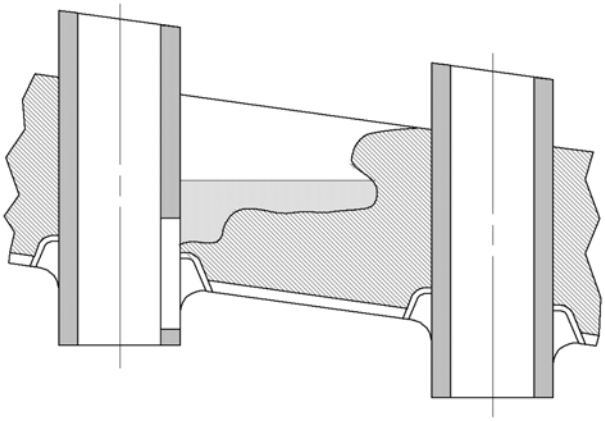

Later Stage 2: As a cavity forms and deepens on the top head surface, the edges of the pool recede back towards the leaking nozzle. A constant leak rate (about 0.1 gpm) results in an equilibrium volume of liquid on the head surface that corrodes predominantly downward through the low-alloy steel head.

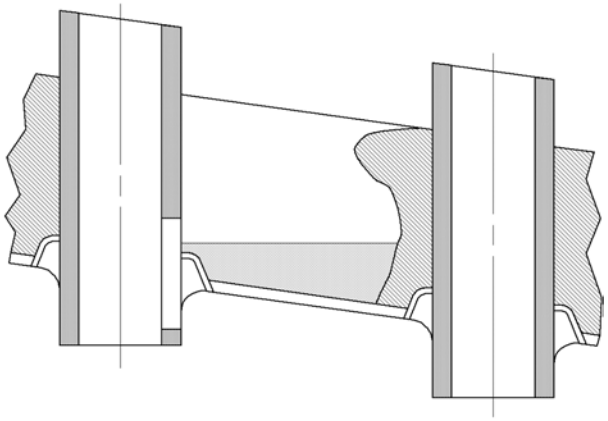

Stage 3: Downward corrosion is arrested by the stainless steel clad. Corrosion continues on the exposed low-alloy steel surfaces due to the equilibrium volume of liquid on the clad surface.

Figure C-7
Cavity Progression for a Top-Down Corrosion Mode

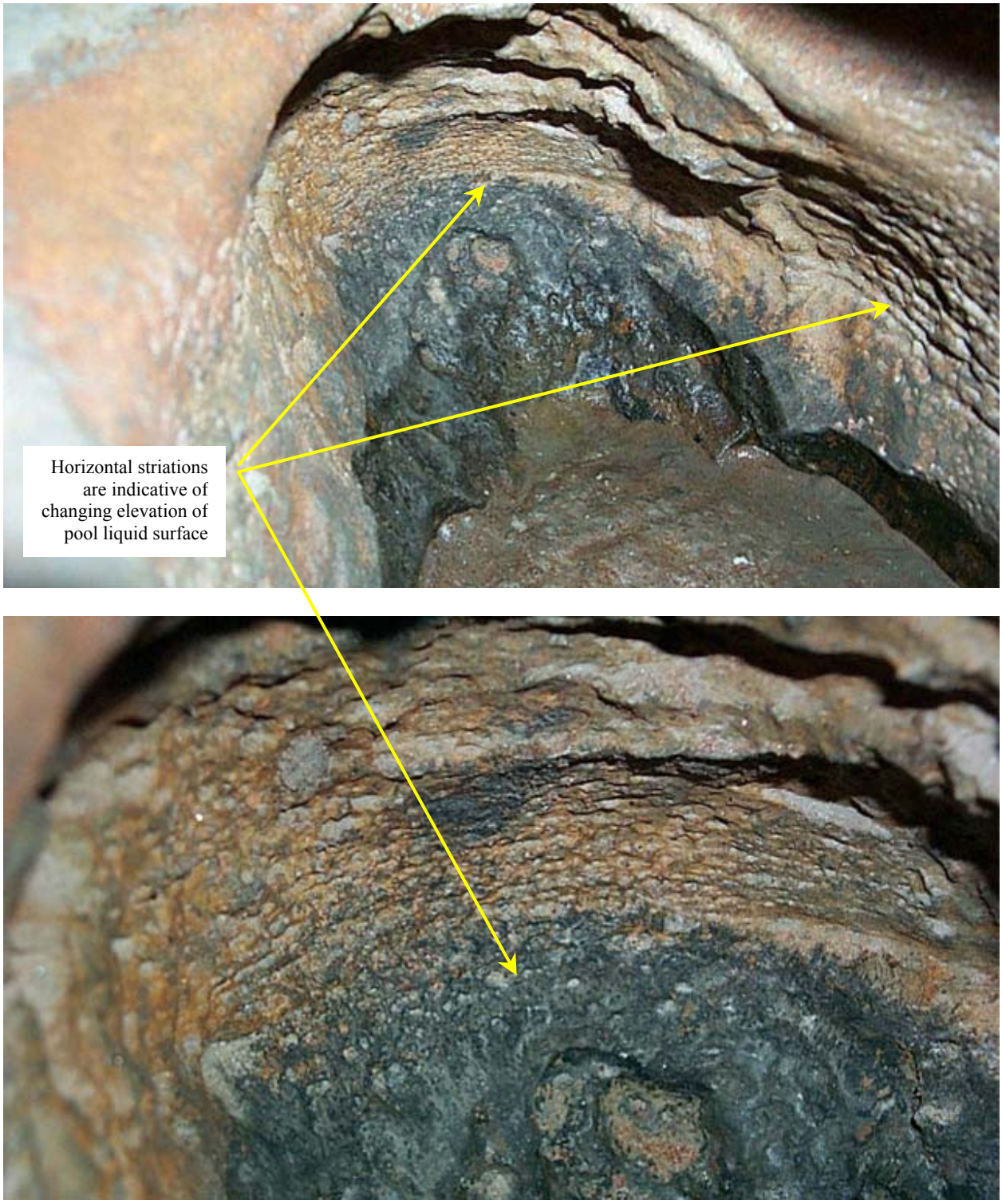

Figure C-8
Photographs of Davis-Besse Wastage Cavity Adjacent to Nozzle #3 [C-9]

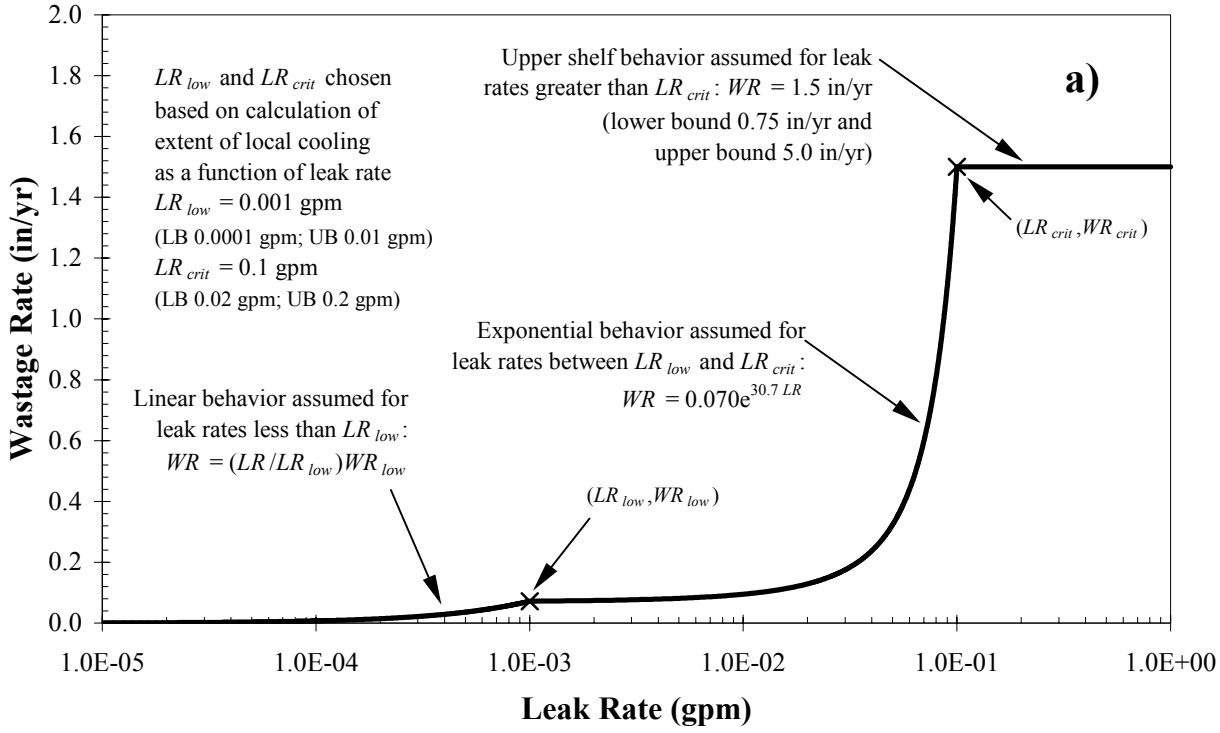

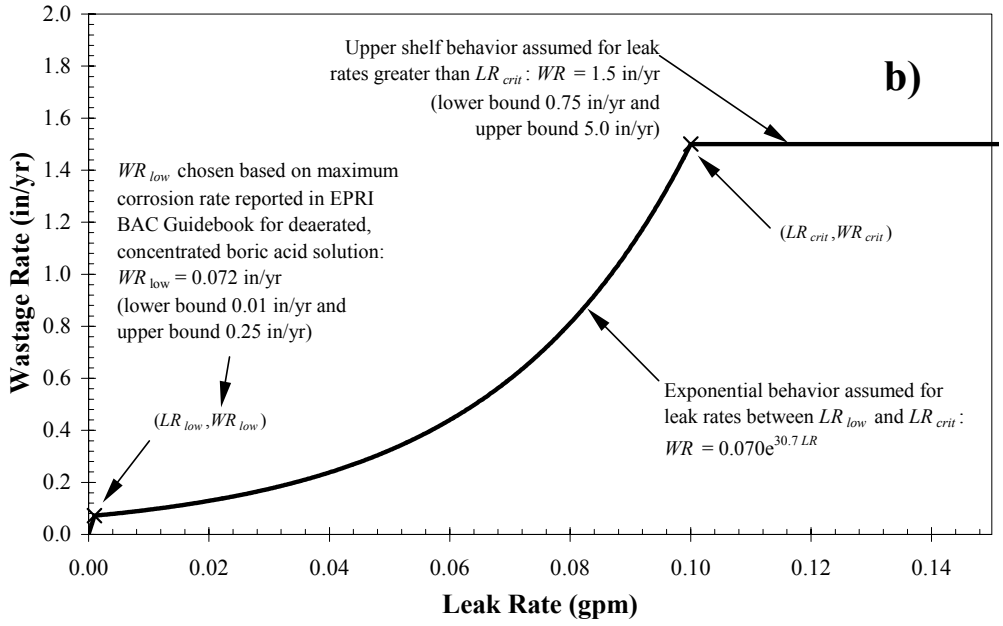

Figure C-9
Assumed Dependence of Linear Wastage Rate on Leak Rate Based on Available Test and Plant Data: a) Log scale for leak rate; b) linear scale for leak rate

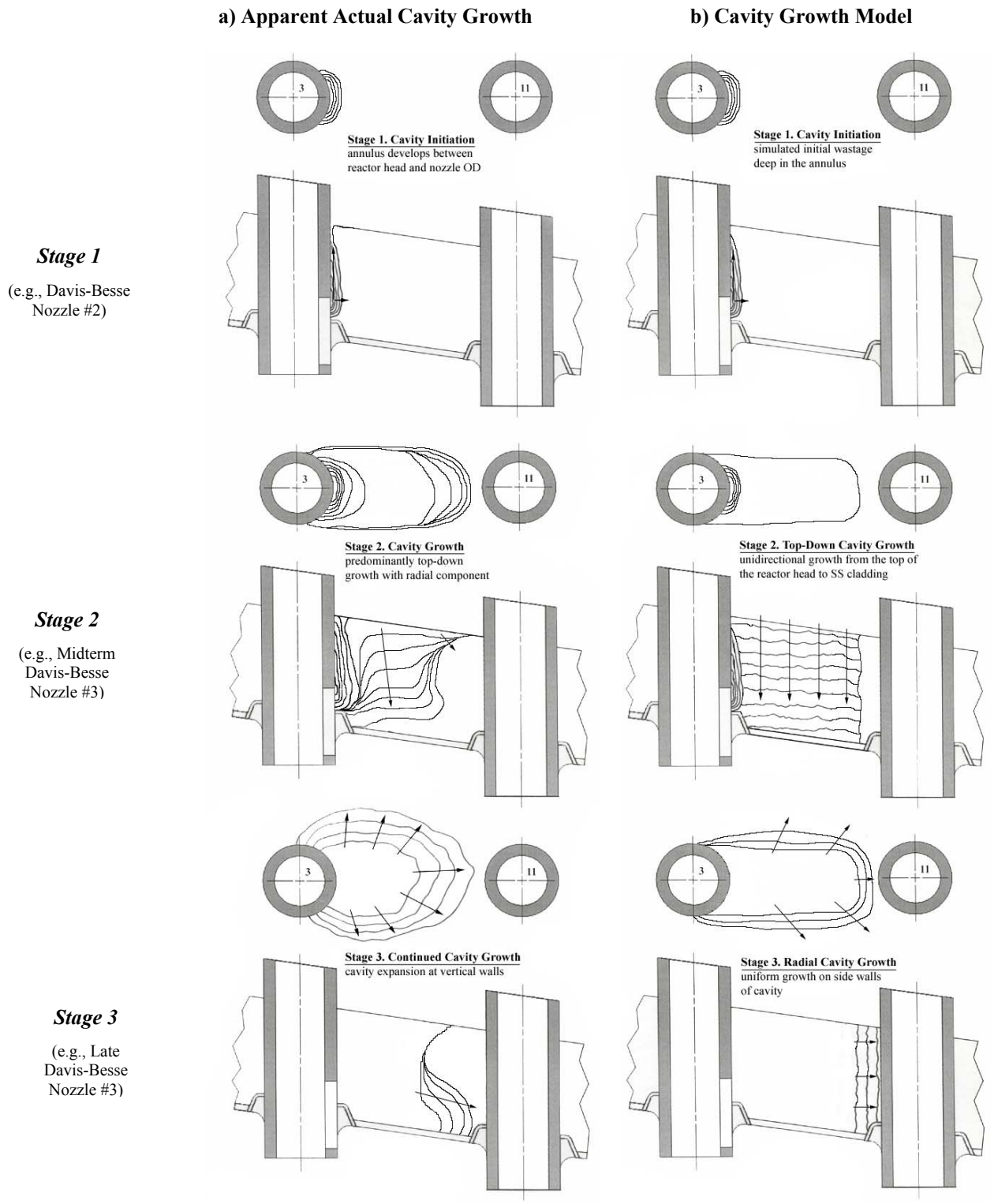

Figure C-10
Development of Wastage Cavity: a) Apparent actual cavity development adjacent to Davis-Besse nozzle #3; b) Cavity growth geometry assumed for the probabilistic wastage model

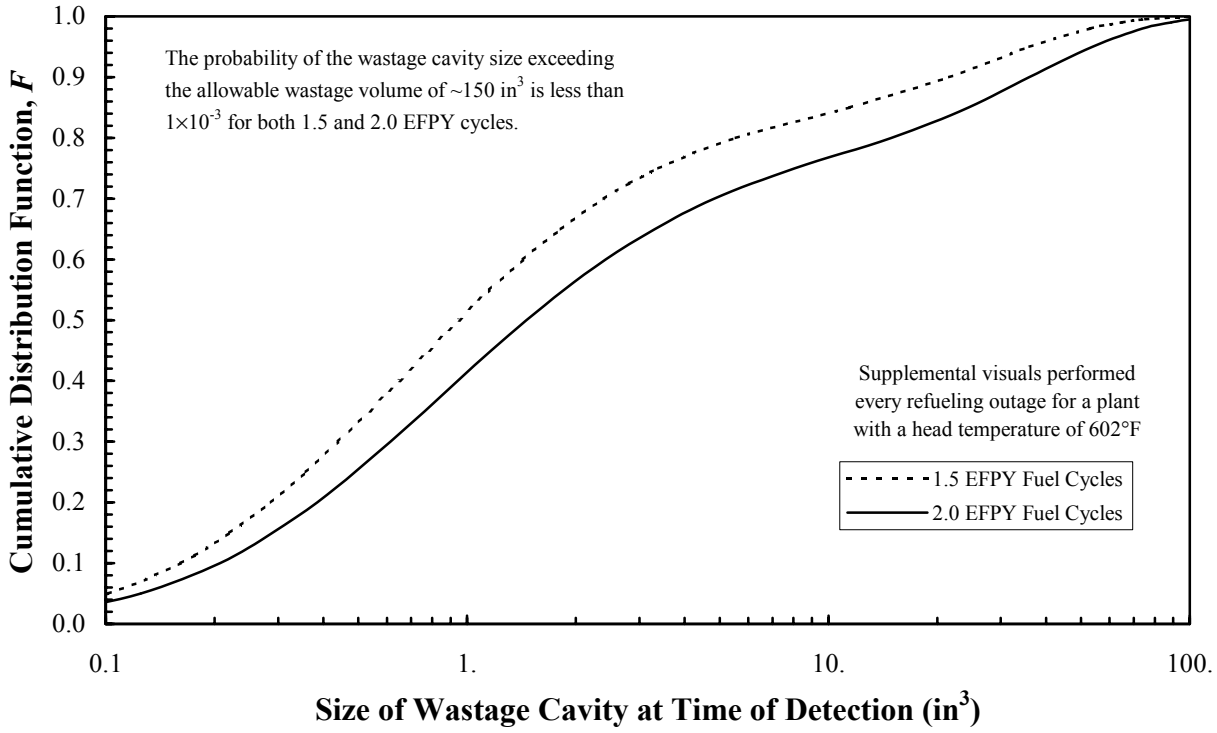

Figure C-11
Results of the Probabilistic Wastage Calculations

D
APPENDIX D: DESCRIPTION OF THE PROBABILISTIC WASTAGE MODEL

One approach for evaluating the potential for wastage due to a leaking RPV head nozzle is a deterministic calculation. However, a probabilistic approach allows the uncertainties associated with the inputs to be fully considered. The end product of the probabilistic wastage model presented here is the statistical distribution of wastage cavity size at the time that the cavity is detected. Detection of the cavity is assumed to be either by observation of boric acid crystal accumulation during a Supplemental Visual inspection or by the unidentified leak rate exceeding the typical technical specification limit of 1.0 gpm, triggering a search for the source of the leakage. This appendix describes the Monte Carlo probabilistic wastage model for a single leaking CRDM nozzle. The appendix is organized as follows:

- WASTAGE MODEL BASICS. Describes the steps used to connect the growth of a postulated axial crack extending above the top of the CRDM nozzle J-groove weld to the resultant wastage rate and wastage cavity volume.
- LEAK RATE TO PRODUCE RAPID CORROSION BASED ON THERMAL ANALYSIS. Briefly describes the thermal analysis used to determine the extent of local cooling due to vaporization of the effluent. The extent of local cooling is the key parameter determining the potential for rapid corrosion.
- STATISTICAL DISTRIBUTIONS USED FOR INPUTS. Defines the parameters of each statistical distribution used to model the inputs necessary for calculating the wastage rate.
- MONTE CARLO CALCULATIONS. Summarizes the steps used to calculate the wastage volume associated with a range of confidence levels (e.g., volume of wastage for which 95% of the trials yielded a smaller result).

Wastage Model Basics

This section describes the basic calculation sequence used to estimate the extent of wastage at any particular point in time. In particular, the following steps are used:

- Predict the crack growth for an axial crack extending above the top of the CRDM J-weld. Crack growth rates are calculated using the standard power-law expression $\dot{a} = A(K - K_{th})^n$ where A, K_{th}, and n are constants and K is the stress intensity factor. The constant A is modified using a standard thermal activation energy of 31.0 kcal/mole to account for the effect of head temperature. Because of uncertainties associated with the chemical environment on the nozzle OD for relatively high leak rates, it is conservatively assumed that the local cooling due to the leakage does not reduce the rate of crack growth.

- Predict the associated leak rate as a function of the crack length above the weld. Past predictions based on crack opening area and displacement (finite element analysis or EPRI algorithm for an axial crack in a pipe) have tended to overpredict leakage for small cracks based on industry experience. Hence, an empirical curve based on available plant data for CRDM nozzles was developed for this model (Figure C-4).

- Predict the wastage rate as a function of the leak rate. This model is based on two key inputs:

    - The estimated critical leak rate, LR_{crit}, which results in sufficient head cooling to permit concentrated liquid over a significant region of the top head surface, where the presence of the aerated, concentrated boric acid solution may lead to relatively high corrosion rates. The nominal value for LR_{crit}, 0.1 gpm, is correlated with a nominal wastage rate of 1.5 in/yr based on the Davis-Besse experience and laboratory testing.

    - A baseline low rate, LR_{low}, of 0.001 gpm, which produces relatively little local cooling, is correlated with a wastage rate of 0.072 in/yr, a conservative value based on the testing reported in the EPRI *Boric Acid Corrosion Guidebook* [D-8] for deaerated and low-oxygen, concentrated boric acid solutions.

    For leak rates below LR_{low}, a linear relationship starting at zero leak rate and zero wastage rate is assumed. For rates between LR_{low} and LR_{crit}, the profile is assumed to follow an exponential relationship reflecting the role of increased cooling on corrosion rates. This is illustrated in Figure C-9. For leak rates above LR_{crit}, the constant upper shelf wastage rate, nominally 1.5 in/yr, is assumed. This behavior may be conservative since higher leak rates could tend to "wash" the corrosion sites of the most concentrated boric acid.

- Compute the associated wastage volume (loss of material). This is modeled in the following fashion, as shown in Figure C-10:

    - Stage 1: The initial wastage "front" (exposed area being wasted) is assumed to be a region of the CRDM nozzle penetration hole extending up from the top of the weld a distance equal to one fourth of the total distance to the top head surface and over an arc extending a total of 30°. The active corrosion area is assumed to increase in height at four times the wastage rate and circumferential extent at twice the wastage rate on each side. The maximum circumferential extent of the wastage front is assume to be 180°.

    - Stage 2: Once the leak rate reaches LR_{crit}, there is assumed to be sufficient cooling to permit concentrated boric acid solution to cause wastage at the top surface of the head. Based on the Davis-Besse experience [D-1], an area measuring 7 inches by 3.5 inches, with the leaking nozzle located at one end, is assumed to be subject to wastage at the upper shelf wastage rate WR_{crit} once LR_{crit} is reached. The model assumed that this top-down mode causes additional volume loss independent of the amount of material corroded during Stage 1.

    - Note that the results of the probabilistic wastage model are relatively insensitive to the assumption of a top-down progression in Stage 2 versus continued radial growth of the cavity at the upper shelf wastage rate. Under this alternative progression, rapid corrosion would begin once the annulus opens up to the point that oxygen can penetrate deep into the cavity. However, the rate of material volume loss would be

similar because half the surface area of the low-alloy steel bore is comparable to the assumed 25 in^2 (7 by 3.5 inches) area for the top-down corrosion front.

- Stage 3: Once the top-down corrosion mode removes material all the way down to the inside surface cladding, additional material loss is assumed to occur at the WR_{crit} wastage rate on the sides of the cavity.

- The wastage volume at the time of detection is recorded. As mentioned, detection may be by observation of boric acid accumulation during a Supplemental Visual inspection or by the leak rate exceeding the typical technical specification limit for unidentified leak rate, 1.0 gpm. The volume of boric acid (H_3BO_3) deposits produced by the leaking primary water is calculated using a boron mass balance assuming that the boron concentration in the primary water decreases linearly from 1500 ppm at the start of the cycle down to 0 ppm at the end of the cycle. This assumed dependence of boron concentration versus time produces a conservatively low estimate of the volume of deposits produced.

Later sections of this appendix describe how this calculation methodology is incorporated in a Monte Carlo probabilistic analysis.

Leak Rate to Produce Rapid Corrosion Based on Thermal Analysis

Large local cooling creates the conditions for rapid corrosion by allowing aerated, concentrated boric acid solution to pool on the top head surface. Calculations have also shown that an aggressive chemical environment (e.g., low pH) is more likely to occur for solution temperatures approaching 212°F [D-2]. The extent of cooling along the leak path is primarily a function of the leak rate since the rate of heat transfer to completely vaporize the effluent is directly proportional to the leak rate. Therefore, an analysis was performed to determine the extent of cooling as a function of leak rate [D-2].

Using a simple enthalpy balance, Figure D-1 shows the size of the effluent heat sink produced as a function of the leak rate and the steam quality or superheat of the escaping steam. The assumption in this figure of atmospheric pressure for the exiting flow is based on two-phase pressure drop calculations that have shown that early in the cavity growth progression the pressure in the cavity becomes nearly atmospheric pressure [D-2]. For leaking primary water at 600°F, 45% of the effluent will flash to steam without any heat input. Heat input from the head material to the effluent will act to increase the quality to saturated conditions and then superheat the steam back to a temperature of 600°F.

The second step in the thermal analysis was to construct a finite element model of an example head and apply thermal boundary conditions including a uniform heat sink on a 45° or 90° arc surface on the OD of a CRDM nozzle along a postulated leak path. Figure D-2 shows an example temperature field resulting from this analysis for the case of a total 45° arc surface heat sink with a magnitude of 1860 Btu/h. This size heat sink corresponds to complete vaporization of a 0.007 gpm leak. Figure D-3 summarizes the results of several such finite element cases by showing the average metal surface temperature in the annulus along the leak path as a function of heat sink magnitude.

The results of the thermal analysis were applied as follows. For a leak rate of 0.001 gpm, Figure D-1 shows that a heat sink of roughly 300 Btu/h would be expected for complete effluent vaporization. Then Figure D-3 shows that the extent of cooling would be expected to be relatively minor, on the order of 10°F. For a leak rate of 0.01 gpm and the corresponding heat sink of 3000 Btu/h, the extent of cooling is calculated to approach 100°F, still not enough cooling to support a liquid pool developing on the head top surface. On the other hand, a leak rate of 0.1 gpm is calculated to be sufficient to cool the local metal surface to temperatures below the boiling point of water at atmospheric pressure (212°F). Since cooling below this temperature cannot be supported, the actual heat sink magnitude in the annulus region must be less than that corresponding to complete effluent vaporization. In this case, the steam quality exiting the annulus would be less than 100%, indicating development of a liquid pool on the head top surface.

Statistical Distributions Used for Inputs

Due to inherent uncertainties, many of the variables on which the potential wastage depends are better represented by statistical distributions than by single values. The use of appropriately chosen statistical distributions allows the possibility for unlikely, extreme values to be accounted for in a quantitative fashion.

In this appendix, all variables used to compute wastage are assigned one of three types of statistical distribution, listed below along with the corresponding probability density function $f(x)$:

UNIFORM:
$$f(x)=\begin{cases}\dfrac{1}{b-a}, & a\le x\le b\\ 0, & x<a, x>b\end{cases}$$

TRIANGULAR:
$$f(x)=\begin{cases}\dfrac{2(x-a)}{(b-a)(c-a)}, & a\le x\le c\\ \dfrac{2(b-x)}{(b-a)(b-c)}, & c\le x\le b\end{cases}$$
; min. a, max. b, mode c

LOG-TRIANGULAR:
$$f(x)=\begin{cases}\dfrac{2(\ln x-\ln a)}{(\ln b-\ln a)(\ln c-\ln a)}, & a\le x\le c\\ \dfrac{2(\ln b-\ln x)}{(\ln b-\ln a)(\ln b-\ln c)}, & c\le x\le b\end{cases}$$
; min. a, max. b, mode c

The cumulative distribution function $F(x)$ (CDF) is the integral of the probability density function $f(x)$ (PDF) and thus represents the probability that the variable of interest is equal to or less than the value x. Further characteristics of these distributions—such as formulas for the

mean, mode, and median—can be found in standard statistics references (e.g., see Chapter 6 of [D-3]).

The values for the statistical input distributions for the probabilistic wastage model are listed in Table D-1. This table is constructed in the following fashion:

- The two leftmost columns describe the variable of interest and the variable nomenclature.
- The next two columns list the nominal value and the applicable units.
- The next four columns define the statistical distribution used to model each variable and the associated parameter values (e.g., *a*, *b*, and *c* for a triangularly distributed variable). Triangular and log-triangular distributions are commonly used for variables with limited available data and are hence used for the majority of the inputs.

The following list summarizes the basis for each input parameter in Table D-1.

- FRACTION OF CYCLE WHEN LEAK BEGINS. The use of a uniform distribution reflects the assumption that a leak is equally likely to initiate at any point during a cycle.
- STRESS INTENSITY FACTOR. Used in projecting crack growth rates, the values for this input distribution are based on finite element calculations that consider all operating stresses including welding residual stresses and assume a through-wall axial crack extending 0.5 to 1.5 inches above the top of the J-groove weld.
- CRACK GROWTH RATE POWER LAW COEFFICIENT. The statistical distribution for this coefficient is based on the evaluation of Alloy 600 crack growth rate data presented in report MRP-55 [D-4]. The same log-triangular distribution used for the probabilistic evaluation of nozzle ejection discussed in Appendix A was also used for the wastage model. The upper bound of the distribution accounts for the physical upper limit to the rate of SCC crack growth.
- LEAK RATE FOR CRACK 0.5-INCH ABOVE WELD. The distribution used for this leak rate (2×10^{-6} gpm nominal with 10^{-6} and 10^{-4} triangular bounds) is based on industry experience with such cracks. The leak rate is estimated based on the small volumes of boric acid deposit accumulations typically observed adjacent to leaking CRDM nozzles. Further details are available in MRP-44, Part 2 [D-5], MRP-48 [D-6], and Reference [D-7].
- LEAK RATE FOR CRACK 1.3-INCH ABOVE WELD. This distribution is based on the Davis-Besse experience as evaluated in the Davis-Besse root cause report [D-1] with statistical bounds chosen in light of the variability of crack geometry.
- LEAK RATE YIELDING WASTAGE RATE WR_{low}. The values for this input distribution were chosen because they result in a relatively low level of local cooling and relatively small flow velocities. As discussed above in the section describing the thermal analysis, the nominal value of 0.001 gpm for LR_{low} is expected to produce only about 10°F of local cooling. The bounds to this parameter cover a total range of two orders of magnitude in order to account for the uncertainties in the thermal analysis.
- CRITICAL LEAK RATE YIELDING UPPER SHELF WASTAGE RATE WR_{crit}. The nominal value of 0.1 gpm was chosen based on the results of the thermal analysis, and also on the Davis-Besse experience [D-1] that indicated rapid corrosion beginning for a leak rate in the range of 0.04 to

0.20 gpm. For this leak rate, the thermal analysis shows that the extent of local cooling is sufficient for a pool of concentrated boric acid solution to form on the top head surface. The lower bound of 0.02 gpm for this parameter accounts for uncertainties in the thermal analysis. This lower bound also addresses the concern that relatively high corrosion rates could possibly occur in a highly concentrated molten boric acid solution at temperatures significantly higher than 212°F (e.g., 450°F). Molten boric acid is known to be slow to lose moisture at temperatures up to roughly 450°F.

- WASTAGE RATE AT LEAKAGE RATE LR_{low}. The nominal value of 0.072 in/yr is based on laboratory test data summarized in the EPRI *Boric Acid Corrosion Guidebook* [D-8]. This value is considered to be conservative because it is somewhat greater than the maximum value reported for corrosion of low-alloy steel in low-oxygen, concentrated boric acid solutions.

- UPPER-SHELF WASTAGE RATE. This parameter describes the wastage rate applied in the model after the leak rate reaches LR_{crit}. It describes wastage from the top head surface down toward the cladding (Stage 2 in Figures C-7 and C-10). The nominal value of 1.5 in/yr is based on the Davis-Besse experience (the size of the nozzle #3 cavity and the probable time interval of rapid corrosion) and laboratory test data reported in EPRI Boric Acid Guidebook [D-8] for aerated, concentrated boric acid solutions. The upper bound value of 5 in/yr accounts for the high rates reported for some tests.

- DETECTION SENSITIVITY FOR BORIC ACID CRYSTAL RELEASE. The nominal value of 500 in^3 was assumed in the body of this document; see the heading "Volume of Boric Acid Deposits Detectable by Supplemental Visual Inspection." The upper- and lower-bound parameters for the triangular distribution account for the uncertainty in this parameter.

Monte Carlo Calculations

The sequence of steps listed in "Wastage Model Basics" were implemented in a Monte Carlo simulation in order to predict the probability associated with different levels of wastage. The simulation also determines the likelihood that the upper shelf wastage rate (WR_{crit}) is reached before the cavity is detected and the likelihood that the top-down wastage mode proceeds to the point that a relatively large area of the inside surface cladding is exposed (e.g., over a 25 in^2 area). The Monte Carlo analysis is carried out as follows:

- For all trials, the following constant values are applied:

- The maximum industry head temperature (T_{head}) of 602°F for al lplants other than Davis-Besse, for which a replacement head is now being installed, is assumed for the crack growth calculation.

- A standard crack growth rate activation energy (Q_g) of 31.0 kcal/mol [D-4] is assumed to adjust the crack growth rate parameter A from the standard reference temperature of 617°F to the assumed head temperature of 602°F. Per MRP-55 [D-4] the apparent stress intensity factor threshold K_{th} and power-law exponent n are taken to be the recommended values of 9 MPa√m and 1.16, respectively.

- For each trial, each statistical distribution in Table D-1 is sampled using a random number generator, yielding a value from the permissible range for each input according to the CDF for

the distribution used. For example, the stress intensity factor *K* is assigned a value according to the applicable triangular distribution. The value is most likely close to the mode (65 MPa√m) but could be anywhere between the minimum of 55 MPa√m and the maximum of 75 MPa√m.

- Using all of the inputs sampled in this fashion from the respective statistical distributions, the total wastage volume is calculated using the approach outlined under "Wastage Model Basics" above. For each trial, the wastage volume at 0.1-EFPY intervals is computed up through 50 total EFPY.

- A total of 100,000 trials are executed in this fashion, and the wastage volumes for each stored.

- The full array of 100,000 wastage volumes are sorted from lowest to highest, permitting the values associated with specific confidence levels to be identified. For example, the median wastage volume (50% confidence) is that representing the $50{,}000^{th}$ value in the sorted list, while the 90% one-sided upper-bound volume is the $90{,}000^{th}$ value in the sorted list (i.e., only 10,000 of the trials produced larger volumes). The resulting curve of wastage volume versus confidence level is the cumulative distribution function (CDF) for the wastage volume. This distribution can then be compared to the wastage volume required to maintain code margins.

References

D-1 *Root Cause Analysis Report: Significant Degradation of the Reactor Pressure Vessel Head*, Davis-Besse Nuclear Power Station report CR 2002-0891, April 2002.

D-2 White, G., C. Marks, and S. Hunt. *Technical Assessment of Davis-Besse Degradation,* prepared for meeting with NRC technical staff, May 22, 2002, Rockville, MD.

D-3 Law, A. M. and W. D. Kelton. *Simulation Modeling and Analysis*, Second Edition. New York: McGraw-Hill, Inc., 1991.

D-4 *Crack Growth Rates for Evaluating Primary Water Stress Corrosion Cracking (PWSCC) of Thick-Wall Alloy 600 Material (MRP-55)*, EPRI, Palo Alto, CA: July 2002.

D-5 *PWR Materials Reliability Program, Interim Alloy 600 Safety Assessments for US PWR Plants (MRP-44): Part 2: Reactor Vessel Top Head Penetrations*, EPRI, Palo Alto, CA: 2001. TP-1001491, Part 2.

D-6 *PWR Materials Reliability Program Response to NRC Bulletin 2001-01 (MRP-48)*, EPRI, Palo Alto, CA: 2001. 1006284.

D-7 *Probability of Detecting Leaks in RPV Upper Head Nozzles by Visual Inspections*, by Steve Hunt and Mark Fleming, September 2002. [Appendix B of this report]

D-8 *Boric Acid Corrosion Guidebook, Revision 1: Managing Boric Acid Corrosion Issues at PWR Power Stations*, EPRI, Palo Alto, CA: 2001. 1000975.

Table D-1
Input Statistical Distributions Used in Monte Carlo Calculations of Wastage

Quantity / Description	*Symbol*	*Nominal Value*	*Units*	*Statistical Distribution*	*Parameter 1* Triangular = *c* Log-triang = c	*Parameter 2 (lower bound)* Triangular = *a* Log-triang = *a* Uniform = *a*	*Parameter 3 (upper bound)* Triangular = *b* Log-triang = *b* Uniform = *b*
Fraction of Fuel Cycle Completed When Leak Begins	f_{t0}	0.5	–	Uniform		0.0	1.0
Stress Intensity Factor Driving Axial Crack Growth Above Top of Weld	K	65	MPa√m	Triangular	65	55	75
Crack Growth Rate Power Law Coefficient $\times 10^{13}$	A_{ref}	15.1	$(m/s) \times (MPa\sqrt{m})^{-1.16}$	Log-triang	15.1	1.65	137.6
Leak Rate for Crack Extending 0.5" Above Top of Weld	LR_0	2.0E-06	gpm	Log-triang	2.0E-06	1.0E-06	1.0E-04
Leak Rate for Crack Extending 1.3" Above Top of Weld	LR_1	0.15	gpm	Log-triang	0.15	0.001	1.0
Leak Rate Yielding Wastage Rate WR_{low}	LR_{low}	0.001	gpm	Log-triang	0.001	0.0001	0.01
Critical Leak Rate Yielding Upper Shelf Rapid Corrosion Rate WR_{crit}	LR_{crit}	0.10	gpm	Log-triang	0.10	0.02	0.20
Wastage Rate at Leakage Rate LR_{low}	WR_{low}	0.072	in/yr	Triangular	0.072	0.010	0.250
Upper-Shelf Wastage Rate for Leak Rates Greater than LR_{crit}	WR_{crit}	1.5	in/yr	Triangular	1.5	0.75	5.0
Suppl. Visual Detection Sensitivity for Boric Acid Crystal Release	BAC_{det}	500	in^3	Triangular	500	250	1000

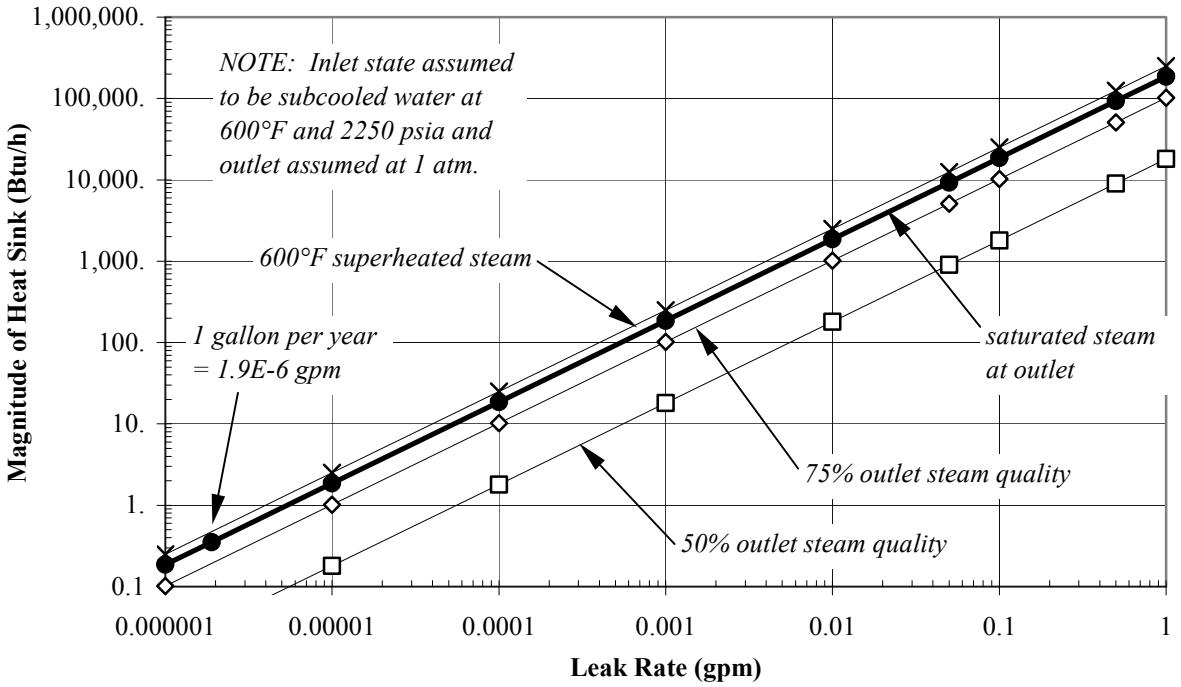

Figure D-1
Expansion Cooling Heat Sink Rate Versus Leak Rate

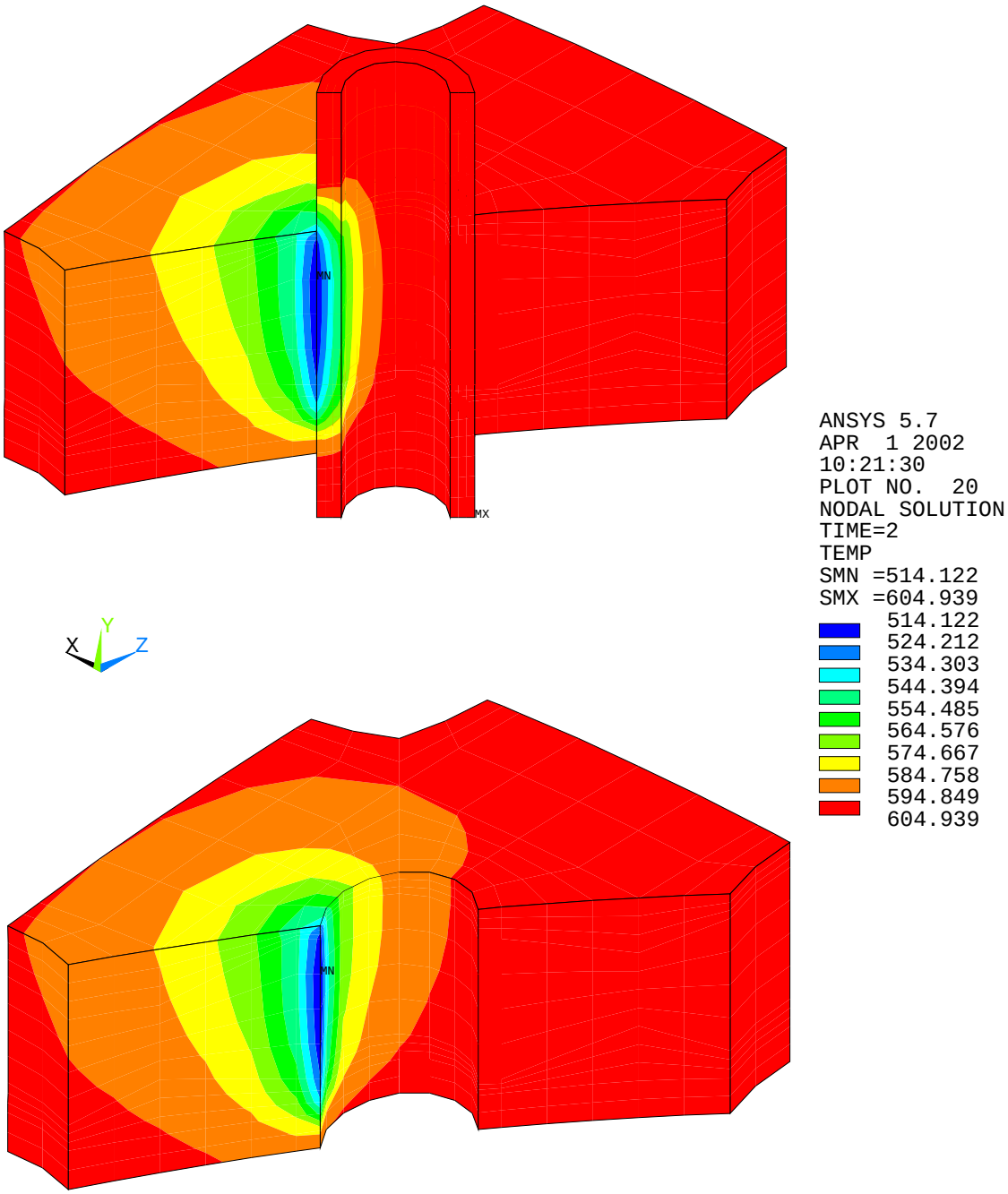

Figure D-2
Example Thermal Analysis Results: Temperature Contours (°F) for a Uniform 1860 Btu/h Heat Sink on 45° Total Arc Surface Corresponding to Complete Vaporization of a 0.007 gpm Leak (Heat Transfer Coefficient on Inside Head Surface of 110 Btu/h-ft^2-°F)

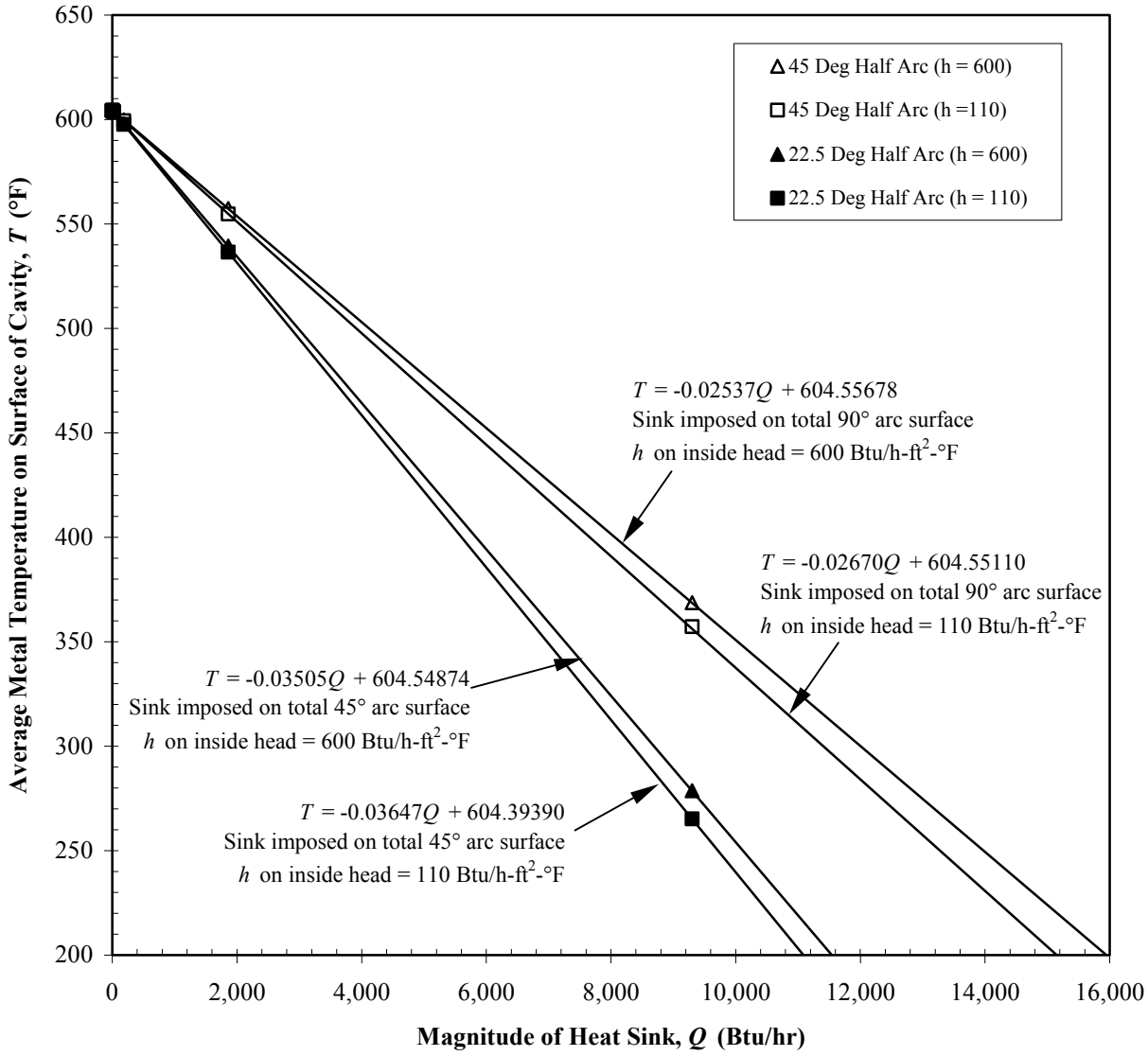

Figure D-3
Average Metal Temperature Along Small Cavity Leak Path Versus Heat Sink Magnitude

E
APPENDIX E: ALLOWABLE WASTAGE VOLUME AT RPV HEAD CRDM NOZZLES

The purpose of this calculation is to determine the volume of low-alloy steel that can be lost from the top surfaces of reactor vessel heads by boric acid corrosion without the stresses in the remaining material exceeding the ASME Code allowable values [E-1].

1. Previous NSSS Vendor Safety Analyses

   Safety analyses prepared by the NSSS vendors in the early 1990's showed that about 6 in^3 of material could be lost and still meet ASME Code stress requirements [E-2, E-3, E-4]. These calculations were not directed towards determining the allowable material loss, but rather to confirm that about 6 in^3 of material loss is acceptable. The 6 in^3 volume was based on six years of leakage with a material loss rate of about 1.07 in^3 per year determined from tests performed by Combustion Engineering [E-5].

2. Allowable Corrosion Volume Based on Finite Element Analysis

   Finite element analyses were performed of a typical PWR vessel head to determine the amount of wastage that can be accommodated and still remain within ASME Code allowable primary membrane and primary membrane plus bending stresses. No credit was taken for elastic-plastic performance of the low-alloy steel head base material or for the membrane pressure capability of unsupported cladding. These factors provide additional margin above that determined using normal elastic stress analysis methods.

   The analyses were performed using the ANSYS finite element software for a model of a vessel head as shown in Figure E-1. The model consists of a 1/8 symmetry sector of the vessel head including the head shell, all of the CRDM nozzles, and the vessel flange. Welding residual stresses were simulated by use of constraint equations between the nozzle OD surface and the shell in the region of the J-groove weld. Typical specified bolt preload was applied to the flange. Operating pressure was applied out to the inner o-ring sealing diameter, and operating temperature was applied to all elements.

   Two conditions were evaluated. The first was a case similar to that which occurred at Davis-Besse nozzle #3, where a pool of borated water apparently developed on the top surface of the head between two nozzles and then corroded down through the low-alloy steel material. The second was a hypothetical case where the corrosion occurs uniformly around a single nozzle.

a. Allowable Wastage Volume – Corrosion Located Between Nozzles

Figure E-2 shows the elements on the top surface of the vessel head that were assumed to be lost due to wastage that occurs between two nozzles as was discovered at Davis-Besse nozzle #3. The elements selected for modeling the wastage were selected based on the actual shape of the Davis-Besse wastage.

Analyses were performed after removing each layer of material except for the last layer. After each new volume of material was removed, ANSYS computed the primary membrane and primary membrane plus bending stress at a path through the center of the corroded ligament as shown in Figure E-2.

Figure E-3 shows the primary membrane and primary membrane plus bending stress through the center of the remaining ligament for increasing volumes of wastage. Also shown on this figure are the allowable membrane (Sm) and membrane plus bending (1.5Sm) stresses at a temperature of 650°F.

These calculations show that approximately 150 in^3 of the low-alloy steel head material can be lost and still meet the ASME Code allowables for primary membrane and membrane plus bending stresses.

b. Allowable Wastage Volume – Corrosion Distributed Around Nozzle

A check calculation was made to confirm that the previous case of wastage distributed between two adjacent nozzles is more limiting than the case of wastage uniformly distributed around a nozzle.

Figure E-4 shows the location of the assumed wastage. Calculations were performed for the cases of one and two rows of elements adjacent to the nozzle corroded.

After each volume of material was removed, ANSYS computed the primary membrane and primary membrane plus bending stresses at a path midway between two adjacent nozzles as shown in Figure E-4. Figure E-5 shows these stresses for the two volumes of wastage. Like Figure E-3, also shown on Figure E-5 are the allowable membrane (Sm) and membrane plus bending (1.5Sm) stresses at the 650°F design temperature.

These calculations confirm that the previous case of wastage located between two adjacent nozzles is conservative relative to wastage of the same volume of material uniformly distributed around a single nozzle.

3. Allowable Corrosion Volume for Other Head Designs

The finite element analyses described in paragraph 2 are for the case of a typical PWR vessel head similar to the Davis-Besse head. These results are considered representative for other vessels as well since the design analyzed had a relatively high diameter to thickness (D/T) ratio and resultant relatively low margins of excess thickness over that required to meet the Code minimum wall thickness.

In summary, the above calculations show that all vessels should be able to accommodate wastage of up to about 150 in^3 and still meet ASME Code primary membrane and membrane plus bending stress requirements.

References

E-1. *Section II – Material Properties, and Section III – Division 1 – Subsection NB – Class 1 Components*, ASME Boiler and Pressure Vessel Code, July 1, 2002 Edition.

E-2. *Safety Evaluation for B&W-Design Reactor Vessel Head Control Rod Drive Mechanism Nozzle Cracking*, BAW-10190P (Proprietary), BAW-10190 (Non-Proprietary), B&W Nuclear Technologies, May and June 1993.

E-3 *Safety Evaluation of the Potential for and Consequence of Reactor Vessel Head Penetration Alloy 600 ID Initiated Nozzle Cracking*, CEN-607, ABB Combustion Engineering Nuclear Operations, May 1993.

E-4 *Alloy 600 Reactor Vessel Head Adaptor Tube Cracking Safety Evaluation*, WCAP-13565, Rev. 1 (Proprietary and Non-Proprietary), Westinghouse Electric Corporation, February 1993.

E-5 *Boric Acid Corrosion Guidebook, Revision 1: Managing Boric Acid Corrosion Issues at PWR Power Stations*, EPRI, Palo Alto, CA: 2001. 1000975. pp. 4-54 to 4-56 (Test Reference M).

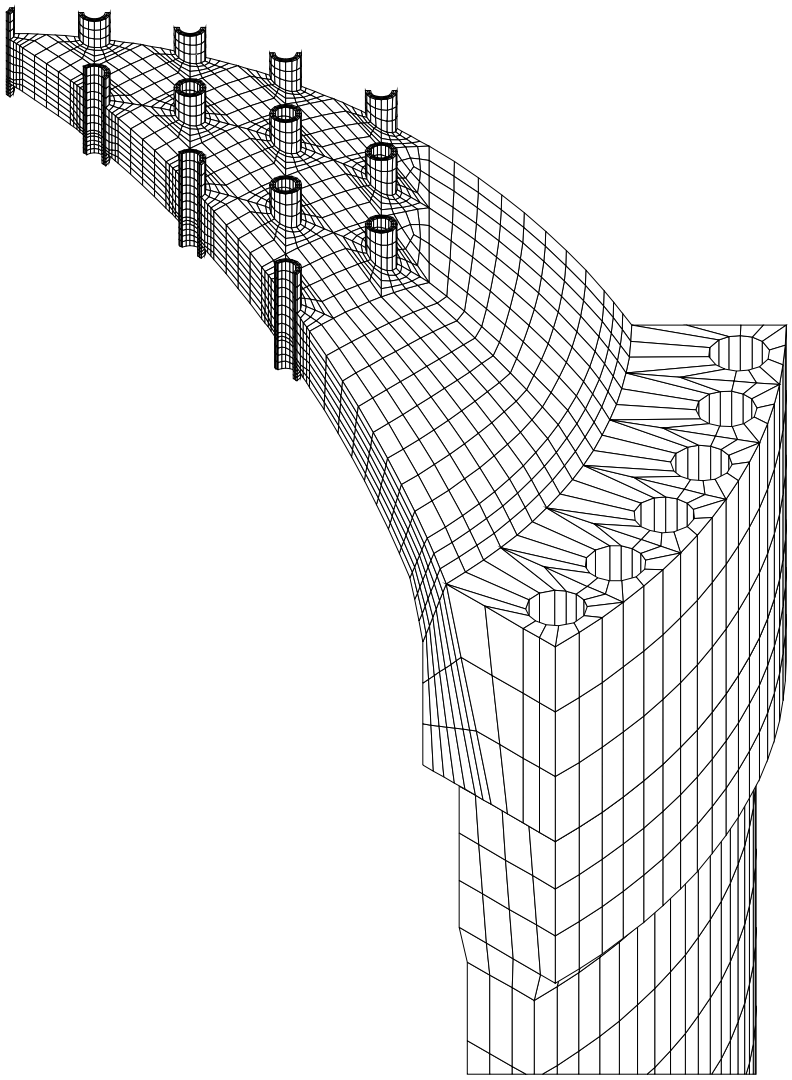

Figure E-1
Finite Element Model of Typical PWR Head Used for Allowable Wastage Volume Calculations

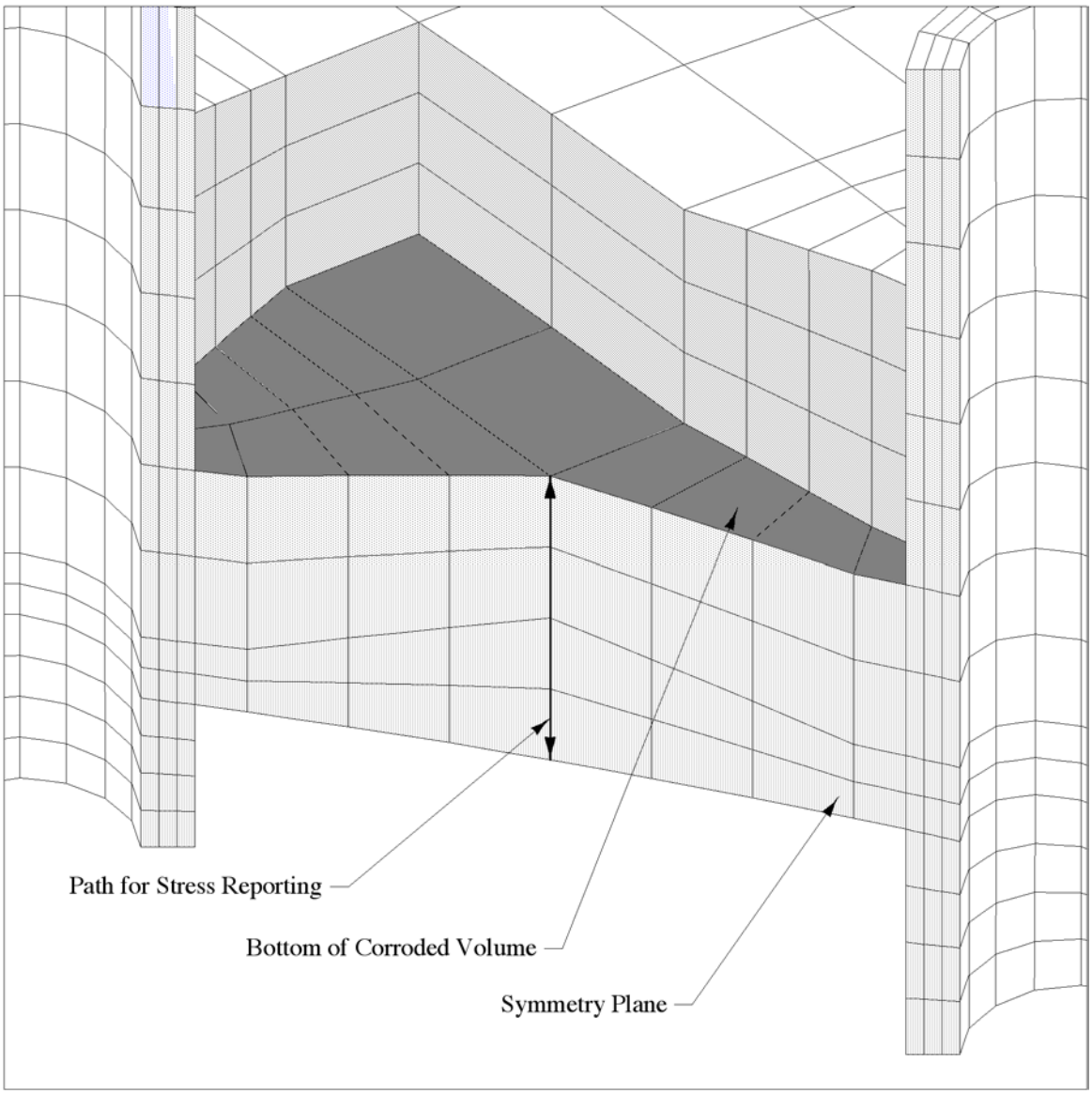

Figure E-2
Finite Element Model – Wastage Between Adjacent Nozzles

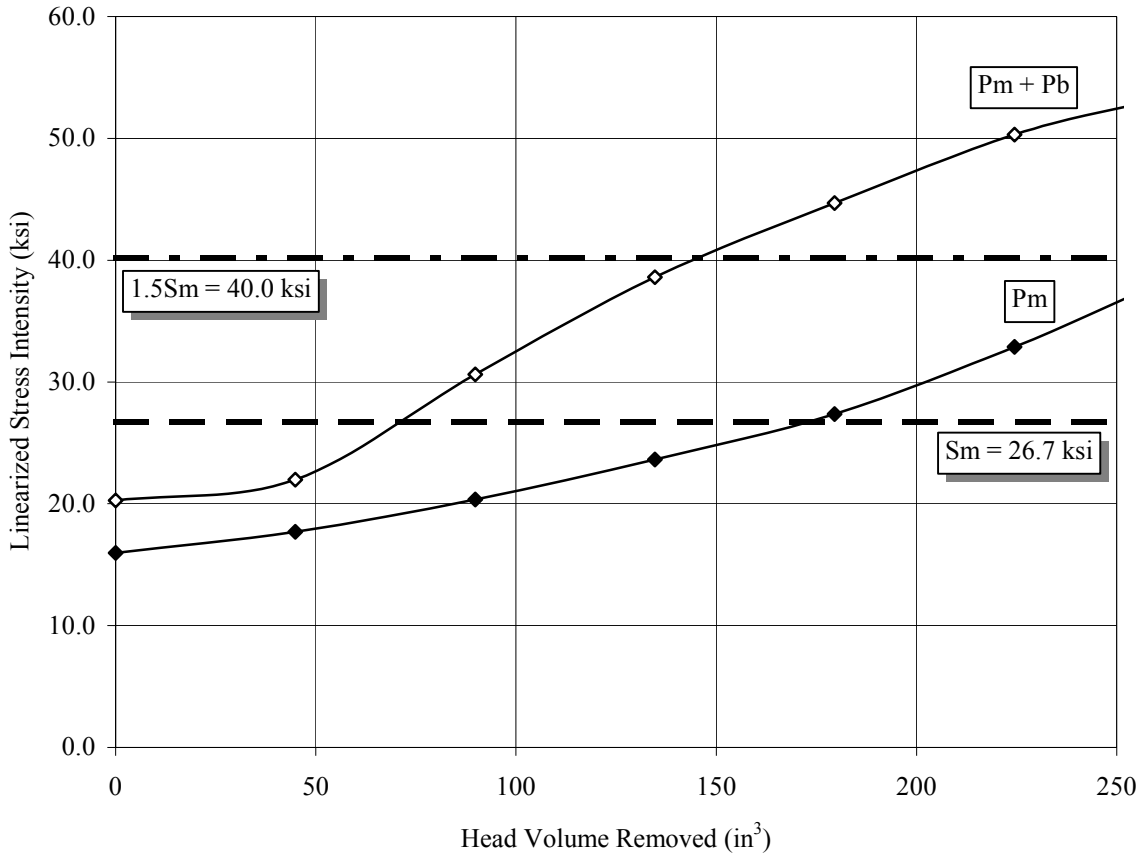

Figure E-3
Finite Element Analysis Results – Wastage Between Adjacent Nozzles

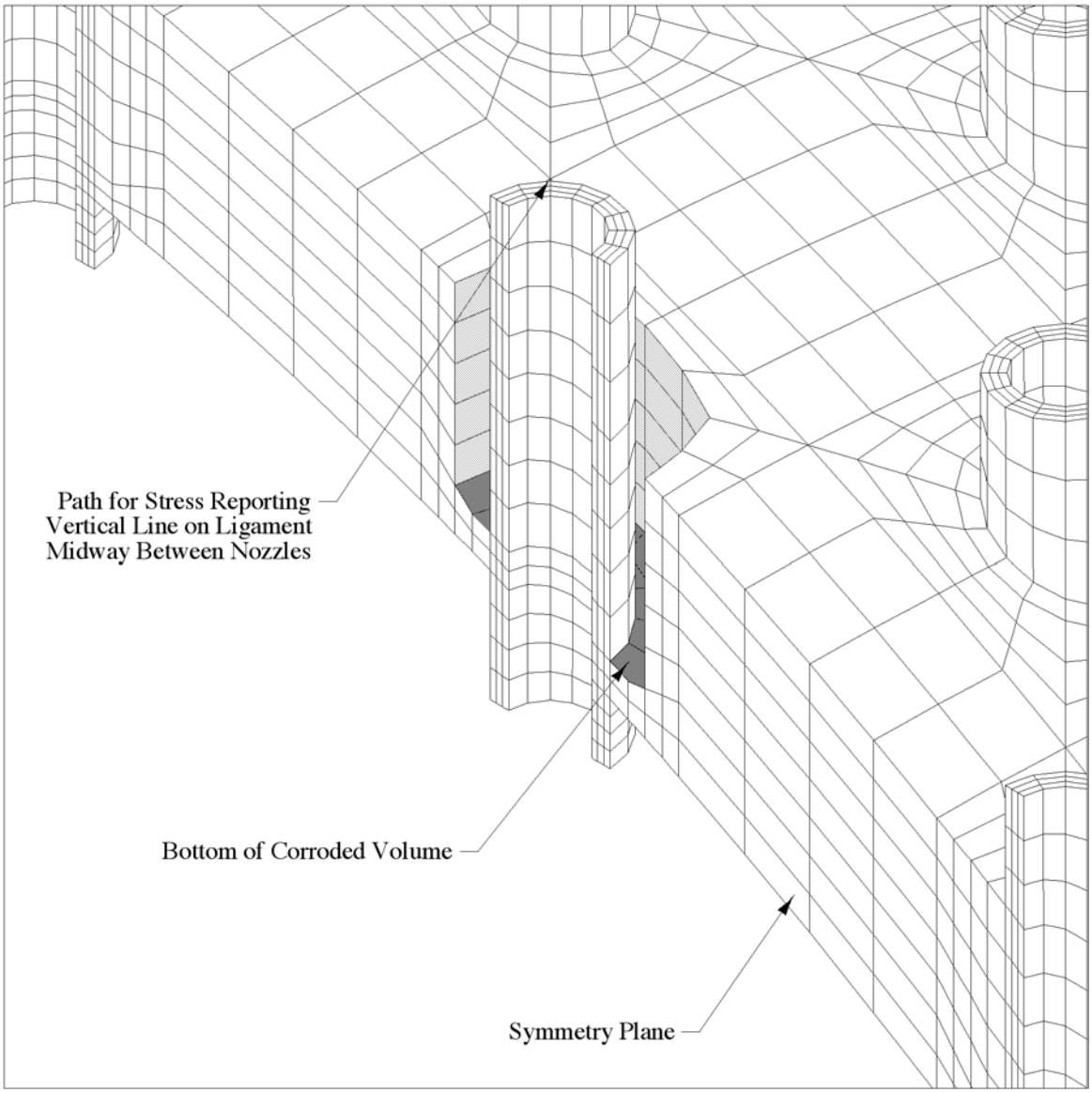

Figure E-4
Finite Element Model – Wastage Distributed Around Single Nozzle

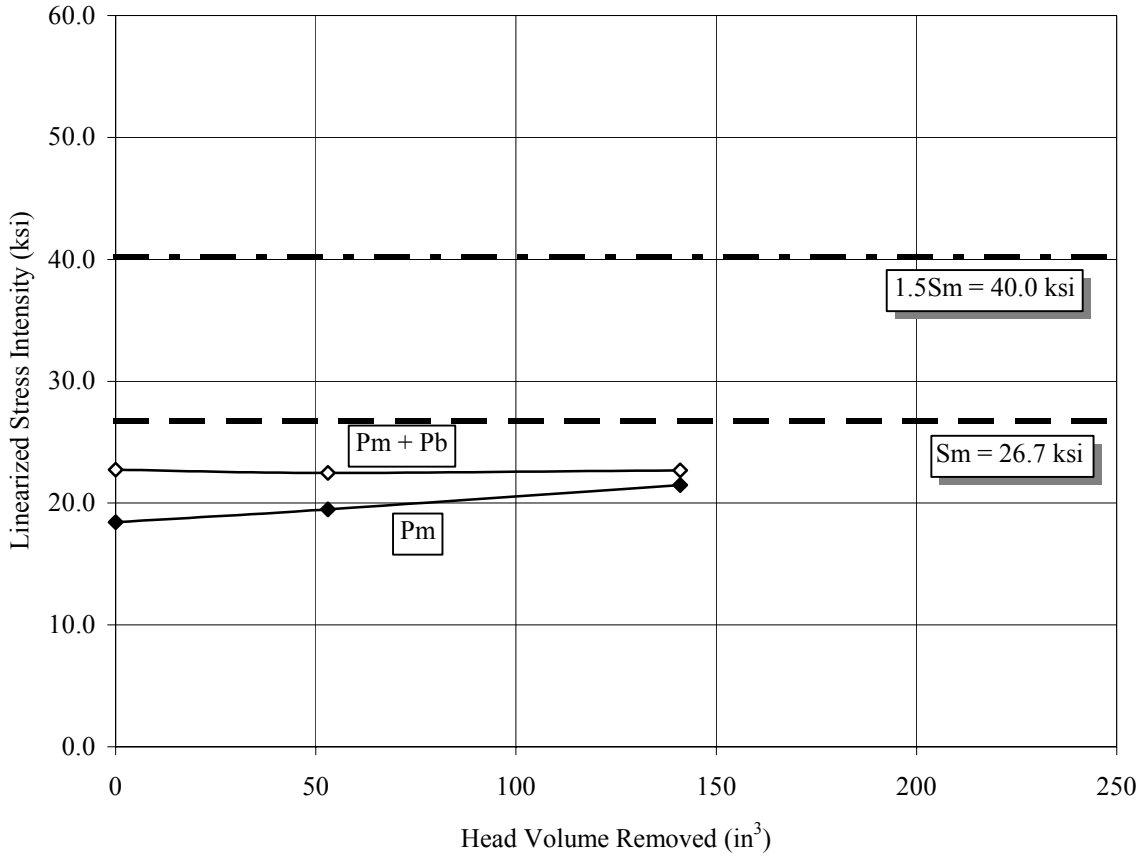

Figure E-5
Finite Element Analysis Results – Wastage Distributed Around Single Nozzle